Analyzing the quantum approximate optimization algorithm: ansätze, symmetries, and Lie algebras

Sujay Kazi •, 1, 2, 3 Martín Larocca •, 2, 4, * Marco Farinati •, 5 Patrick J. Coles •, 6, 2 M. Cerezo •, 7, † and Robert Zeier •, ‡

1 Courant Institute of Mathematical Sciences, New York University, New York, New York 10012, USA
2 Theoretical Division, Los Alamos National Laboratory, Los Alamos, New Mexico 87545, USA
3 Department of Electrical and Computer Engineering, Duke University, Durham, NC 27708, USA
4 Center for Nonlinear Studies, Los Alamos National Laboratory, Los Alamos, New Mexico 87545, USA
5 Departamento de Matemática, FCEN, UBA - IMAS CONICET.
6 Normal Computing Corporation, New York, New York, USA
7 Information Sciences, Los Alamos National Laboratory, Los Alamos, NM 87545, USA
8 Forschungszentrum Jülich GmbH, Peter Grünberg Institute,
Quantum Control (PGI-8), 54245 Jülich, Germany
(Dated: July 11, 2025)

The Quantum Approximate Optimization Algorithm (QAOA) has been proposed as a method to obtain approximate solutions for combinatorial optimization tasks. In this work, we study the underlying algebraic properties of three QAOA ansätze for the maximum-cut (maxcut) problem on connected graphs, while focusing on the generated Lie algebras as well as their invariant subspaces. Specifically, we analyze the standard QAOA ansatz as well as the orbit and the multi-angle ansätze. We are able to fully characterize the Lie algebras of the multi-angle ansatz across arbitrary connected graphs, finding that they only fall into one of just six families. Besides the cycle and the path graphs, the Lie dimensions for every graph are exponentially large in the system size, meaning that multi-angle ansätze are extremely prone to exhibiting barren plateaus. Then, a similar quasigraph-independent Lie-algebraic characterization beyond the multi-angle ansatz is impeded as the circuit exhibits additional "hidden" symmetries besides those naturally arising from a certain paritysuperselection operator and all automorphisms of the considered graph. Disregarding the "hidden" symmetries, we can upper bound the dimensions of the orbit and the standard Lie algebras, and the dimensions of the associated invariant subspaces are determined via explicit character formulas. To finish, we conjecture that (for most graphs) the standard Lie algebras have only components that are either exponential or that grow, at most, polynomially with the system size. This would imply that the QAOA is either prone to barren plateaus, or classically simulable. More generally, our work provides a symmetry framework and tools to analyze any desired variational quantum algorithm.

I. INTRODUCTION

Variational models, such as the Quantum Approximate Optimization Algorithm (QAOA) [1, 2], hold the promise to make practical use of intermediate-scale quantum computers [3–7]. At their core, these schemes train a parametrized quantum circuit to minimize a loss function encoding the solution to a given task of interest. For example, QAOA aims at finding approximate solutions to the maximum-cut (maxcut) problem by encoding the edges of a graph as interaction terms in an Ising-type Hamiltonian, and training a circuit to prepare the ground states of said Hamiltonian.

One of the critical design choices that can make or break a variational model is the choice of an ansatz for the parametrized quantum circuit [8]. Indeed, it has been shown that certain circuit architectures can lead to trainability barriers such as exponentially suppressed loss function gradients [9–11] (i.e., barren plateaus), or optimization landscapes plagued with local-minima [12–19].

Importantly, given that we do not yet posses large-scale quantum computers to heuristically test performance at scale, it is crucial to look for theoretical characterizations capable of predicting whether an ansatz will run into issues or not. One such analysis is the study of the generated Lie algebra [20], defined as the Lie closure of the infinitesimal generators of the parametrized gates. Importantly, the Lie algebra of the circuit captures the ultimate breadth of unitaries that can be expressed via different parameter choices, and its precise characterization is an extremely powerful tool as it enables the study of barren plateaus [21–24], overparametrization [25, 26], as well as the classical simulability of the model [27].

Given the critical importance of the Lie algebra, it comes at no surprise that its analysis has gained significant attention [20, 28–40]. Still, a careful inspection of the literature reveals that many Lie-algebra studies are restricted to two cases: circuits whose gates are generated by single Pauli operators, or ansätze where generators are very structured linear combinations of Paulis, for example invariant under some symmetry group. The first case corresponds to circuits where each rotation is individually parametrized, while the second one contains circuits with correlated gate angles. The reason why the Lie-algebra analysis is restricted to the aforementioned cases is that the computation of the Lie algebra becomes

^{*} larocca@lanl.gov

[†] cerezo@lanl.gov

[‡] r.zeier@fz-juelich.de

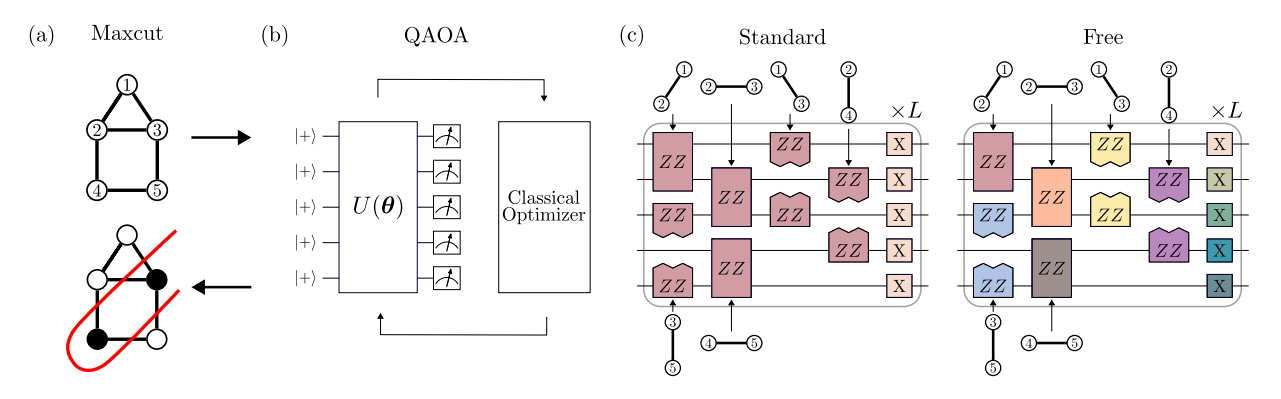


Figure 1. Maxcut, QAOA and ansätze. (a) Given a graph, the maxcut problem is to determine a partition of the vertices into two complementary sets, such that the number of edges between those sets is as large as possible. (b) The QAOA algorithm is a hybrid quantum-classical algorithm that can be used to approximately solve the maxcut problem. The success of QAOA hinges on the ability to optimize the parametrized quantum circuit $U(\vec{\theta})$. Crucially, the trainability of QAOA can be linked to certain algebraic properties of $U(\vec{\theta})$. (c) Here we depict two of the considered QAOA ansätze: the standard and the multi-angle (or free) ansätze [see, e.g., Figs. 2 and 6]. In the image, a gate with ZZ indicates a two-qubit entangling gate generated by a $Z_w Z_{\bar{w}}$ interaction, while the X gate indicates a single-qubit rotation around the x-axis. Boxes with the same color share the same parameter. Hence, each gate in the free ansatz is individually parametrized and generated by a single Pauli operator, which makes its Lie algebra tractable across all graphs. In the standard case, all single-qubit gates share the same parameter, and similarly for all two-qubit gates. This means that the infinitesimal generators of the circuit are given by a sum of Paulis, which limits the ability to treat these cases.

extremely challenging for arbitrary generators consisting of linear combinations of Paulis.

In this work, we contribute to the literature of symmetry and Lie-algebra characterization of quantum circuits by studying the algebraic properties of three QAOA ansätze for maxcut. These include the standard ansatz introduced in the original QAOA manuscript [1]. Here, there are only two generators where certain Paulis are summed over all the edges and vertices of the graph, respectively. Then, we consider the orbit ansatz proposed in [41] where the generators are instead defined by summing operators according to the automorphism group of the graph. Finally, we also study the multi-angle [42, 43] (or free) ansatz, where one assigns a single parameter to each gate in the standard ansatz.

In the case of multi-angle QAOA ansatz, we give a complete characterization of the Lie algebra for any graph, finding that they fall within one of six families. In particular, in all graph families (except for the cycle and the path graphs) the dimension of the Lie algebra grows exponentially with the number of vertices in the graph. We then analyze the implications of these results, and show that multi-angle case is prone to exhibiting barren plateaus, even when using a single layer of the ansatz.

In the orbit and the standard cases, we argue that a full characterization of the Lie algebra across all graphs is likely quite challenging (with some notable exceptions as the path, cycle and complete graphs, for which we characterize the Lie algebra, see also [34, 36, 44]). To this end, we take a closer look at the symmetries of the Lie algebra [20], i.e., the set of operators that commute with the parametrized unitary. Firstly, we show how the symmetries of the graph get promoted to symmetries at the

quantum level, and find that while the standard and the orbit ansätze respect them, the multi-angle ansatz does not (and this is precisely why we can characterize it so well). Then, we show that the orbit and the standard ansätze exhibit additional symmetries beyond the "natural" symmetries arising from the parity-superselection operator $X^{\otimes n}$ and the automorphisms of the considered graph. These "hidden" symmetries make the Lie algebra highly graph dependent and harder to study. We can associate the natural symmetries to a "natural" Lie algebra that is semi-universal [32, 45] and its dimension provides an upper bound for the dimensions of the orbit and the standard Lie algebras. Moreover, the dimensions of the invariant subspaces associated to the "natural" symmetries are determined via explicit character formulas. Finally, we conjecture that for the vast majority of graphs that the dimensions of the largest invariant component for the natural Lie algebra and the standard Lie algebra only differ by a polynomial factor. If this is the case, then our work has important implications regarding the trainability and classical simulability of QAOA. In summary, we develop a symmetry framework and much needed tools to systematically analyze QAOA and general variational quantum algorithms.

We also point to related work [46–49] applicable to large-girth D-regular graphs which establishes concentration results for the loss function with respect to variations in the QAOA angles (see Sec. XI). These concentration results have been obtained in the context of smart initialization techniques [9, 50, 51] and follow as the optimal angles for the problem Hamiltonian are rescaled with $1/\sqrt{D}$ as D increases. In contrast, we aim at developing tools to analyze general connected graphs.

II. FRAMEWORK

From maxcut to QAOA

We recall the maxcut problem [52–55] and define notation that will be used throughout the manuscript. An undirected, unweighted, graph G (without loops) [56] is defined by its vertex set $V = \{1, \dots, n\}$ and its edge set E consisting of unordered pairs $\{w, \tilde{w}\}\$ of vertices $w, \tilde{w} \in V$ with $w \neq \tilde{w}$. Given a graph G, the (optimization variant of the) maxcut problem is to find a partition of its vertices into two complementary sets such that the number of edges between those sets is as large as possible [see Fig. 1(a)]. Mathematically, this is formalized by noting that a vertex subset $W \subset V$ determines a bipartition (or cut) of the vertices of a graph into the disjoint sets W and $V \setminus W$. A natural way of quantifying the cut value is by assigning to each vertex a value of 0 or 1, depending on the subset it belongs to. Therefore, we represent a cut through a bitstring $x \in \{0,1\}^n$ with cut value $\sum_{\{w,\tilde{w}\}\in E} |x_w - x_{\tilde{w}}|$. An optimal solution to the maxcut problem is identified by a maximum cut that observes the maximum cut value for the considered graph. Despite the seemingly simplicity of this task, finding the maximum cut value is known to be NP-hard [57, 58].

Due to the NP-hardness of maxcut, there has been significant interest in classical approximation algorithms [59–62], including randomized ones. Let $c \in (0,1]$ denote the expected approximation ratio of an algorithm guaranteeing that the (expected) cut value of the computed cut is lower bounded by c times the maximum cut value of the considered graph. Goemans and Williamson [63] devised a randomized classical algorithm based on semidefinite programming which guarantees that the expected approximation ratio is at least $c_{\rm GW} \approx 0.87856$. As shown in [64, 65], there are graphs for which the expected approximation ratio obtained via [63] saturates the lower bound c_{GW} . Moreover, approximating maxcut with an approximation ratio of $c \ge 16/17$ is NP-hard [66].

Quantum computers can also be used to find approximate solutions to the maxcut problem [1, 67, 68]. Obtaining the maximum cut value can be mapped to finding the ground state energy of the n-qubit Ising Hamiltonian

$$H_p := \sum_{\{w,\tilde{w}\}\in E} Z_w Z_{\tilde{w}},\tag{1}$$

where Z_k denotes the Pauli-z operator acting on the k-th qubit. One can therefore attempt to obtain the maxcut variationally by defining the cost function

$$C(\vec{\theta}) = \langle \psi(\vec{\theta}) | H_p | \psi(\vec{\theta}) \rangle,$$
 (2)

where $|\psi(\vec{\theta})\rangle$ is a quantum state parametrized by $\vec{\theta}$, and solving the optimization task $\arg\min_{\vec{\theta}} C(\vec{\theta})$. In QAOA, the state $|\psi(\vec{\theta})\rangle$ is obtained as follows [see Fig. 1(b)]:

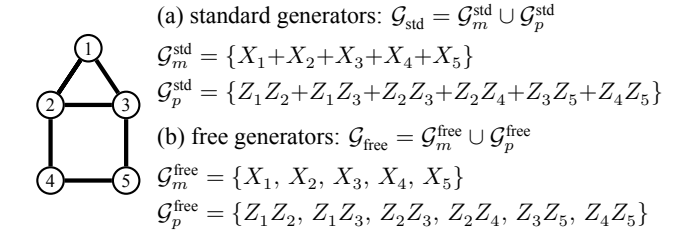


Figure 2. Example of house graph. Generators for the (a) standard and (b) the free ansatz.

First, one initializes n qubits to the fiduciary state

$$|+\rangle^{\otimes n} = \frac{1}{\sqrt{2^n}} \sum_{x \in \{0,1\}^n} |x\rangle, \qquad (3)$$

where $|x\rangle$ denotes the computational basis state in an n-qubit Hilbert space $\mathcal{H} := (\mathbb{C}^2)^{\otimes n}$. Henceforth, d := $\dim(\mathcal{H}) = 2^n$ denotes the dimension of \mathcal{H} . The initial state is sent through a parametrized quantum circuit with L layers of the form

$$U(\vec{\theta}) = \prod_{\ell=1}^{L} \left[\prod_{k=1}^{|\mathcal{G}_m|} e^{-i\theta_{m\ell k} H_{mk}} \right] \left[\prod_{k=1}^{|\mathcal{G}_p|} e^{-i\theta_{p\ell k} H_{pk}} \right]$$
(4)

for suitable sets \mathcal{G}_p and \mathcal{G}_m of hermitian generators $H_{pk} \in$ \mathcal{G}_p and $H_{mk} \in \mathcal{G}_m$. The real parameters $\theta_{p\ell k}$ and $\theta_{m\ell k}$ are collected in the vector $\vec{\theta}$. Then, $|\psi(\vec{\theta})\rangle = U(\vec{\theta})|+\rangle^{\otimes n}$ is measured in the computational basis, and the measurement outcomes are classically post-processed to estimate the cut value. This is the starting point for the hybrid quantum-classical optimization as illustrated in Fig. 1.

In the original QAOA manuscript [1], the standard generator sets are [see Fig. 2(a)]

$$\mathcal{G}_p^{\text{std}} := \{ H_p \} \text{ with } H_p = \sum_{\{w, \tilde{w}\} \in E} Z_w Z_{\tilde{w}},$$
 (5a)

$$\mathcal{G}_m^{\text{std}} := \{ H_m \} \text{ with } H_m := \sum_{v \in V} X_v.$$
 (5b)

As we can see, in the standard ansatz, only two parameters are used per layer. One of the drawbacks of this approach is that it hinders the circuit's expressiveness and one usually requires a large number L of layers to achieve a good approximation ratio. We detail two ansätze with more parameters per layer. To mitigate this issue, and pack more parameters per later (thus making QAOA better suited for near-term quantum computers) several modifications to the QAOA generators have been proposed. First, we consider the the multiangle [42, 43, 69, 70], or free ansatz, the sets of generators of which are [see Fig. 2(b)]

$$\mathcal{G}_{p}^{\text{free}} := \{ Z_{w} Z_{\tilde{w}} \text{ for } \{ w, \tilde{w} \} \in E \},$$

$$\mathcal{G}_{m}^{\text{free}} := \{ X_{v} \text{ for } v \in V \}.$$
(6a)

$$\mathcal{G}_m^{\text{free}} := \{ X_v \text{ for } v \in V \}. \tag{6b}$$

This approach assigns one parameter per layer for each edge and vertex. Occasionally, a variant of the free ansatz with $\tilde{\mathcal{G}}_p^{\text{free}} := \mathcal{G}_p^{\text{std}} = \{H_p\}$ is experimentally more suitable. Then, in the orbit ansatz of [41] not all parameters are independent, but rather they are correlated following orbits of the automorphism group of a graph. The orbit ansatz is then a middle ground between the standard and the free one in terms of the number of generators and we analyze the orbit ansatz in Sec. VII as an upper bound to the standard ansatz.

Given the above freedom in choosing an ansatz for the QAOA, a natural question that arises is: Which one should we choose? Clearly, having more trainable parameters at the same depth is an appealing idea. However, increasing the expressiveness of an ansatz (for instance by adding experimentally more independent parameters) can also lead to barren plateaus and trainability issues [9, 21, 71]. In the following subsection, we explore symmetry methods for analyzing the free, standard, orbit ansätze and their expressiveness through the lens of Lie algebras.

B. Lie algebras and symmetries

For ease of notation, let us focus here on a general variational quantum algorithms with L layers described by a unitary

$$U(\vec{\theta}) = \prod_{\ell=1}^{L} \prod_{k=1}^{|\mathcal{G}|} e^{-i\theta_{\ell k} H_k} . \tag{7}$$

Here, \mathcal{G} is the set of hermitian generators $H_k \in \mathcal{G}$, and $\theta_{\ell k}$ the trainable real parameters that we collect in the vector $\vec{\theta} \in \mathbb{R}^{L \times |\mathcal{G}|}$. Note that this case recovers as a special case the unitary in Eq. (4) with $\mathcal{G} = \mathcal{G}_p \cup \mathcal{G}_m$. In what follows we now outline different symmetry methods that can be used to analyze variational quantum algorithms. In particular, we illustrate these techniques in Table I for a low-dimensional computational example. Further details are deferred to Appendix A 1.

As a first analysis tool, the (real) Lie algebra $\mathfrak{g} = \langle i\mathcal{G} \rangle_{\mathrm{Lie}}$ is the Lie closure of its generators $iH_k \in i\mathcal{G}$, i.e., it contains all real-linear combinations of repeated commutators of $iH_1, \ldots, iH_{|\mathcal{G}|}$ [72–74]. Recall that the commutator of $A, B \in \mathbb{C}^{d \times d}$ is given by [A, B] := AB - BA. Thus $\mathfrak{g} \subseteq \mathfrak{u}(d) \subseteq \mathbb{C}^{d \times d}$ is a subalgebra of the unitary Lie algebra $\mathfrak{u}(d)$ of skew-hermitian matrices. In our context, the Lie algebra is sometimes denoted as the dynamical Lie algebra [75] in order to emphasize its relation to the unitary time evolution. The corresponding Lie group $\exp(\mathfrak{g}) \subseteq \mathbb{U}(d)$ is then contained in the unitary group $\mathbb{U}(d)$. The Lie algebra \mathfrak{g} plays a key role as it determines reachability properties [20, 21, 75, 76], e.g., it characterizes the set of quantum states $\exp(\mathfrak{g}) |\psi\rangle$ that are accessible from a given initial state $|\psi\rangle$, when evolved by a unitary as in Eq. (7).

Table I. Symmetry analysis for the house graph. Based on the given generators, the commutant $\mathcal C$ and its center $\mathcal Z(\mathcal C)$ determine the invariant subspaces, but, in general, *not* the generated Lie algebra $\mathfrak g$ (refer to Sec. II B and Appendix A 1). For the standard ansatz, the center $\mathcal Z(\mathfrak g)$ of $\mathfrak g$ has support on all invariant subspaces (refer also to Sec. VII).

Ansatz	Dimension						
Free							
Commutant C	2						
Center $\mathcal{Z}(\mathcal{C})$	2						
Center $\mathcal{Z}(\mathfrak{g})$	0						
Lie algebra g	510	$\mathfrak{su}(16)$	\oplus	$\mathfrak{su}(16)$			
Invariant subs	spaces	\mathbb{C}^{16}	\oplus	\mathbb{C}^{16}			
Standard		$\overline{}$	$\overline{}$				
Invariant subs	spaces	$\mathbb{C}^{10} \oplus \mathbb{C}^5 \oplus \mathbb{C}$	1 ⊕	$\mathbb{C}^{10} \oplus \mathbb{C}^5 \oplus \mathbb{C}^1$			
Lie algebra g	248	$\mathfrak{su}(10) \oplus \mathfrak{su}(5) \oplus \mathfrak{u}($	1) ⊕	$\mathfrak{su}(10) \oplus \mathfrak{su}(5) \oplus \mathfrak{u}(1)$			
Center $\mathcal{Z}(\mathfrak{g})$	2	support on all invariant subspaces					
Center $\mathcal{Z}(\mathcal{C})$	6						
Commutant C	6						

As a second analysis tool, the linear symmetries of the generators \mathcal{G} are given by the *commutant*

$$\mathcal{C} = \mathsf{com}(\mathcal{G}) = \{ S \in \mathbb{C}^{d \times d} \text{ s.t. } [S, H_k] = 0 \text{ for all } H_k \in \mathcal{G} \}.$$
(8)

Note that the commutant $\mathfrak{com}(\mathfrak{g}) = \mathfrak{com}(i\mathcal{G}) = \mathfrak{com}(\mathcal{G})$ of the Lie algebra \mathfrak{g} is equal to the commutant of its generators $i\mathcal{G}$. Also, \mathcal{C} is closed under complex-linear combinations and matrix multiplication, thus constituting an associative subalgebra (under matrix multiplication) of $\mathbb{C}^{d\times d}$. The commutant \mathcal{C} and its center

$$\mathcal{Z}(\mathcal{C}) = \{ Z \in \mathcal{C} \text{ s.t. } [Z, S] = 0 \text{ for all } S \in \mathcal{C} \}$$
 (9)

determine the invariant subspaces of $\mathcal{H} = \mathbb{C}^d$ under the action of \mathcal{G} , i.e., $\mathcal{I} \subseteq \mathcal{H}$ is an invariant subspace if $H_k v \in \mathcal{I}$ for all $v \in \mathcal{I}$ and $H_k \in \mathcal{G}$. And, the invariant subspaces induced by the action of \mathcal{G} , \mathfrak{g} , and $\exp(\mathfrak{g})$ all agree. Elements of the commutant correspond to conserved quantities, since $\langle \psi | e^{itH_j} S e^{-itH_j} | \psi \rangle = \langle \psi | S | \psi \rangle$, meaning that the expectation of S is constant under the time evolution by any of the generators H_j .

An invariant subspace $\mathcal{J} \neq 0$ is *irreducible* if it contains no invariant subspaces distinct from 0 and \mathcal{J} itself. The dimension $\dim[\mathcal{Z}(\mathcal{C})]$ of the center $\mathcal{Z}(\mathcal{C})$ specifies how many inequivalent irreducible subspaces occur (see Appendix A 1). The invariant subspaces are revealed by a basis change so that the block decomposition

$$\mathcal{C} \simeq \bigoplus_{\lambda=1}^{\dim[\mathcal{Z}(\mathcal{C})]} \mathbb{C}^{m_{\lambda} \times m_{\lambda}} \otimes \mathbb{1}_{d_{\lambda}} \text{ and } \mathfrak{g} \simeq \bigoplus_{\lambda=1}^{\dim[\mathcal{Z}(\mathcal{C})]} \mathbb{1}_{m_{\lambda}} \otimes \mathfrak{g}_{\lambda}, (10)$$

holds for certain Lie algebras $\mathfrak{g}_{\lambda} \subseteq \mathfrak{u}(d_{\lambda}) \subseteq \mathbb{C}^{d_{\lambda} \times d_{\lambda}}$ with $\dim[\mathfrak{com}(\mathfrak{g}_{\lambda})] = 1$. The commutant \mathcal{C} fixes the dimensions $d_{\lambda} \geqslant 1$ and multiplicities $m_{\lambda} \geqslant 1$, but does *not* uniquely determine the Lie algebra \mathfrak{g} (or the \mathfrak{g}_{λ}). For

completeness, the corresponding decomposition

$$\mathcal{H} \simeq igoplus_{\lambda=1}^{\dim[\mathcal{Z}(\mathcal{C})]} \mathbb{C}^{m_{\lambda}} \otimes \mathcal{H}_{\lambda} \,,$$

of the state space under the action of \mathfrak{g} and $\exp(\mathfrak{g})$ identifies the subspaces $\mathcal{H}_{\lambda} = \mathbb{C}^{d_{\lambda}}$ as invariant and irreducible.

As a third analysis tool, the Lie algebra $\mathfrak{g} \subseteq \mathfrak{u}(d)$ observes its *reductive* decomposition [77, 78]

$$\mathfrak{g} \cong \mathcal{Z}(\mathfrak{g}) \oplus [\oplus_i \mathfrak{s}_i] \cong [\mathfrak{com}(\mathfrak{g}) \cap \mathfrak{g}] \oplus [\oplus_i \mathfrak{s}_i] \tag{11}$$

which includes its center $\mathcal{Z}(\mathfrak{g})$ and its semisimple part $\oplus_{j}\mathfrak{s}_{j}$ consisting of a direct sum of simple Lie algebras \mathfrak{s}_{j} . The center $\mathcal{Z}(\mathfrak{g})$ can be readily obtained from the commutant $\mathcal{C} = \mathfrak{com}(\mathfrak{g})$ and the generators \mathcal{G} . But identifying the simple Lie algebras \mathfrak{s}_{j} (such as $\mathfrak{su}(r)$, $\mathfrak{so}(r)$, and $\mathfrak{sp}(r)$ for suitable $r \geq 2$ [72]) is usually more challenging, both for computations [20, 74, 79, 80] and analytic approaches. The reductive decomposition of Eq. (11) can be either interpreted as an intrinsic vector-space decomposition of \mathfrak{g} with $[\mathfrak{s}_{j_1},\mathfrak{s}_{j_2}] = 0$ or as being extrinsically embedded into $\mathfrak{g} \subseteq \mathfrak{u}(d) \subseteq \mathbb{C}^{d \times d}$.

This embedding can be specified by an explicit representation which constitutes our fourth analysis tool. A representation γ of \mathfrak{g} is a linear map from \mathfrak{g} to $\mathfrak{u}(m) \subseteq \mathbb{C}^{m \times m}$ with $m \geqslant 1$ such that $\gamma([g_1, g_2]) = [\gamma(g_1), \gamma(g_2)]$ for $g_1, g_2 \in \mathfrak{g}$ [72]. Notable examples are the standard representation κ with $\kappa(g) = g$ for $g \in \mathfrak{g} \subseteq \mathfrak{u}(d)$, the trivial representation ϵ with $\epsilon(g) = 0 \in \mathbb{C}$, and the dual $\overline{\gamma}$ of γ with $\overline{\gamma}(g) = -[\gamma(g)]^t$. Identifying a representation precisely characterizes the occurring symmetries but this is usually more difficult to achieve.

Table I highlights significant differences between the free and standard ansatz for the example of the house graph. For the free ansatz, the commutant and its center are both two dimensional which results into two inequivalent irreducible subspaces. The commutant and center for the standard ansatz are, however, both six dimensional and one obtains six inequivalent irreducible subspaces which refine the ones for the free ansatz. We will further explore the free ansatz in Sec. III, while Sections V-VI start the discussion of the standard ansatz.

III. THE MULTI-ANGLE OR FREE ANSATZ

We now apply the framework established in Sec. II to the free ansatz of QAOA which is based on the problem and mixer Hamiltonians in $\mathcal{G}_p^{\text{free}}$ and $\mathcal{G}_m^{\text{free}}$ from Eq. (6). These generators define the *free-mixer Lie algebra*

$$\mathfrak{g}_{\mathrm{free}} := \langle i\mathcal{G}_{\mathrm{free}} \rangle_{\mathrm{Lie}} \subseteq \mathbb{C}^{2^n \times 2^n} \text{ where } \mathcal{G}_{\mathrm{free}} := \mathcal{G}_p^{\mathrm{free}} \cup \mathcal{G}_m^{\mathrm{free}}.$$

As a first observation, all generators $H_j \in \mathcal{G}_{\text{free}}$ commute with $X^{\otimes n}$ (and trivially with $\mathbb{1}_{2^n}$). Here, $X^{\otimes n}$ acts as bit-flip (or \mathbb{Z}_2) symmetry, i.e., $X^{\otimes n}|x\rangle = |\neg x\rangle$ where \neg is the bitwise NOT operation. Alternatively, $X^{\otimes n}$ can be interpreted as a parity superselection operator. The

Table II. Free ansatz. Six families of connected graphs with $n \ge 2$ vertices are identified by their generated Lie algebras.

Graph	Example	Bipartite	Lie algebra g _{fre} dimension	$\mathfrak{g} \subseteq \mathfrak{su}(2^n) \subseteq \mathbb{C}^{2^n \times 2^n}$ reductive decomposition
Path	0000	yes	$2n^2-n$	$\mathfrak{so}(2n)$
Cycle		$\begin{array}{c} \text{if } n \\ \text{is even} \end{array}$	$4n^2-2n$	$\mathfrak{so}(2n) \oplus \mathfrak{so}(2n)$
Even- even		yes	$2^{2n-2}-2^{n-1}$	$\mathfrak{so}(2^{n-1}) \oplus \mathfrak{so}(2^{n-1})$
Odd- odd		yes	$2^{2n-2}+2^{n-1}$	$\mathfrak{sp}(2^{n-1}) \oplus \mathfrak{sp}(2^{n-1})$
Even- odd	%	yes	$2^{2n-2}-1$	$\mathfrak{su}(2^{n-1})$
Archetypal		no	$2^{2n-1}-2$	$\mathfrak{su}(2^{n-1}) {\oplus} \mathfrak{su}(2^{n-1})$

states $|x\rangle$ and $|\neg x\rangle$ then have the same expectation value relative to H_p . We show in Lemma 15(a) of Appendix B 1 that the commutant

$$C_{\text{free}} := \text{com}(G_{\text{free}}) = \text{span}_{\mathbb{C}}\{I^{\otimes n}, X^{\otimes n}\}$$
 (12)

of all matrices simultaneously commuting with all $H_j \in \mathcal{G}_{\text{free}}$ consists solely of complex-linear combinations of $I^{\otimes n}$ and $X^{\otimes n}$. Clearly, $X^{\otimes n}$ has two distinct eigenvalues +1 and -1 which both have multiplicity $d/2=2^{n-1}$ and it is equivalent to

$$X^{\otimes n} \simeq Z_1 = \mathbb{1}_{d/2} \oplus (-\mathbb{1}_{d/2})$$

by switching to an eigenbasis. Thus the \mathbb{Z}_2 symmetry enforces a two-fold splitting of the Hilbert space into equally-sized invariant subspaces and no further splitting is possible as the commutant $\mathcal{C}_{\text{free}}$ is two dimensional for the free ansatz. This symmetry analysis is true for any connected graph and, more generally, we completely determine all possible free-mixer Lie algebras for any graph:

Theorem 1 (Free-mixer Lie algebras). Given the generators $\mathcal{G}_{\text{free}}$ of the free QAOA ansatz for any connected graph, the generated Lie algebras $\mathfrak{g}_{\text{free}}$ fall into one of the six families depicted in Table II.

Theorem 1 identifies only six families of connected graphs with different Lie algebras and free-mixer generators: path graphs; cycle graphs; bipartite graphs of even-even, odd-odd, and even-odd type (not equal to a path or a cycle graph); and finally any other graph:

Definition 1 (Archetypal graph). An archetypal graph is connected but neither bipartite nor a cycle graph.

The classification of Theorem 1 includes one generic class given by the archetypal graphs from the last row of Table II. Thus the Lie algebra for archetypal graphs is given by its particularly simple and semiuniversal reductive decomposition $\mathfrak{su}(2^{n-1}) \oplus \mathfrak{su}(2^{n-1})$, while a more diverse set of Lie algebras is obtained for bipartite and cycle

Table III. Pauli-string bases associated to Table III. For Pauli strings consisting of $A \in \{X, Y, Z, I\}$, let #A denote the number of A in a Pauli string. Also, $\#A|_{V_1}$ indicates the number of A in V_1 for a vertex bipartition $V = V_1 \uplus V_2$ with $|V| = n \ge 2$. Refer also to Table V and Appendix B.

Connected graph	Pauli-string basis for g _{free}	Dimension of \mathfrak{g}_{free}			
Path	$I \cdot IXI \cdot I$ $I \cdot I \left\{ {{_Z^Y}} \right\} X \cdot X \left\{ {{_Z^Y}} \right\} I \cdot I$	$2n^2-n$			
Cycle	$\begin{split} & \text{I} \cdot \text{I} \text{XI} \cdot \text{I}, \ X \cdot \text{X} \text{IX} \cdot \text{X} \\ & \text{I} \cdot \text{I} \left\{ \frac{Y}{Z} \right\} \text{X} \cdot \text{X} \left\{ \frac{Y}{Z} \right\} \text{I} \cdot \text{I} \\ & \text{X} \cdot \text{X} \left\{ \frac{Y}{Z} \right\} \text{I} \cdot \text{I} \left\{ \frac{Y}{Z} \right\} \text{X} \cdot \text{X} \end{split}$	$4n^2-2n$			
$\begin{aligned} & \textbf{Bipartite} \\ & \neq \text{cycle or path} \\ & \text{with } V = V_1 \uplus V_2 \end{aligned}$	$\# Y + \# Z$ is even and $\# I \neq n \text{ and } \# X \neq n \text{ and}$ $\# X + \# Y _{V_1} + \# Z _{V_1} \text{ is odd}$	$2^{2n-2}-2^{n-1}$ (even-even) $2^{2n-2}-1$ (even-odd) $2^{2n-2}+2^{n-1}$ (odd-odd)			
Archetypal	$\#\mathbf{Y} + \#\mathbf{Z}$ is even and $\#\mathbf{I} \neq n$ and $\#\mathbf{X} \neq n$	$2^{2n-1}-2$			

graphs. But a path or cycle graph has trivial solutions to the maxcut problem, while a polynomial algorithm exist for bipartite and planar graphs [81]. Archetypal graphs cover all hard instances for the maxcut problem as well as easy instances such as planar graphs (as for the house graph in the last row of Table II). Thus only archetypal graphs (or suitable subsets thereof) matter in practice.

The statement of Theorem 1 is striking in light of the large number of non-isomorphic connected graphs: one obtains twenty-two graphs for five vertices, but already more than eleven million for ten vertices. Their number grows at least exponentially with the number of vertices. But one can intuitively understand that the possible classes of Lie algebras collapse to the few cases in Theorem 1 as the generators from the free ansatz break almost all symmetries arising from a specific graph.

Inspecting the families of Lie algebras in Table II, the cases of $\mathfrak{so}(2^{n-1}) \oplus \mathfrak{so}(2^{n-1})$, $\mathfrak{sp}(2^{n-1}) \oplus \mathfrak{sp}(2^{n-1})$, and $\mathfrak{su}(2^{n-1}) \oplus \mathfrak{su}(2^{n-1})$ nicely respect the block structure induced by the eigenspaces of $X^{\otimes n}$. The case of $\mathfrak{su}(2^{n-1})$ for the even-odd bipartite case is more intriguing, but $\mathfrak{su}(2^{n-1})$ is represented in a suitable block-diagonal basis as $M \oplus (-M^t)$ for complex $2^{n-1} \times 2^{n-1}$ matrices M (see Appendix B 7). For path graphs, $\mathfrak{so}(2n)$ is represented using a direct sum $\eta_+ \oplus \eta_-$ of spinor representations η_\pm of degree 2^{n-1} as detailed in Appendix B 4. The spinor representation η_+ is also utilized to map the simple parts of $\mathfrak{so}(2n) \oplus \mathfrak{so}(2n)$ to their respective blocks.

Table III highlights explicit Pauli-string bases for the associated free-mixer Lie algebra of each family of connected graphs from Table II, while Appendix B and Table V provide more details. For archetypal graphs, all Pauli strings appear that have an even parity #Y + #Z and differ from I··I and X··X (see Table III). The extensive proofs leading to the results in this section are detailed in Appendices B and C. Appendix B employs Liealgebraic proof techniques, while Appendix C emphasizes graph properties.

IV. IMPLICATIONS FOR THE FREE ANSATZ

We collect relevant consequences of Thm. 1. First, we clarify that the free ansatz of QAOA can—in principle—reach at least one maximum cut (i.e., an optimal solution for maxcut) using a finite number of layers for archetypal graphs from Def. 1 (see Cor. 1 below), thus constituting a strict improvement over previous known convergence results, namely reachability in the infinite-layer limit [82]. The argument relies on three ingredients: (1) the initial state and the target maxcut state belong to the same invariant subspace, (2) $\exp(\mathfrak{g}_{\text{free}})$ acts transitively on this invariant subspace, and (3) each unitary $U \in \exp(\mathfrak{g}_{\text{free}})$ can be generated in a finite number of layers.

For the second ingredient, the free-mixer Lie algebra $\mathfrak{g}_{\text{free}} = \mathfrak{su}(2^{n-1}) \oplus \mathfrak{su}(2^{n-1})$ for archetypal graphs (see Theorem 1) acts transitively on both invariant subspaces \mathcal{H}_+ and \mathcal{H}_- of $X^{\otimes n}$ (see App. B1) which constitute the +1 and -1 eigenspaces of $X^{\otimes n}$ and are spanned by all Hadamard basis states $|b_1\rangle \cdots |b_n\rangle$ with $b_j \in \{+, -\}$ for respectively an even or an odd number of minus signs (i.e. $b_i = -$). For the first ingredient, \mathcal{H}_+ contains both the initial state $|+\rangle^{\otimes n}$ and at least one ground state of H_p as we detail now: Consider a maximum cut $x \in \{0,1\}^n$ (see Sec. IIA) and let $\neg x$ denote its bitwise negation, which is also a maximum cut. Thus the state $|x_{+}\rangle =$ $(|x\rangle + |\neg x\rangle)/\sqrt{2}$ is a ground state of H_p and also belongs to \mathcal{H}_+ as $X^{\otimes n}(|x\rangle + |\neg x\rangle)/\sqrt{2} = (|x\rangle + |\neg x\rangle)/\sqrt{2}$. Finally, our third ingredient relies on general arguments which establish that reachable unitaries can be obtained in a finite number of products [83–85]:

Lemma 1. We consider the standard ansatz with the generators $\{H_p, H_m\}$ and the free ansatz with the generators $\mathcal{G}_{\text{free}} = \mathcal{G}_p^{\text{free}} \cup \mathcal{G}_m^{\text{free}}$. In both cases, if a target quantum state is reachable from a given initial state, then it can be also obtained in a finite number of layers.

Proof. Based on the assumed reachability, the target state can be obtained for the standard ansatz using products of the form $\prod_{\ell=1}^L e^{-i\theta_{\ell m} H_m} e^{-i\theta_{\ell p} H_p}$ or $\prod_{\ell=1}^L e^{-i\theta_{\ell p} H_p} e^{-i\theta_{\ell m} H_m}$ with angles $\theta_{\ell m}$, $\theta_{\ell p}$ which can be zero. General results in control theory on the so-called order of generation [83–85] imply a finite upper bound on the length of products required to reach all possible unitaries in $\exp(\mathfrak{g}_{\text{free}})$. Clearly, we can restrict ourselves to the first form of the product by enlarging L by one. This establishes the result for the standard ansatz.

For the free ansatz, we need to consider arbitrary products of the form $\prod_{j=1}^r e^{-i\theta_j H_j}$ with angles θ_j and generators $H_j \in \mathcal{G}_{\text{free}}$, where the length r of the products is again bounded by a finite integer \tilde{L} . Clearly, we can rewrite all these products in the form of Eq. (4) with $L = \tilde{L} + 1$, suitable angles $\theta_{m\ell k}$ and $\theta_{p\ell k}$ which are possibly zero, as well as $H_{mk} \in \mathcal{G}_m = \mathcal{G}_m^{\text{free}}$ and $H_{pk} \in \mathcal{G}_p = \mathcal{G}_p^{\text{free}}$. This completes the proof.

The length of the products required to obtain all reachable unitaries has to be greater or equal to the dimen-

sion of the generated Lie algebra [25, 83, 84, 86], but we lack general upper bounds as they depend on the particular generators. These arguments neglect that the target ground state could possibly be reached with a much smaller depth. By combining our three ingredients for the free-mixer ansatz, we can at least rule out an infinite depth as compared to the usual convergence argument for QAOA [1, 82], while not contradicting results on reachability deficits for QAOA [87] which apply to a fixed number of layers. Initial results beyond the free ansatz are discussed at the end of Sec. VI.

Corollary 1. The free QAOA ansatz can reach a maxcut state with a finite number of layers for any archetypal graph from Def. 1

In this context, one might wonder how effective QAOA will be for the free ansatz. Unfortunately, the following results argue that barren plateaus dominate such optimization landscapes. Recall that the QAOA cost function $C(\vec{\theta}) = \langle \psi(\vec{\theta}) | H_p | \psi(\vec{\theta}) \rangle$ from Eq. (2) utilizes the unitaries $U(\vec{\theta})$ in the circuit from Eq. (7) and $U(\vec{\theta})$ depends on the parameters $\vec{\theta}$ with real entries θ_{ϑ} . For simplicity, the entries θ_{ϑ} of $\vec{\theta}$ are now indexed by the numbers ϑ . Let $\partial_{\vartheta}C(\vec{\theta})$ denote the partial derivative of $C(\vec{\theta})$ with respect to the ϑ -th parameter θ_{ϑ} in $\vec{\theta}$. Sampling the parameters $\vec{\theta}$ according to a given distribution $d\vec{\theta}$ over a chosen parameter domain δ_L induces a distribution on the associated unitaries $U(\vec{\theta})$ of an L-layered circuit [71]. We define the second-order moment operators

$$\begin{split} M_{e^{\mathfrak{g}}} &:= \int_{U \in e^{\mathfrak{g}}} d\mu_{e^{\mathfrak{g}}}(U) \; U^{\otimes 2} \otimes \bar{U}^{\otimes 2} \; \text{ and } \\ M_{L} &:= \int_{\vec{\theta} \in \delta_{L}} d\vec{\theta} \; [U(\vec{\theta})]^{\otimes 2} \otimes [\bar{U}(\vec{\theta})]^{\otimes 2}. \end{split}$$

Then, $\mathcal{A}_L := M_L - M_{e^{\mathfrak{g}}}$ is a positive semi-definite operator that quantifies how much the second moments arising from $U(\vec{\theta})$ differ from those of the Haar measure over $e^{\mathfrak{g}}$. We say that a distribution $d\vec{\theta}$ results in an ε -approximate unitary 2-design for the unitaries $U(\vec{\theta}) \subseteq e^{\mathfrak{g}}$ if

$$\|\mathcal{A}\|_{\infty} = \|M_L - M_{e^{\mathfrak{g}}}\|_{\infty} \leqslant \varepsilon.$$

Here, $\left\| \cdot \right\|_{\infty}$ denotes the Schatten ∞ -norm (or operator norm) which is given by the largest singular value of its argument. We refer to [88–99] (and references therein) for many similar definitions and notions related to approximate unitary 2-designs. We now obtain:

Corollary 2. For the free ansatz, consider any archetypal graph from Def. 1 with n>3 vertices and |E| edges. Recall the QAOA cost function $C(\vec{\theta})$ from Eq. (2) and its partial derivative $\partial_{\vartheta}C(\vec{\theta})$ with respect to the ϑ -th parameter θ_{ϑ} in $\vec{\theta}$. Assume that the multi-angle QAOA circuit has enough layers such that the distribution of unitaries is an ε -approximate unitary 2-design. Then, the expectation value of the partial derivatives is $E_{\vec{\theta}}[\partial_{\vartheta}C(\vec{\theta})]=0$

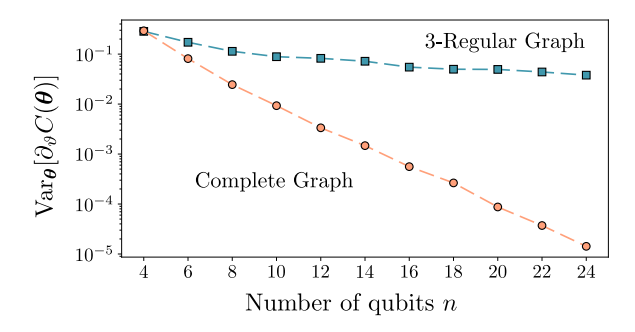


Figure 3. Gradient concentration for a single layer of the multi-angle QAOA applied to certain regular graphs. For each number of vertices |V|=n, we pick a random 3-regular or a complete graph. The variance of the gradients is obtained by sampling 100 parameter values. The cost function $C(\vec{\theta})$ has been renormalized so that its values lie in [-1,1]. Refer also to the discussion in Sec. XI.

and their variance is given by (with $d = 2^n$)

$$\operatorname{Var}_{\vec{\theta}}[\partial_{\vartheta}C(\vec{\theta})] = 4d^2|E|/[(d^2-4)(d+2)] \leq 4n^2/2^n.$$

The proof of Corollary 2 is given in Appendix D, it shows that, if the circuit is deep enough so that its unitaries form an approximate unitary 2-design over $e^{\mathfrak{g}}$, then the partial derivatives of the cost function will, in average, vanish exponentially with the system size. Thus the cost function will exhibit barren plateaus. This result can be further understood by recalling that the Lie algebra is a measure of expressiveness for the parametrized unitaries [21] and that highly expressive ansätze are known to exhibit barren plateaus [71]. Indeed, for any archetypal graph from Def. 1, the Lie algebra is exponentially large, which implies exponentially small gradients [22].

As previously mentioned, Corollary 2 holds for a multiangle QAOA circuit when the generated unitaries form an ε -approximate unitary 2-design. This is fulfilled when the number of layers L is bounded from below as [22]

$$L \geqslant \frac{\log(1/\varepsilon)}{\log(1/\|\mathcal{A}_L\|_{\infty})}.$$
 (13)

Clearly, the exact value of L will depend on the specific graph considered, as well as on the parameter distribution and the chosen parameter domain. Still, empirical evidence suggests in meaningful scenarios (as for Pauli generators and parameters θ_{ϑ} that are independently and uniformly sampled from $[-2\pi, 2\pi]$) that the circuit unitaries become an ε -approximate unitary 2-design if $L \in \Omega(\text{poly}(n))$ [21]. However, a general analytical characterization of $\|\mathcal{A}_L\|_{\infty}$ is still lacking and beyond the scope of this work. We refer the reader to [93, 100–102] for inspiration on how to tackle these and related questions.

While our results hint at the fact that the multi-angle QAOA will not be trainable for deep circuits, they—in

principle—do not preclude the possibility of good approximation ratios being reachable for very shallow circuits with, e.g., $L \in \mathcal{O}(\log(n))$. Thus, one may wonder if shallow multi-angle QAOA are trainable, i.e., if they will be barren plateau-free. However, we can find graphs for which the free ansatz exhibits exponentially vanishing gradients already for a single layer. Usually, one does not expect single layered or shallow circuits to have trainability issues when they are either composed of few local entangling gates or have a small number of parameters [11, 103]. However, a single layer of the free ansatz can simultaneously be highly entangling and contain up to a polynomial number of parameters in n. For instance, consider the case of an D-regular graph. For constant D, each layer of the circuit will not be highly entangling, and thus one can expect sufficiently large gradients. However, if D scales with n, then a single layer can be sufficiently expressive to observe barren plateaus. This intuition is exemplified in Fig. 3 where we compare the gradient scaling for random 3-regular and complete graphs. Therein the gradients for 3-regular graphs are quite large, while $\operatorname{Var}_{\vec{\theta}}[\partial_{\vartheta}C(\vec{\theta})]$ decays exponentially with n for complete graphs as highlighted by the straight line in the log-linear plot of Fig. 3. A similar behavior of enlargement of barren plateaus with increasing D even for a single layer was also observed in [104, Fig. 9 of App. C] for the standard ansatz.

In summary, freeing the QAOA generators and assigning a single parameter to each gate can certainly help to reduce the circuit depth, but such an uncontrolled increase in expressiveness may be undesirable. As illustrated, for example, by Corollary 2 and Fig. 3, this might lead to severe trainability issues. Although more expressible ansätze are generally expected to allow for reduced circuit depths (as in the case of hardware efficient ansätze [105]), oftentimes such additional expressiveness needs to be well-directed. Following the ideas in geometric deep learning [106], it is usually possible to restrict the expressiveness without sacrificing performance by building ansätze that actively exploit the symmetries in the problem. Unfortunately, the free ansatz breaks one of the essential symmetries of the maxcut QAOA given by the automorphism group of the considered graph.

V. SYMMETRIES OF THE STANDARD ANSATZ

In Sec. III, we have completely characterized the possible Lie algebras and their symmetries for the free ansatz for any possible graph. We would ideally aim at a similar general result for the standard ansatz. We now explore the standard ansatz and show how even characterizing the corresponding linear symmetries as given by the commutant becomes a much more intricate task.

Recall that the standard generators $\mathcal{G}_{\text{std}} = \{H_p, H_m\}$ from Eq. (5) generate the Lie algebra $\mathfrak{g}_{\text{std}} := \langle i\mathcal{G}_{\text{std}} \rangle_{\text{Lie}}$. Clearly, the free-mixer Lie algebra $\mathfrak{g}_{\text{free}} \supseteq \mathfrak{g}_{\text{std}}$ con-

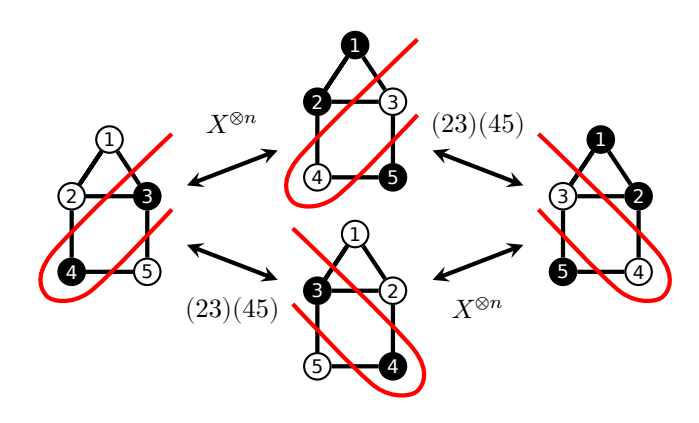


Figure 4. Symmetries in the standard-ansatz QAOA. The free-mixer symmetries $I^{\otimes n}$ and $X^{\otimes n}$ are complemented by symmetries arising from graph automorphism such as the permutation (23)(45) for the house graph. These symmetries naturally act on quantum states (see text).

tains the Lie algebra $\mathfrak{g}_{\mathrm{std}}$ for the standard ansatz. Conversely, the corresponding symmetries observe the inclusion $\mathrm{span}_{\mathbb{C}}\{I^{\otimes n},X^{\otimes n}\}=\mathcal{C}_{\mathrm{free}}\subseteq\mathcal{C}_{\mathrm{std}}$ of commutants. Here, $X^{\otimes n}$ induces a \mathbb{Z}_2 symmetry given by the bit-wise negation $X^{\otimes n}|x\rangle=|\neg x\rangle$. The matrix group generated by the matrices $I^{\otimes n}$ and $X^{\otimes n}$ is given by

$$\mathbb{Z}_2 := \langle I^{\otimes n}, X^{\otimes n} \rangle_{\text{group}}. \tag{14}$$

Then, $|x\rangle$ and $X^{\otimes n}|x\rangle = |\neg x\rangle$ have the same expectation value with respect to H_p and these states clearly correspond to the same cut value. This is visualized in Fig. 4 for the maximum cut vectors [see Fig. 5(e)] for the example of the house graph.

One additional class of symmetries arises from the automorphism group $\operatorname{Aut}(G) \subseteq \mathcal{S}_n$ [56] of the underlying graph G. Here, $\operatorname{Aut}(G)$ is the subgroup of vertex permutations from the symmetric group \mathcal{S}_n [107] that map the edge set E of G to itself, i.e.,

$$\operatorname{Aut}(G) = \{ \sigma \in \mathcal{S}_n \mid \{ \sigma(k), \sigma(\ell) \} \in E \text{ iff } \{k, \ell\} \in E \}.$$

The action $\sigma \cdot |x\rangle := |x_{\sigma^{-1}(1)}, \dots, x_{\sigma^{-1}(n)}\rangle$ is naturally extended to any $\sigma \in \mathcal{S}_n$ via the representation map $\zeta(\sigma) \in \mathbb{C}^{d \times d}$ (with $d = 2^n$). For example, the transposition $(1, 2) \in \mathcal{S}_2$ operating on two qubits is given by

$$\zeta[(1,2)] = \text{SWAP} = \begin{pmatrix} 1 & 0 & 0 & 0 \\ 0 & 0 & 1 & 0 \\ 0 & 1 & 0 & 0 \\ 0 & 0 & 0 & 1 \end{pmatrix}.$$

The general form of ζ is uniquely defined for any number n of qubits as any element of the symmetric group \mathcal{S}_n can be written as a product of transpositions (j, j+1) with $j \in \{1, \ldots, n-1\}$ [107]. Henceforth, 1 denotes the identity permutation.

One verifies that $|x\rangle$ and $\sigma \cdot |x\rangle$ have the same cut value for any $\sigma \in \operatorname{Aut}(G)$ as one can check that $(\langle x|\zeta(\sigma)^{\dagger})H_p(\zeta(\sigma)|x\rangle) = \langle x|H_p|x\rangle$. Figure 4 shows the house graph, where the maximum cut vectors from Fig. 5(e) are permuted by the automorphism (2,3)(4,5).

As $X^{\otimes n}$ commutes with $\zeta(\sigma)$ for any permutation $\sigma \in \mathcal{S}_n$, the group of natural symmetries of the standard ansatz of QAOA is defined as the direct product

$$\mathbb{G}_{\text{nat}} := \mathbb{Z}_2 \times \zeta[\text{Aut}(G)] \tag{15}$$

of the group \mathbb{Z}_2 as specified in Eq. (14) and the subgroup given by the image of the automorphism group Aut(G)under the representation ζ . We emphasize their linear structure and define the natural symmetries as

$$S_{\text{nat}} := \operatorname{span}_{\mathbb{C}} \{ \mathbb{G}_{\text{nat}} \} \subseteq C_{\text{std}}. \tag{16}$$

We can always choose a linear-independent basis of the natural symmetries S_{nat} as

$$\mathcal{B}_{\text{nat}} = \{b_1, \dots, b_{\dim(\mathcal{S}_{\text{nat}})}\},\tag{17}$$

while the dimension $\dim(\mathcal{S}_{\mathrm{nat}}) \leq 2|\mathrm{Aut}(G)|$ is in general not equal to $2|\operatorname{Aut}(G)|$. One example with $\dim(\mathcal{S}_{\operatorname{nat}})$ $2|\operatorname{Aut}(G)|$ is presented in Fig. 10, and $\operatorname{Aut}(G) = \mathcal{S}_n$ with n > 3 provides another one as \mathbb{G}_{nat} then contains too many elements for all of them to be linear independent. Here, $|\operatorname{Aut}(G)|$ denotes the number of elements in the automorphism group Aut(G). For the house graph, \mathcal{S}_{nat} has a basis given by

$$\mathcal{B}_{\text{nat}} = \{ I^{\otimes n}, X^{\otimes n}, \zeta[(2,3)(4,5)], X^{\otimes n} \zeta[(2,3)(4,5)] \},$$
(18)

where the corresponding action of the group of natural symmetries is visualized in Fig. 4.

At this point, it is worth asking whether the natural symmetries are the only symmetries in the commutant, i.e., whether there is an equality in Eq. (16). But even for the house graph, the commutant C_{std} has dimension six (see Table I) while S_{nat} has dimension four. Indeed, the one-dimensional projectors P_3 and P_6 complement the natural symmetries as detailed in Fig. 5(b) and (c). We are using projectors $P_j \in \mathbb{C}^{d \times d}$ (with $d = 2^n$) that observe $P_j^2 = P_j = P_j^{\dagger}$ to specify invariant subspaces \mathcal{H}_j as the image of the corresponding projector P_j .

Thus not all symmetries in the commutant C_{std} are in general contained in S_{nat} . We can extend any basis \mathcal{B}_{nat} from Eq. (17) of the natural symmetries \mathcal{S}_{nat} to a basis

$$\mathcal{B}_{\text{ext}} = \{b_1, \dots, b_a; \ \tilde{b}_1, \dots, \tilde{b}_{\tilde{a}}\}\$$

of all symmetries $\mathcal{C}_{\mathrm{std}}$ where $q = \dim(\mathcal{S}_{\mathrm{nat}})$ and $\tilde{q} =$ $\dim(\mathcal{C}_{\mathrm{std}}) - \dim(\mathcal{S}_{\mathrm{nat}})$. Hence, any symmetry $S \in \mathcal{C}_{\mathrm{std}}$ can be linearly expanded as

$$S = \left(\sum_{j=1}^{q} c_j b_j\right) + \left(\sum_{k=1}^{\tilde{q}} \tilde{c}_k \tilde{b}_k\right),\tag{19}$$

where $c_j, \tilde{c}_k \in \mathbb{C}$. We say a symmetry $S \in \mathcal{C}_{\mathrm{std}}$ is a hidden symmetry if $\tilde{q} \neq 0$ and there exists a $k \in \{1, \dots, \tilde{q}\}$ in Eq. (19) with $\tilde{c}_k \neq 0$. This definition is independent of the choice of \mathcal{B}_{nat} or its extension \mathcal{B}_{ext} to a full basis of $C_{\rm std}$. Formally, the hidden symmetries can also be

(a) Graph G, automorphisms Aut(G), symmetries C_{std} , center $\mathcal{Z}(C_{std})$:

(b) Invariant-subspace decomposition of symmetries:

$$\begin{array}{llll} & \text{Symmetries} & \text{Projectors} & \text{Ione-dim. } P_j = \left| \psi_j \right> \! \left< \psi_j \right| / \left< \psi_j \right| \psi_j \rangle \\ & \text{Basis \mathcal{B}_{inv}} & P_1 & P_2 & P_3 & P_4 & P_5 & P_6 \\ & \text{Dimension} & 10 & 5 & 1 & 10 & 5 & 1 \\ & \text{Subspace} & + & + & + & - & - & - \\ & \text{Vectors} & \left| \psi_3 \right> = + \left| 00100 \right> - \left| 00111 \right> - \left| 01000 \right> + \left| 01011 \right> \\ & & + \left| 10100 \right> - \left| 10111 \right> - \left| 11000 \right> + \left| 11011 \right> \\ & \left| \psi_6 \right> = + \left| 00100 \right> - \left| 00111 \right> - \left| 01000 \right> + \left| 01011 \right> \\ & - \left| 10100 \right> + \left| 10111 \right> + \left| 11000 \right> - \left| 11011 \right> \end{array}$$

(c) Natural and hidden symmetries:

Figure 5. Symmetry decomposition of the standardansatz QAOA for the house graph. (a) graph, automorphisms, symmetries; (b) invariant subspaces \mathcal{H}_j as in Table I and projectors P_j which are explicitly shown in Fig. 16 in App. H. This includes their dimension, their respective position in the +1 and the -1 eigenspace of $X^{\otimes 5}$ (denoted by + or -), and explicit one-dimensional projectors. (c) natural and hidden symmetries; (d) transformation from \mathcal{B}_{inv} in (b) to $\mathcal{B}_{\mathrm{ext}}$ in (c), $\mathcal{B}_{\mathrm{ext}}$ is not unique as shown by the red, nonzero entries in the last two rows; (e) maximum cut vectors and their (nonzero) support in the invariant subspaces.

identified with all nonzero elements of the quotient vector space of the commutant C_{std} with respect to the natural symmetries S_{nat} .

The structure of the hidden symmetries and their relation to the invariant subspaces (see Sec. IIB) are highlighted in Fig. 5 which details the symmetries of standard-ansatz QAOA for the house graph. Following Table I, Figure 5(b) describes the commutant \mathcal{C}_{std} as the complex span of six (orthogonal) projectors P_j , which define the basis $\mathcal{B}_{\mathrm{inv}}$ of $\mathcal{C}_{\mathrm{std}}$ and uniquely identify the respective irreducible invariant subspaces. (In general, these invariant subspaces are not irreducible but only isotypical as detailed in App. A1.) For reference, Fig. 16 in App. H provides the explicit matrix form of the projectors in Figure 5. The one-dimensional projectors P_3 and P_6 are specified via their respective invariant, one-dimensional subspaces that are respectively spanned by the vectors $|\psi_3\rangle$ and $|\psi_6\rangle$. Part (c) of Figure 5 clarifies that the natural symmetries \mathcal{B}_{nat} in Eq. (18) can be extended to a full basis \mathcal{B}_{ext} of the commutant \mathcal{C}_{std} by adding the one-dimensional projectors P_3 and P_6 . But this choice is not unique as all projectors P_j with $j \in \{2, 3, 5, 6\}$ are

hidden symmetries. This is directly implied by the red, nonzero entries in the last two rows in Fig. 5(d), which details the basis change from the basis \mathcal{B}_{inv} of \mathcal{C}_{std} to \mathcal{B}_{ext} . Consequently, the description via natural and hidden symmetries provides an additional dimension complementing the decomposition into invariant subspaces. We refer to Appendix A 2 and particularly Fig. 10 for a more intricate example that is—in contrast to the house graph—not multiplicity-free [in the sense that $m_{\lambda} \neq 1$ in Eq. (10)]. Both Figures 5 and 10 demonstrate the highly complex structure of the symmetries in the standard ansatz.

It is instructive to reinterpret a vector $|\psi\rangle$ spanning a one-dimensional invariant subspace (as in Fig. 5) as a simultaneous eigenvector of a set of generators \mathcal{G} , i.e.,

$$H |\psi\rangle = \beta(H, |\psi\rangle) |\psi\rangle \text{ for all } H \in \mathcal{G}.$$
 (20)

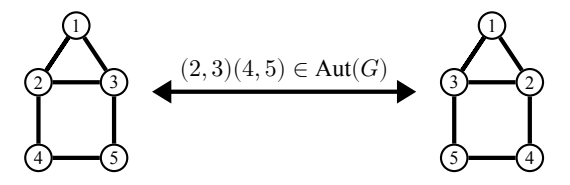
The two formulations can be easily shown to be equivalent. The eigenvalues $\beta(H,|\psi\rangle)$ for the respective generators $H \in \mathcal{G}$ and the simultaneous eigenvector $|\psi\rangle$ uniquely identify the corresponding one-dimensional representation up to multiplicity (see App. A 2). The multiplicity can be different from one. Instead of relying on a complete irreducible decomposition, other methods can be—in principle—used to identify these simultaneous eigenvectors more directly [108–111]. The condition in Eq. (20) is a necessary condition for the existence of quantum many-body scars [112–114], where $\mathcal G$ contains local terms (or sums of local terms) H_j for a parametrized class of Hamiltonians $H = \sum_j r_j H_j$ with parameters $r_j \in \mathbb R$. These classes of Hamiltonians are studied in the search and analysis of counterexamples to the eigenstate thermalization hypothesis [111, 115–121].

Combining locality in generators with the preservation of symmetries (such as natural symmetries in standard ansatz) can give rise to additional symmetries [32, 45, 122], while the absence of symmetries [20, 28] allows for universality as in the case of all one- and two-qubit gates [123, 124]. In particular, the collection of k-local unitaries (that act on at most k qubits with k < n) cannot in general generate all n-local unitaries while respecting the same symmetries for both k- and n-local unitaries. However, symmetries for the standard ansatz also arise as possible generators are restricted not only based on locality but also based on graph connectivity. We discuss these points in more detail in Sec. XI.

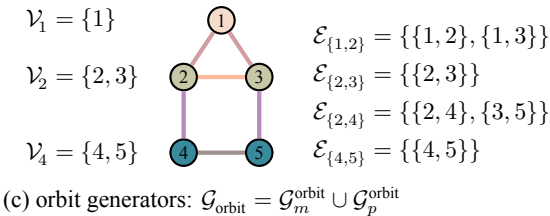
VI. LIE-ALGEBRA HIERARCHY: FROM THE FREE TO THE STANDARD ANSATZ

We continue to study the symmetries of the standard ansatz. In this section, we explore various Lie algebras that lie between $\mathfrak{g}_{\text{free}}$ and the standard-mixer Lie algebra $\mathfrak{g}_{\text{std}}$ or, alternatively, between $\mathfrak{u}(2^n)$ and $\mathfrak{g}_{\text{std}}$. The Lie algebras $\mathfrak{g}_{\text{std}}$ is contained in these intermediate Lie algebras which provide an additional approach for its characterization. In particular, we analyze the group of natural

(a) automorphism group $Aut(G) = \{1, (2,3)(4,5)\} \subseteq S_5$



(b) vertex and edge orbits



c) orbit generators:
$$\mathcal{G}_{\text{orbit}} = \mathcal{G}_{p}^{\text{orbit}} \cup \mathcal{G}_{p}^{\text{orbit}}$$

$$\mathcal{G}_{m}^{\text{orbit}} = \{\underline{X}_{1}, \underline{X}_{2} + \underline{X}_{3}, \underline{X}_{4} + \underline{X}_{5}\}$$

$$\mathcal{G}_{p}^{\text{orbit}} = \{\underline{Z}_{1}Z_{2} + \underline{Z}_{1}Z_{3}, \underline{Z}_{2}Z_{3}, \underline{Z}_{2}Z_{4} + \underline{Z}_{3}Z_{5}, \underline{Z}_{4}Z_{5}\}$$

Figure 6. Orbit generators for the house graph. (a) automorphisms, (b) vertex and edge orbits, (c) generators.

symmetries $\mathbb{G}_{\mathrm{nat}}$ from Sec. V and how this group acts on the state space $\mathcal{H} = \mathbb{C}^d$ and the intermediate Lie algebras. For a given graph G, Eq. (15) defines $\mathbb{G}_{\mathrm{nat}}$ as a direct product of $\mathbb{Z}_2 = \langle I^{\otimes n}, X^{\otimes n} \rangle_{\mathrm{group}}$ and the automorphism group $\mathrm{Aut}(G)$ acting as qubit permutations $\zeta(\sigma) \in \mathbb{C}^{d \times d}$ for $\sigma \in \mathrm{Aut}(G)$.

As a first step we introduce the orbit ansatz: Given a graph G with vertices $v \in V$ and edges $\{w_1, w_2\} \in E$, we recall the vertex and the edge orbits (see Fig. 6)

$$\mathcal{V}_v := \{ \sigma(v) \text{ for } \sigma \in \operatorname{Aut}(G) \} \text{ and }$$

$$\mathcal{E}_{\{w_1, w_2\}} := \{ \{ \sigma(w_1), \sigma(w_2) \} \text{ for } \sigma \in \operatorname{Aut}(G) \}$$

and define the sets of generators for the *orbit ansatz* as

$$\mathcal{G}_p^{\text{orbit}} := \Big\{ \sum_{\{w,\tilde{w}\} \in \mathcal{E}_{f_v,\tilde{w}}\}} Z_w Z_{\tilde{w}} \text{ for } \{v,\tilde{v}\} \in E \Big\}, \quad (21a)$$

$$\mathcal{G}_{m}^{\text{orbit}} := \Big\{ \sum_{\tilde{v} \in \mathcal{V}_{v}} X_{\tilde{v}} \text{ for } v \in V \Big\}.$$
 (21b)

We introduce the Lie algebra for the orbit ansatz as

$$\mathfrak{g}_{\mathrm{orbit}} := \langle i \mathcal{G}_{\mathrm{orbit}} \rangle_{\mathrm{Lie}} \text{ where } \mathcal{G}_{\mathrm{orbit}} := \mathcal{G}_p^{\mathrm{orbit}} \cup \mathcal{G}_m^{\mathrm{orbit}}.$$

Interestingly, the generators of the orbit ansatz can also be obtained by suitably symmetrizing the free-mixer generators. To this end, we first define three symmetrization operations on a given matrix $M \in \mathbb{C}^{d \times d}$:

$$\tau_{\mathbb{Z}_2}(M) := \frac{1}{2} [I^{\otimes n} M I^{\otimes n} + X^{\otimes n} M X^{\otimes n}], \qquad (22a)$$

$$\tau_{\text{aut}}(M) := \frac{1}{|\text{Aut}(G)|} \sum_{\sigma \in \text{Aut}(G)} \zeta[\sigma] M \zeta[\sigma^{-1}], \qquad (22b)$$

$$\tau_{\text{nat}}(M) := \tau_{\text{aut}}[\tau_{\mathbb{Z}_2}(M)] = \tau_{\mathbb{Z}_2}[\tau_{\text{aut}}(M)]. \tag{22c}$$

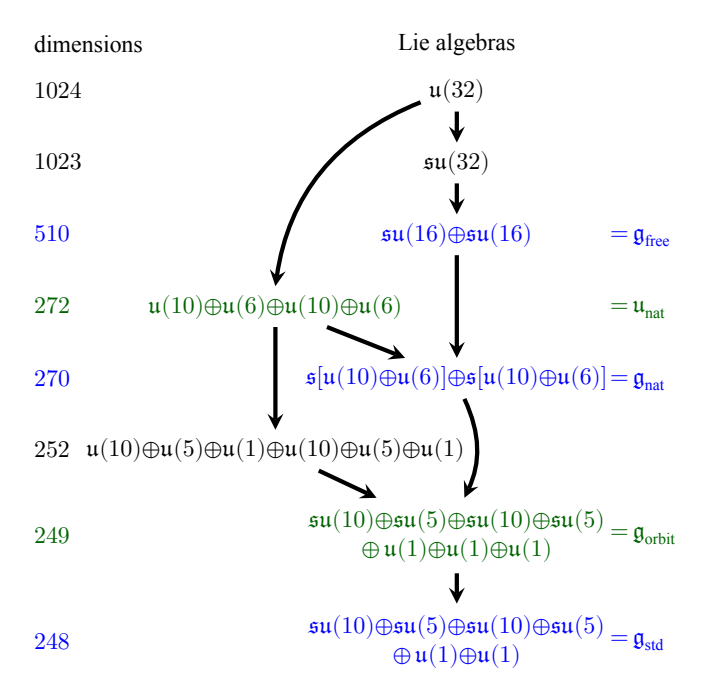


Figure 7. Lie-algebra inclusions for the house graph. The Lie algebras $\mathfrak{g}_{\mathrm{free}}$, $\mathfrak{u}_{\mathrm{nat}}$, $\mathfrak{g}_{\mathrm{nat}}$, $\mathfrak{g}_{\mathrm{orbit}}$, and $\mathfrak{g}_{\mathrm{std}}$ are shown with their inclusion relations and dimensions. The decomposition $\mathfrak{s}[\mathfrak{u}(10)\oplus\mathfrak{u}(6)]\cong\mathfrak{su}(10)\oplus\mathfrak{su}(6)\oplus\mathfrak{u}(1)$ has unitary blocks $\mathfrak{u}(10)$ and $\mathfrak{u}(6)$ where the 16-dimensional block has zero trace (which details more than the reductive decomposition).

Here, Eq. (22c) follows as the actions of \mathbb{Z}_2 and $\operatorname{Aut}(G)$ commute as detailed in Sec. V. Also, the free-mixer generators from Eq. (6) commute with X^{\otimes^n} [see Lemma 15(a)]. Thus the orbit-ansatz generators in Eq. (21b) are recovered up to suitable scalar factors by symmetrizing the free-ansatz generators, i.e., for every $g \in \mathcal{G}_{\operatorname{orbit}}$, there exists a positive integer z and $\tilde{g} \in \mathcal{G}_{\operatorname{free}}$ such that

$$g = z \,\tau_{\text{nat}}(\tilde{g}) = z \,\tau_{\text{aut}}(\tilde{g}). \tag{23}$$

The symmetrization operation $\tau_{\rm nat}$ from Eq. (22c) will be a key tool to better characterize the Lie algebra $\mathfrak{g}_{\rm std}$ associated to the standard ansatz. Let us define

$$\mathfrak{u}_{\mathrm{nat}} := \mathrm{span}_{\mathbb{R}} \{ \tau_{\mathrm{nat}}(g) \text{ for } g \in \mathfrak{u}(d) \},$$
 (24)

as well as

$$\mathfrak{g}_{\text{nat}} := \operatorname{span}_{\mathbb{R}} \{ \tau_{\text{nat}}(g) \text{ for } g \in \mathfrak{g}_{\text{free}} \}$$

$$= \operatorname{span}_{\mathbb{R}} \{ \tau_{\text{aut}}(g) \text{ for } g \in \mathfrak{g}_{\text{free}} \} \subseteq \mathfrak{u}_{\text{nat}}. \tag{25}$$

Both $\mathfrak{g}_{\mathrm{nat}}$ and $\mathfrak{u}_{\mathrm{nat}}$ form Lie algebras as they are closed under commutator due to (for $M_j \in \mathbb{C}^{d \times d}$)

$$[\tau_{\text{nat}}(M_1), \, \tau_{\text{nat}}(M_2)] = \tau_{\text{nat}}([M_1, \, M_2]).$$

Figure 7 highlights the corresponding Lie-algebra inclusion relations for the house graph. The structure of the centers of the considered Lie algebras is involved and

we detail their structure for the house graph in terms of the projectors P_j from Figure 5:

$$\begin{split} \mathcal{Z}(\mathfrak{u}_{\mathrm{nat}}) &= \mathrm{span}_{\mathbb{R}}\{iP_{1}, i(P_{2} + P_{3}), iP_{4}, i(P_{5} + P_{6})\}, \\ \mathcal{Z}(\mathfrak{g}_{\mathrm{nat}}) &= \mathrm{span}_{\mathbb{R}}\{i(-3P_{1} + 5P_{2} + 5P_{3}), \\ &i(-3P_{4} + 5P_{5} + 5P_{6})\}, \\ \mathcal{Z}(\mathfrak{g}_{\mathrm{orbit}}) &= \mathrm{span}_{\mathbb{R}}\{i(-3P_{1} + 5P_{2} + 5P_{3} - 3P_{4} + 5P_{5} + 5P_{6}), \\ &i(-1P_{1} + 2P_{2} - 1P_{4} + 2P_{5}), \\ &i(+1P_{1} - 3P_{2} + 5P_{3} - 1P_{4} + 3P_{5} - 5P_{6})\}, \\ \mathcal{Z}(\mathfrak{g}_{\mathrm{std}}) &= \mathrm{span}_{\mathbb{R}}\{i(-1P_{1} + 2P_{2} - 1P_{4} + 2P_{5}), \\ &i(+1P_{1} - 3P_{2} + 5P_{3} - 1P_{4} + 3P_{5} - 5P_{6})\}. \end{split}$$

On a more general note, Lemma 43 in Appendix G highlights how the center $\mathcal{Z}(\mathfrak{g})$ of a compact Lie algebra \mathfrak{g} (i.e. $\mathfrak{g} \subseteq \mathfrak{u}(m)$ for a suitable m) is contained in the center $\mathcal{Z}(\mathcal{C})$ of its commutant \mathcal{C} , i.e., $\mathcal{Z}(\mathfrak{g}) \subseteq \mathcal{Z}(\mathcal{C})$. But the projectors P_j to (certain) invariant subspaces (or more precisely to the isotypical subspaces as detailed in Appendix A) span the center $\mathcal{Z}(\mathcal{C})$ of the commutant. Thus the above decomposition of the centers associated to the house graph is no longer that surprising. We can readily derive a general strict hierarchy among the Lie algebras and their commutants considered so far:

Proposition 2 (Lie-algebra and commutant hierarchy). For any graph G, we observe $\mathcal{C}(\mathfrak{g}_{nat}) = \mathcal{S}_{nat}$ and the following chain of inclusions:

$$\begin{array}{cccc} \mathfrak{g}_{\mathrm{std}} & \subseteq & \mathfrak{g}_{\mathrm{orbit}} & \subseteq & \mathfrak{g}_{\mathrm{nat}} & \subseteq & \mathfrak{g}_{\mathrm{free}}, \\ \mathcal{C}(\mathfrak{g}_{\mathrm{std}}) & \supseteq & \mathcal{C}(\mathfrak{g}_{\mathrm{orbit}}) & \supseteq & \mathcal{C}(\mathfrak{g}_{\mathrm{nat}}) & \supseteq & \mathcal{C}(\mathfrak{g}_{\mathrm{free}}). \end{array}$$

The power of the hierarchy in Prop. 2 resides in the fact that $\mathfrak{g}_{\mathrm{nat}}$ can be characterized efficiently and therefore provides an accessible upper bound to $\mathfrak{g}_{\mathrm{orbit}}$ and $\mathfrak{g}_{\mathrm{std}}$.

Proof of Proposition 2. The inclusion relations on the commutants directly follow from the inclusion relations on the Lie algebras. The inclusion relation $\mathfrak{g}_{\rm std}\subseteq\mathfrak{g}_{\rm orbit}$ is a consequence of the form of the generators in Eq. (21b), similar as for $\mathfrak{g}_{\rm std}\subseteq\mathfrak{g}_{\rm free}$. We obtain $\mathfrak{g}_{\rm nat}$ by symmetrizing the basis of $\mathfrak{g}_{\rm free}$ via Eq. (22c) which implies $\mathfrak{g}_{\rm nat}\subseteq\mathfrak{g}_{\rm free}$. Moreover, $\mathfrak{g}_{\rm orbit}\subseteq\mathfrak{g}_{\rm nat}$ as $\mathfrak{g}_{\rm orbit}$ is generated by the symmetrized generators of $\mathfrak{g}_{\rm free}$ which are contained in $\mathfrak{g}_{\rm nat}$. Thus we are only left with verifying that the characterizations of $\mathfrak{g}_{\rm orbit}$ via Eq. (21) and Eq. (23) are equivalent, but this is detailed before Eq. (23).

We continue by discussing the structure of the symmetrized Lie algebras $\mathfrak{g}_{\rm nat}$ and $\mathfrak{u}_{\rm nat}$ for archetypal graphs following Def. 1. In this regard, we again point the reader to the example of the house graph in Figure 7 and the above discussed structure of the associated centers. For archetypal graphs, the following Proposition 3 shows that $\mathfrak{g}_{\rm nat}$ differs from $\mathfrak{u}_{\rm nat}$ by just a pair of Lie-algebra elements from the center $\mathcal{Z}(\mathfrak{u}_{\rm nat})$ of $\mathfrak{u}_{\rm nat}$ which can be interpreted as $\mathfrak{g}_{\rm nat}$ being semi-universal [32, 45].

Proposition 3. For any archetypal graph from Def. 1,

$$\operatorname{span}_{\mathbb{R}}\{\mathfrak{g}_{\operatorname{nat}} \cup \{iP_{+}, iP_{-}\}\} = \mathfrak{u}_{\operatorname{nat}}, \tag{26}$$

where $P_{\pm} := (I^{\otimes n} \pm X^{\otimes n})/2$ (see Sec. B 1) projects to the two invariant subspaces. The reductive decomposition is

$$\mathfrak{g}_{\mathrm{nat}} \oplus \mathfrak{u}(1) \oplus \mathfrak{u}(1) \cong \mathfrak{u}_{\mathrm{nat}}$$
 (27)

and the elements iP_+ and iP_- are chosen to respectively span each of the two abelian subalgebras $\mathfrak{u}(1)$.

Proof. Recall that $\mathfrak{g}_{\text{free}} \cong \mathfrak{su}(2^{n-1}) \oplus \mathfrak{su}(2^{n-1})$ holds for any archetypal graph (see Theorem 1). This implies

$$\tau_{\mathbb{Z}_2}[\mathfrak{u}(2^n)] \cong \mathfrak{u}(2^{n-1}) \oplus \mathfrak{u}(2^{n-1}) \cong \mathfrak{g}_{\text{free}} \oplus \mathfrak{a}_1 \oplus \mathfrak{a}_2,$$
 (28)

where \mathfrak{a}_i are one-dimensional abelian Lie algebras that are respectively spanned by iP_+ or iP_- . We apply the symmetrization operation $\tau_{\rm aut}$ to Eq. (28) and obtain

$$\begin{split} \mathfrak{u}_{\mathrm{nat}} &= \tau_{\mathrm{aut}}[\tau_{\mathbb{Z}_2}[\mathfrak{u}(2^n)]] \cong \tau_{\mathrm{aut}}[\mathfrak{g}_{\mathrm{free}}] \oplus \tau_{\mathrm{aut}}[\mathfrak{a}_1] \oplus \tau_{\mathrm{aut}}[\mathfrak{a}_2] \\ &\cong \tau_{\mathrm{aut}}[\mathfrak{g}_{\mathrm{free}}] \oplus \mathfrak{a}_1 \oplus \mathfrak{a}_2 \cong \mathfrak{g}_{\mathrm{nat}} \oplus \mathfrak{a}_1 \oplus \mathfrak{a}_2, \end{split}$$

where the second isomorphism follows from the fact $I^{\otimes n}$ and $X^{\otimes n}$ commute with any automorphism. The definition of \mathfrak{g}_{nat} implies the third isomorphism.

One can naturally extend the symmetrization from Equation (22c) to quantum states $|\psi\rangle \in \mathcal{H}$ via

$$\hat{\tau}_{\mathrm{nat}}(|\psi\rangle) := \frac{1}{2|\mathrm{Aut}(G)|} (I^{\otimes n} + X^{\otimes n}) \sum_{\sigma \in \mathrm{Aut}(G)} \zeta[\sigma] \ |\psi\rangle$$

and we introduce the related symmetrized subspace

$$\mathcal{H}_{\mathrm{nat}} := \{\hat{\tau}_{\mathrm{nat}}(|\psi\rangle) \text{ for all } \psi \in \mathcal{H}\} \subseteq \mathcal{H}_{+} \subseteq \mathcal{H}.$$

For the house graph, the symmetrized subspace \mathcal{H}_{nat} has a dimension of ten and corresponds to the projector P_1 in Figure 5. Consider a maximum cut $x \in \{0,1\}^n$ (see Sec. II A) and the corresponding ground state $|x\rangle \in \mathcal{H}$ of H_p with ground state energy E. The action of $(X^{\otimes n})^b \zeta(\sigma)$ with $b \in \{0,1\}$ and $\sigma \in \zeta$ maps $|x\rangle$ to another ground state $(X^{\otimes n})^b \zeta(\sigma) |x\rangle$ with

$$H_p(X^{\otimes n})^b \zeta(\sigma) |x\rangle = E(X^{\otimes n})^b \zeta(\sigma) |x\rangle,$$

which follows as H_p and $(X^{\otimes n})^b \zeta(\sigma)$ commute. Clearly, $\hat{\tau}_{\text{nat}}(|x\rangle) \in \mathcal{H}_{\text{nat}}$ is another ground state of H_p .

Proposition 4. Let G denote a connected graph with at least two vertices. (a) \mathcal{H}_{nat} contains at least one ground state of H_p . (b) If G is any archetypal graph from Def. 1, then $\exp(\mathfrak{g}_{nat})$ acts transitively on \mathcal{H}_{nat} .

Proof. Statement (a) has been verified directly before the proposition and (b) follows from Proposition 3.

The dimension of the space $\mathcal{H}_{\mathrm{nat}}$ will be further characterized via character computations in Sec. VIIIB. Even though Prop. 4(b) verifies the transitivity of $\exp(\mathfrak{g}_{nat})$ on \mathcal{H}_{nat} for archetypal graphs, $\exp(\mathfrak{g}_{\text{std}})$ is in general not transitive on \mathcal{H}_{nat} . This will be exemplified in Sec. IX for graphs G with |Aut(G)| = 1.

VII. PARTIAL RESULTS FOR THE STANDARD ANSATZ AND PARTICULAR GRAPHS

In order to illustrate the results and methods of the previous sections, we now analyze concrete cases given by path, cycle, and complete graphs. We are able to completely determine the standard-ansatz Lie algebra for the path graphs and we provide upper bounds for the cycle and the complete graphs. The solvability of these cases may be related to the well-known fact that the corresponding maxcut problems have trivial solutions.

Standard ansatz for path graphs

We determine the standard-ansatz Lie algebra \mathfrak{g}_{std} for path graphs P_n . Applying Theorem 1, $\mathfrak{g}_{std} \subseteq \mathfrak{g}_{nat} \subseteq$ $\mathfrak{g}_{\text{free}} = \mathfrak{so}(2n)$. The Lie algebra $\mathfrak{g}_{\text{free}}$ is spanned (up to factors of i) by the $2n^2-n$ Pauli strings (see Table III)

$$I \cdot IXI \cdot I$$
 and $I \cdot I \begin{Bmatrix} Y \\ Z \end{Bmatrix} X \cdot X \begin{Bmatrix} Y \\ Z \end{Bmatrix} I \cdot I$,

or equally, the basis consists of (with $1 \le j < k \le n$)

$$iX_j, iY_jX_{j+1} \cdots X_{k-1}Y_k, iY_jX_{j+1} \cdots X_{k-1}Z_k,$$
 (29a)

$$iZ_jX_{j+1}\cdots X_{k-1}Y_k, iZ_jX_{j+1}\cdots X_{k-1}Z_k.$$
 (29b)

The automorphism group of the path graph is given by

$$\operatorname{Aut}(P_n) = \{\mathbf{1}, \, \tilde{\sigma}_n\} \subseteq \mathcal{S}_n \text{ where } \bar{n} := \lfloor n/2 \rfloor \text{ and}$$

$$\tilde{\sigma}_n := \begin{cases} (1\,n)(2\,n-1)\cdots(\bar{n}\,\bar{n}+1) & \text{for } n \text{ even,} \\ (1\,n)(2\,n-1)\cdots(\bar{n}\,\bar{n}+2) & \text{for } n \text{ odd.} \end{cases}$$
(30)

Note that $\bar{n} = n/2$ for even n and $\bar{n} = (n-1)/2$ otherwise. Let us introduce the indices $o \in \{1, ..., \bar{n}\}$ and $p, q \in$ $\{1,\ldots,n\}$ with p < n+1-q and $p \neq q$. Symmetrizing the Pauli strings associated to $\mathfrak{g}_{\text{free}}$ following Eq. (25), basis elements for \mathfrak{g}_{nat} are given as

$$iX_{\bar{n}+1}$$
 if n is odd, $iX_o + iX_{n+1-o}$, (31a)

$$iP_{oo}^{YY}, iP_{oo}^{ZZ}, iP_{oo}^{YZ} + iP_{oo}^{ZY},$$
 (31b)

$$iP_{oo}^{YY}, iP_{oo}^{ZZ}, iP_{oo}^{YZ} + iP_{oo}^{ZY},$$
 (31b) $iP_{pq}^{YY} + iP_{qp}^{YY}, iP_{pq}^{ZZ} + iP_{qp}^{ZZ}, iP_{pq}^{YZ} + iP_{qp}^{ZY},$ (31c)

where

$$P_{ab}^{AB} := A_a X_{a+1} \cdot X_{n-b} B_{n+1-b}$$
 with $a+b \leq n$.

We count the number of possibilities for the different cases in Eq. (31) before and after the symmetrization. Recall that there are $\binom{n}{2} = n(n-1)/2$ pairs (\tilde{p}, \tilde{q}) with $\tilde{p}, \tilde{q} \in \{1, \dots, n\}$ and $\tilde{p} + \tilde{q} \leqslant n$. Thus 2n(n-1) basis elements from Eq. (29) are symmetrized to the cases (31b)-(31c) and n different elements from Eq. (29) result in the cases (31a), which agrees with the total of $2n^2-n$ basis elements in Eq. (29). For n even, there are \bar{n} cases in (31a), n cases for iP_{oo}^{YY} and iP_{oo}^{ZZ} , \bar{n} cases for $iP_{oo}^{YZ}+iP_{oo}^{ZY}$, and n(n-2) cases in (31c). For n odd, there are $\bar{n}+1$ cases in (31a), $2\bar{n}$ cases for iP_{oo}^{YY} and iP_{oo}^{ZZ} , \bar{n} cases for $iP_{oo}^{YZ} + iP_{oo}^{ZY}$, and $(n-1)^2$ cases in (31c). Both for even and odd n, a total of n^2 basis elements are provided in Eq. (31). Thus we have shown

Lemma 5. For a path graph P_n with n vertices, \mathfrak{g}_{nat} has dimension n^2 and is spanned by the elements in Eq. (31).

There are different strategies to identify $\mathfrak{g}_{\rm nat}$ as $\mathfrak{u}(n)$ based on explicit isomorphisms, subalgebra chains, and by ruling out all other possibilities (see, e.g., [20, 125]). And detailed arguments in Appendix E 1 verify the following statement:

Lemma 6. For a *n*-vertex path graph P_n , $\mathfrak{g}_{nat} \cong \mathfrak{u}(n)$.

As a last step in our analysis of the standard ansatz for the path graph, we prove in Appendix E 2 that $\mathfrak{g}_{\text{std}} = \mathfrak{g}_{\text{nat}} \cong \mathfrak{u}(n)$:

Proposition 7 (Path graphs). For a path graph P_n with n vertices, the associated standard-mixer Lie algebra $\mathfrak{g}_{\rm std}$ is equal to $\mathfrak{g}_{\rm nat}$. Moreover, its basis is given by Eq. (31) and its reductive decomposition is $\mathfrak{u}(n) \cong \mathfrak{su}(n) \oplus \mathfrak{u}(1)$.

B. Standard ansatz for cycle graphs

Similarly as in Sec. VII A, we now consider the standard ansatz for cycle graphs C_n . The free-mixer Lie algebra observes $\mathfrak{g}_{\text{std}} \subseteq \mathfrak{g}_{\text{nat}} \subseteq \mathfrak{g}_{\text{free}} = \mathfrak{so}(2n) \oplus \mathfrak{so}(2n)$ (see Theorem 1) and Table III states an explicit basis of $\mathfrak{g}_{\text{free}}$ given (up to factors of i) by $4n^2-2n$ Pauli strings

$$\begin{split} & \text{I} \cdot \text{I} \text{XI} \cdot \text{I}, & \text{X} \cdot \text{X} \text{IX} \cdot \text{X}, \\ & \text{I} \cdot \text{I} \left\{ \begin{smallmatrix} \mathbf{Y} \\ \mathbf{Z} \end{smallmatrix} \right\} \text{X} \cdot \text{X} \left\{ \begin{smallmatrix} \mathbf{Y} \\ \mathbf{Z} \end{smallmatrix} \right\} \text{I} \cdot \text{I}, & \text{X} \cdot \text{X} \left\{ \begin{smallmatrix} \mathbf{Y} \\ \mathbf{Z} \end{smallmatrix} \right\} \text{I} \cdot \text{I} \left\{ \begin{smallmatrix} \mathbf{Y} \\ \mathbf{Z} \end{smallmatrix} \right\} \text{X} \cdot \text{X}. \end{split}$$

Equivalently, we can write the basis of \mathfrak{g}_{free} as

$$iX_a,\,iX_aX^{\otimes n},\,iQ^{YY}_{ab},\,iQ^{ZZ}_{ab},\,iQ^{YZ}_{ab},\,\,\text{and}\,\,iQ^{ZY}_{ab} \quad \ (32)$$

where $1 \leqslant a \leqslant n$, $1 \leqslant b \leqslant n-1$, and

$$Q_{ab}^{AB} := A_{\iota(a)} X_{\iota(a+1)} \cdot X_{\iota(a+b-1)} B_{\iota(a+b)}$$
 where

$$\iota(c) = \iota_n(c) := \begin{cases} n & \text{if } c \bmod n = 0, \\ c \bmod n & \text{otherwise.} \end{cases}$$

The automorphism group of a cycle graph with n vertices is given by the dihedral group [126, 127] that is generated by the permutations $(1 \cdot 2 \cdot \dots \cdot n)$ and $\tilde{\sigma}_n$ where $\tilde{\sigma}_n$ is defined in Eq. (30), i.e.,

$$\operatorname{Aut}(C_n) = \langle (1 \, 2 \cdots n), \, \tilde{\sigma}_n \rangle_{\operatorname{group}}.$$

In order to determine \mathfrak{g}_{nat} , we apply the symmetrization τ_{nat} from Eq. (22c) to the basis elements of \mathfrak{g}_{free} from Eq. (32). We introduce the notation

$$\tilde{Q}_0 := \sum_{\tilde{a}=1}^n X_{\tilde{a}}, \ \tilde{Q}_n := \sum_{\tilde{a}=1}^n X_{\tilde{a}} X^{\otimes n}, \ \tilde{Q}_b^{AB} := \sum_{\tilde{a}=1}^n Q_{\tilde{a}b}^{AB}.$$

and obtain 3(n-1) + 2 different basis elements

$$i\tilde{Q}_0 = n \,\tau_{\text{nat}}(iX_a), \ i\tilde{Q}_n = n \,\tau_{\text{nat}}(iX_aX^{\otimes n}),$$
 (33a)

$$i\tilde{Q}_b^{YY} = n\,\tau_{\rm nat}(iQ_{ab}^{YY}),\; i\tilde{Q}_b^{ZZ} = n\,\tau_{\rm nat}(iQ_{ab}^{ZZ}), \eqno(33b)$$

$$i(\tilde{Q}_b^{YZ} + \tilde{Q}_b^{ZY}) = 2n\,\tau_{\rm nat}(iQ_{ab}^{YZ}) = 2n\,\tau_{\rm nat}(iQ_{ab}^{ZY}) \quad (33c)$$

spanning \mathfrak{g}_{nat} . We have verified the following lemma:

Lemma 8. For a cycle graph C_n with n vertices, \mathfrak{g}_{nat} has dimension 3(n-1)+2 and it is spanned by the basis elements in Eq. (33).

We know that now that $\mathfrak{g}_{\mathrm{std}} \subseteq \mathfrak{g}_{\mathrm{nat}}$ and that the dimension of $\mathfrak{g}_{\mathrm{nat}}$ is given by 3(n-1)+2. We refer to [34, 36] for an explicit proof of the fact that

$$\mathfrak{g}_{\mathrm{std}} = \mathfrak{g}_{\mathrm{nat}} \cong \underbrace{\mathfrak{su}(2) \oplus \cdots \oplus \mathfrak{su}(2)}_{n-1} \oplus \mathfrak{u}(1) \oplus \mathfrak{u}(1).$$

In addition, we point the reader to the original work of Onsager [44].

C. Standard ansatz for the complete graph

We analyze the standard-ansatz Lie algebra $\mathfrak{g}_{\rm std}$ that is contained in $\mathfrak{g}_{\rm nat}$ due to Proposition 2. The following Proposition 9 observes an exponential separation between the dimension of $\mathfrak{g}_{\rm std}$ and $\dim(\mathfrak{g}_{\rm free})=2^{2n-1}-2$ for the complete graph. This suggests that a standard ansatz could in fact be overparametrized [25] and it would be able to solve the (trivial) task of finding the maximum cut for the complete graph, even though the free ansatz would very likely fail due to the presence of barren plateaus (see Corollary 2). We have shown in Appendix E 3 the following characterization:

Proposition 9. Consider the complete graph K_n with $n \ge 3$ vertices. The dimension of $\mathfrak{g}_{\text{std}}$ is bounded from above by a polynomial in n. In particular, we have

$$\dim(\mathfrak{g}_{\text{std}}) \leqslant \dim(\mathfrak{g}_{\text{nat}}) = \begin{cases} \frac{1}{2} \binom{n+3}{3} - 2 & \text{for } n \text{ odd,} \\ \frac{1}{2} \binom{n+3}{3} + \frac{n}{4} - \frac{3}{2} & \text{for } n \text{ even.} \end{cases}$$

The result of Prop. 9 for the complete graph has been independently obtained in [36] as an upper bound to the standard-ansatz Lie algebra $\mathfrak{g}_{\rm std}$. In [36], they have also determined an explicit basis for $\mathfrak{g}_{\rm std}$ and thereby also an explicit formula for the dimension of $\mathfrak{g}_{\rm std}$ in this case. Moreover, they have provided explicit bases for the semisimple part $[\mathfrak{g}_{\rm std},\mathfrak{g}_{\rm std}]$ and the center $\mathcal{Z}(\mathfrak{g}_{\rm std})$.

VIII. INVARIANT SUBSPACES AND REPRESENTATION THEORY

In contrast to Sec. VII which emphasized specific classes of graphs and explicit (Paul-string) bases for the associated Lie algebras, this section aims at general results for characterizing the invariant subspaces connected to the standard ansatz of QAOA. We start in Sec. VIII A with the general representation-theoretic setting and first implications. This is continued in Sec. VIII B with explicit character computations that lead to upper bounds on dimensions of irreducible representations connected to the standard-ansatz Lie algebra $\mathfrak{g}_{\rm std}$.

Setting and immediate implications

Building on the notation and results from Sections V and VI, we now focus even more on invariant subspaces and representation theory related to the standard ansatz. Set $C_{\text{std}} := C(\mathfrak{g}_{\text{std}})$. The invariant subspaces of $\mathfrak{g}_{\text{std}}$, $\mathfrak{g}_{\text{nat}}$, and $\mathfrak{u}_{\mathrm{nat}}$ (or for their semisimple parts) are revealed by suitable basis changes so that the block decompositions

$$\mathfrak{g}_{\mathrm{std}} \simeq \bigoplus_{\lambda=1}^{\dim[\mathcal{Z}(\mathcal{C}_{\mathrm{std}})]} \mathbb{1}_{m_{\lambda}} \otimes \mathfrak{g}_{\lambda},$$
(34a)

$$\mathfrak{g}_{\text{std}} \simeq \bigoplus_{\lambda=1}^{\dim[\mathcal{Z}(\mathcal{C}_{\text{std}})]} \mathbb{1}_{m_{\lambda}} \otimes \mathfrak{g}_{\lambda}, \qquad (34a)$$

$$\mathfrak{g}_{\text{nat}} \simeq \bigoplus_{\mu=1}^{\dim[\mathcal{Z}(\mathcal{S}_{\text{nat}})]} \mathbb{1}_{\tilde{m}_{\mu}} \otimes \tilde{\mathfrak{g}}_{\mu}, \text{ and} \qquad (34b)$$

$$\mathfrak{u}_{\text{nat}} \simeq \bigoplus_{\mu=1}^{\dim[\mathcal{Z}(\mathcal{S}_{\text{nat}})]} \mathbb{1}_{\tilde{m}_{\mu}} \otimes \mathfrak{u}(\tilde{d}_{\mu}) \qquad (34c)$$

$$\mathfrak{u}_{\text{nat}} \simeq \bigoplus_{\mu=1}^{\dim[\mathcal{Z}(\mathcal{S}_{\text{nat}})]} \mathbb{1}_{\tilde{m}_{\mu}} \otimes \mathfrak{u}(\tilde{d}_{\mu})$$
(34c)

hold for suitably chosen Lie algebras

$$\mathfrak{g}_{\lambda} \subseteq \mathfrak{u}(d_{\lambda}) \subseteq \mathbb{C}^{d_{\lambda} \times d_{\lambda}}$$
 and $\tilde{\mathfrak{g}}_{\mu} \subseteq \mathfrak{u}(\tilde{d}_{\mu}) \subseteq \mathbb{C}^{\tilde{d}_{\mu} \times \tilde{d}_{\mu}}$

with $\dim[\mathfrak{com}(\mathfrak{g}_{\lambda})] = \dim[\mathfrak{com}(\tilde{\mathfrak{g}}_{\mu})] = 1$. The decomposition in Eq. (34a) refines the ones in Eqs. (34b)-(34c). The action of the corresponding centers $\mathcal{Z}(\mathfrak{g}_{std})$ and $\mathcal{Z}(\mathfrak{g}_{nat})$ can be quite involved and they can have support on different irreducible blocks in Eq. (34) (see Fig. 7 and the related discussion in Sec. VI). We establish in Appendix F 1 some basic properties of the invariant subspaces corresponding to the Lie algebras $\mathfrak{g}_{\rm free},\,\mathfrak{g}_{\rm nat},\,\mathfrak{g}_{\rm orbit},\,\mathfrak{g}_{\rm std},$ and $\mathfrak{u}_{\mathrm{nat}}$:

Lemma 10. Consider a graph with n vertices and an invariant subspace $W \subseteq \mathbb{C}^{d}$ of any associated Lie algebra $\mathfrak{g} \in \{\mathfrak{g}_{\text{free}}, \mathfrak{g}_{\text{nat}}, \mathfrak{g}_{\text{orbit}}, \mathfrak{g}_{\text{std}}, \mathfrak{u}_{\text{nat}}\}.$ Then $(Z^{\otimes n})W$ is also an invariant subspace of \mathfrak{g} .

For an arbitrary subspace W, $(Z^{\otimes n})W$ may have a nontrivial intersection with W. However, when n is odd and W is a irreducible, invariant subspace of one of our Lie algebras of interest, we can guarantee that W and $(Z^{\otimes n})W$ have a trivial intersection. Recall that a Lie algebra $\mathfrak{g} \in \{\mathfrak{g}_{\text{free}}, \mathfrak{g}_{\text{nat}}, \mathfrak{g}_{\text{orbit}}, \mathfrak{g}_{\text{std}}, \mathfrak{u}_{\text{nat}}\}$ observes the invariant subspaces \mathcal{H}_+ and \mathcal{H}_- of the same dimension given by the +1 and -1 eigenspaces of $X^{\otimes n}$ (see Sec. B1). They are spanned by all Hadamard basis states $|b_1\rangle\otimes\cdots\otimes|b_n\rangle$ with $b_i\in\{+,-\}$ with respectively an even or odd number of minus signs. For odd n, the irreducible subspaces in \mathcal{H}_{+} and \mathcal{H}_{-} match as is verified in Appendix F 2:

Proposition 11 (Odd number of vertices.). Given a graph with an odd number n of vertices, we consider an associated Lie algebra $\mathfrak{g} \in \{\mathfrak{g}_{free}, \mathfrak{g}_{nat}, \mathfrak{g}_{orbit}, \mathfrak{g}_{std}, \mathfrak{u}_{nat}\}.$ The invariant subspaces \mathcal{H}_+ and \mathcal{H}_- have matching decompositions $\mathcal{H}_+ = V_1 \oplus \cdots \oplus V_k$ and $\mathcal{H}_- = W_1 \oplus \cdots \oplus W_k$ into the irreducible, invariant subspaces V_i and W_j with $W_j = (Z^{\otimes n}) V_j$ and $1 \leqslant j \leqslant k$.

В. Character computations

After these preparations, we characterize the invariant subspaces of \mathfrak{g}_{nat} based on explicit character computations [128–130]. This will yield upper bounds on the dimensions of the irreducible representations of \mathfrak{g}_{std} ; recall from Proposition 2 that $\mathfrak{g}_{std} \subseteq \mathfrak{g}_{nat}$.

For $\sigma_1 \in \mathcal{S}_2$, we set the element $\vartheta(\sigma_1) \in \mathbb{Z}_2$ as

$$\vartheta(\sigma_1) := \begin{cases} I^{\otimes n} & \text{for } \sigma_1 = \mathbf{1}, \\ X^{\otimes n} & \text{for } \sigma_1 = (1\,2). \end{cases}$$
 (35)

The permutation group $G_{nat} := S_2 \times Aut(G)$ is represented via $\Upsilon(\sigma_1, \sigma_2) := \vartheta[\sigma_1]\zeta[\sigma_2] \in \mathbb{C}^{d \times d}$ as the group of natural symmetries $\mathbb{G}_{\mathrm{nat}} = \mathbb{Z}_2 \times \zeta[\mathrm{Aut}(G)]$ from Eq. (15). The associated character χ_{nat} is defined as

$$\chi_{\text{nat}}(\sigma_1, \sigma_2) := \text{Tr}[\Upsilon(\sigma_1, \sigma_2)] = \text{Tr}(\vartheta[\sigma_1] \zeta[\sigma_2])$$
(36)

for $\sigma_1 \in \mathcal{S}_2$ and $\sigma_2 \in \operatorname{Aut}(G)$. For a permutation $\sigma \in \mathcal{S}_n$, its cycle type is defined as [107]

$$(1^{b_1}, \dots, n^{b_n}) \tag{37}$$

where b_a denotes the number of cycles of length a in σ . In particular, σ can be uniquely decomposed into a product

$$\sigma = \prod_{a=1}^{c(\sigma)} (z_a, \sigma[z_a], \dots, \sigma^{q_a-1}[z_a])$$
 (38)

of disjoint cycles of length q_a such that $\sigma^{q_a}[z_a] = z_a$, $z_a \in \{1, \ldots, n\}$, and the number of cycles is

$$c(\sigma) := \sum_{a=1}^{n} b_a.$$

For example, the identity $\mathbf{1} = (1) \cdots (n) \in S_n$ can be uniquely written as n cycles of length one. We set

$$\wp(\sigma) := \begin{cases} 1 & \text{if all cycles of } \sigma \text{ are of even length,} \\ 0 & \text{otherwise.} \end{cases}$$

For odd n, no $\tilde{\sigma} \in \mathcal{S}_n$ has only even cycles, i.e., $\wp(\tilde{\sigma}) = 0$. We efficiently compute the character from Eq. (36) which is shown in Appendix F 3:

Lemma 12 (Character formula). We observe

$$\chi_{\text{nat}}(\sigma_1, \sigma_2) = \begin{cases} 2^{c(\sigma_2)} & \text{if } \sigma_1 = \mathbf{1} \text{ or } \wp(\sigma_2) = 1, \\ 0 & \text{otherwise.} \end{cases}$$

We aim to determine the multiplicaties of the irreducible components of the character χ_{nat} . In particular, for each representation index $\nu = (\nu_1, \nu_2)$, we are computing the character χ_{ν} of the group G_{nat} as

$$\chi_{\nu}(\sigma_1, \sigma_2) = \alpha_{\nu_1}(\sigma_1) \beta_{\nu_2}(\sigma_2)$$

where α_{ν_1} and β_{ν_2} are the characters of \mathcal{S}_2 and $\operatorname{Aut}(G)$ with associated representation indices ν_1 and ν_2 as well as $\sigma_1 \in \mathcal{S}_2$ and $\sigma_2 \in \operatorname{Aut}(G)$. The multiplicity of χ_{ν} in χ_{nat} is given by the Schur orthogonality relations [128–130]

$$\mathbf{m}_{\nu} := \frac{1}{2|\operatorname{Aut}(G)|} \sum_{\substack{(\sigma_1, \sigma_2) \in \mathcal{S}_2 \times \operatorname{Aut}(G)}} \bar{\chi}_{\nu}(\sigma_1, \sigma_2) \, \chi_{\operatorname{nat}}(\sigma_1, \sigma_2). \tag{39}$$

By duality (as detailed in Sec. A 1), each multiplicity \mathbf{m}_{ν} corresponds to one of the dimensions \tilde{d}_{μ} in Eq. (34b), while the associated multiplicity \tilde{m}_{μ} is given by the degree $\mathbf{d}_{\nu} := \chi_{\nu}(\mathbf{1}, \mathbf{1})$ of χ_{ν} .

We consider now the example of the house graph and we recall that its automorphism group is isomorphic to S_2 , which has only the trivial and the sign representation with the associated characters χ_t and χ_s . We obtain the following multiplicities and degrees

We evaluate the multiplicity formula in Eq. (39) for $\nu = (t,t)$ using $\chi_{(t,t)}(\sigma_1,\sigma_2) = 1$, while Lemma 12 determines $\chi_{\rm nat}(\sigma_1,\sigma_2)$. We obtain the following formula:

Lemma 13. For the group $G_{nat} = S_2 \times Aut(G)$ and following Eq. (39), the multiplicity of the trivial character $\chi_{(t,t)}$ in the character χ_{nat} from Eq. (36) is given by

$$\mathbf{m}_{(t,t)} = \frac{1}{2|\operatorname{Aut}(G)|} \sum_{\sigma \in \operatorname{Aut}(G)} 2^{c(\sigma)} \left[1 + \wp(\sigma) \right].$$

The summands only depend on the cycle type of the permutations in $\operatorname{Aut}(G)$, and therefore the summation over the whole automorphism group could be replaced by a summation over conjugacy classes. It will be instructive to characterize the multiplicity $\mathbf{m}_{(t,t)}$ for the two limiting cases of large and small automorphism groups $\operatorname{Aut}(G)$:

Proposition 14. Let $\operatorname{Aut}(G)$ denote the automorphism group of a graph G with n vertices. The multiplicity $\mathbf{m}_{(t,t)}$ of the trivial character of $G_{\text{nat}} = \mathcal{S}_2 \times \operatorname{Aut}(G)$ observes the following properties:

- (a) $\operatorname{Aut}(G) = S_n$ implies $\mathbf{m}_{(\mathbf{t},\mathbf{t})} = \left| \frac{n}{2} \right| + 1$, (40a)
- (b) |Aut(G)| = 1 implies $\mathbf{m}_{(t,t)} = 2^{n-1}$, (40b)

(c)
$$\mathbf{m}_{(t,t)} \ge 2^{n-1}/|\text{Aut}(G)|$$
. (40c)

Appendix $\mathbf{F4}$ details the proof of Proposition 14. Proposition 14(a) shows that the trivial multiplicity $\mathbf{m}_{(\mathsf{t},\mathsf{t})}$ is linear in the number n of vertices if the automorphism group is maximal. Using again the duality from Sec. A1 between one of the dimensions \tilde{d}_{μ} in Eq. (34b) and $\mathbf{m}_{(\mathsf{t},\mathsf{t})}$, this dimension \tilde{d}_{μ} of a particular representation of $\mathfrak{g}_{\mathrm{nat}}$ is identified as being equal to $\mathbf{m}_{(\mathsf{t},\mathsf{t})}$. Similarly for a trivial automorphism group with $|\mathrm{Aut}(G)| = 1$, Prop. 14(b) identifies a representation in Eq. (34b) of dimension 2^{n-1} . For small values of $\mathrm{Aut}(G)$ that are, e.g., polynomially bounded in the number n of vertices,

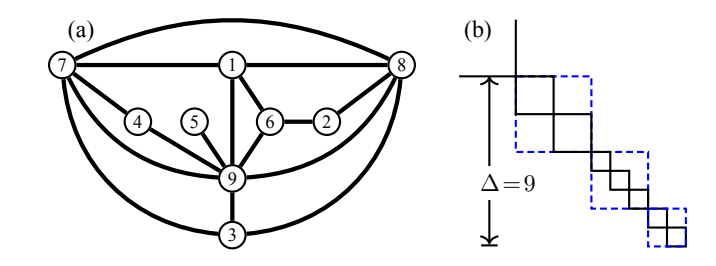


Figure 8. Asymmetric graph with nine vertices and its gap $\Delta = 9 = 2 \times 2 + 1 \times 3 + 1 \times 2$. (a) Graph. (b) $\mathfrak{g}_{\rm std}^+$ acts on the upper-left component \mathcal{H}_+ which splits into irreducible subspaces with the respective dimensions 247, 2, 1, 1 and multiplicities 1, 2, 3, 2. Thus hidden symmetries can entail irreducible subspaces of dimension larger than one.

Prop. 14(c) leads to an exponential lower bound for the corresponding dimension in Eq. (34b).

What does this imply for the standard ansatz of QAOA? Recall from Proposition 2 that $\mathfrak{g}_{\rm std}\subseteq\mathfrak{g}_{\rm nat}$. So, the results in this section and particularly Proposition 14(c) only provide an exponential lower bound on an upper bound for the dimension of an irreducible subspace of $\mathfrak{g}_{\rm std}$ assuming that $|{\rm Aut}(G)|$ is polynomially bounded. But the dimension of this irreducible subspace of $\mathfrak{g}_{\rm std}$ could be smaller. The following Section IX considers the particular case of graphs G with $|{\rm Aut}(G)|=1$ (which are known as asymmetric graphs), which in particular implies that G is archetypal (see Def. 1).

IX. STANDARD ANSATZ FOR CONNECTED ASYMMETRIC GRAPHS

We now explore properties of the standard ansatz for the case of connected asymmetric graphs. Connected asymmetric graphs are connected graphs such that their automorphism group consists only of the identity permutation [131, 132]. Almost all graphs are asymmetric and there are no connected asymmetric graphs for $2 \le n \le 5$. All connected asymmetric graphs are archetypal in the sense of Def. 1. Applying the results of Sec. VI to connected asymmetric graphs with n vertices, one obtains

$$\mathfrak{g}_{\mathrm{std}} \subseteq \mathfrak{g}_{\mathrm{orbit}} = \mathfrak{g}_{\mathrm{nat}} = \mathfrak{g}_{\mathrm{free}} = \mathfrak{su}(2^{n-1}) \oplus \mathfrak{su}(2^{n-1}).$$

Also, Proposition 14(b) shows that the largest dimension for the invariant subspaces of $\mathfrak{g}_{\mathrm{nat}}$ is given by 2^{n-1} . But how much smaller is the largest invariant dimension for the action of the standard-ansatz Lie algebra $\mathfrak{g}_{\mathrm{std}}$?

Appendix B1 introduces a basis change $h \circ \pi_n \circ h$ that transforms the projectors $P_{\pm} = (X^{\otimes n} \pm I^{\otimes n})/2$ into the respective block-diagonal form $I^{\otimes (n-1)} \oplus 0^{\otimes (n-1)}$ and $0^{\otimes (n-1)} \oplus I^{\otimes (n-1)}$. Moreover, the generators H_p and H_m of $\mathfrak{g}_{\mathrm{std}}$ are also transformed into their block-diagonal form $H_p^+ \oplus H_p^-$ and $H_m^+ \oplus H_m^-$, where H_j^+ and H_j^- for $j \in \{p, m\}$ are respectively the upper-left and lower-right components. After these preparations, the Lie algebra

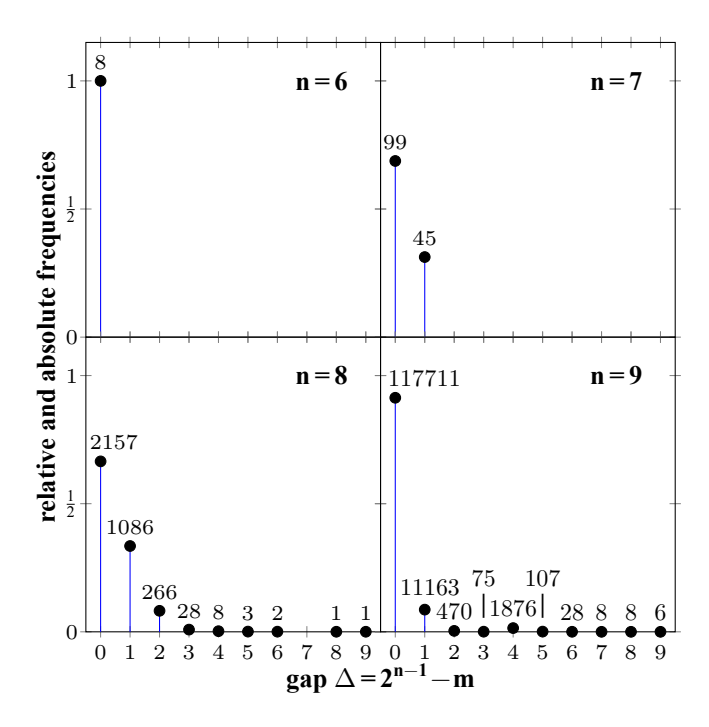


Figure 9. Relative and absolute frequencies for the gap Δ of connected asymmetric graphs with n vertices. The gap concentrates at small values and is tightly bounded.

acting on the upper-left block is defined as

$$\mathfrak{g}_{\mathrm{std}}^+ := \langle H_p^+, H_m^+ \rangle_{\mathrm{Lie}}, \ \ \mathrm{where} \ \ \mathcal{C}_{\mathrm{std}}^+ := \mathfrak{com}(\mathfrak{g}_{\mathrm{std}}^+)$$

is its commutant. Let \mathbf{m} denote the largest dimension of the invariant subspaces of $\mathfrak{g}_{\mathrm{std}}^+$ and the gap from the case of $\mathfrak{g}_{\mathrm{nat}}$ for connected asymmetric graphs is given by

$$\Delta := \mathbf{m}_{(\mathbf{t},\mathbf{t})} - \mathbf{m} = 2^{n-1} - \mathbf{m}. \tag{41}$$

The graph in Fig. 8 with nine vertices yields a largest dimension of $\mathbf{m}=247$ for the action of $\mathfrak{g}_{\mathrm{std}}^+$ and a gap of $\Delta=9=2^{9-1}-\mathbf{m}$. In this example, one observes irreducible subspaces with a dimension larger than one as a consequence of hidden symmetries. Thus additional symmetries beyond natural ones appearing in the standard ansatz cannot be fully explained by quantum many-body scars [112–114] connected to one-dimensional invariant subspaces as discussed at the end of Sec. V.

Figure 9 presents data on values for the gap Δ of connected asymmetric graphs and $6 \le n \le 9$. One observes that the gap concentrates at small values and it is tightly bounded, at least for $n \le 9$. This offers only very limited data, but the difference between the cases of $\mathfrak{g}_{\rm nat}$ and $\mathfrak{g}_{\rm std}$ (as quantified by Δ) is quite small. Similarly, the corresponding dimensions $\dim(\mathcal{C}_{\rm std}^+)$ and $\dim[\mathcal{Z}(\mathcal{C}_{\rm std}^+)]$ for the commutant and its center are detailed in Table IV. Thus the dimension of the commutant $\mathcal{C}_{\rm std}^+$ is much more frequently small than large. Also, the dimension of the center $\mathcal{Z}(\mathcal{C}_{\rm std}^+)$ appears to be quite restricted. One might suggest that Δ will stay polynomially bounded in n:

Table IV. Frequencies for $\dim(\mathcal{C}^+_{\mathrm{std}})$ and $\dim[\mathcal{Z}(\mathcal{C}^+_{\mathrm{std}})]$ of connected asymmetric graphs with n vertices. There are 8, 144, 3552, and 131452 of these graphs for $6 \leq n \leq 9$.

\overline{n}	Frequer	icies for	dim($\mathcal{C}^+_{\mathrm{std}}$	and	dim[$\mathcal{Z}(\mathcal{C}$	(+ (std)	
	$\dim(\mathcal{C}_{\mathrm{std}}^+) = 1$	2	3	4	5	6	7	9	10
6	8								
7	99	45							
8	2157	1086	136		130	13	1	1	15
9	117711	11163	927	708	422	229	42	1	69
	$\dim(\mathcal{C}_{\mathrm{std}}^+) = 11$	12	13	14	17	18	20	21	26
8	4			1	2	2		1	
9	107	8	3	1	20	12	1		10
	$\dim(\mathcal{C}_{\mathrm{std}}^+) = 27$	29	37	38	50	51	65	66	82
8			1				1		1
9	6	1	2	4	2	2		1	
	$\dim[\mathcal{Z}(\mathcal{C}_{\mathrm{std}}^+)] = \ 1$	2	3	4	5				
6	8								
7	99	45							
8	2157	1236	158	1					
9	117711	11680	1287	772	2				

Conjecture 1. Consider the standard ansatz for connected asymmetric graphs with n vertices. The gap Δ as defined in Eq. (41) is polynomially bounded in n.

But, from this data, it is equally possible that Δ will eventually approach the magnitude of 2^{n-1} as n grows. Still, assuming a polynomially bounded Δ , several situations of interest could occur. On the one hand, if the state fully (or partially) belong to one of the polynomially sized subspace, then the action of QAOA could likely be simulated therein [27, 133]. Then, if the state belongs to an exponentially large invariant subspace, and we have full control in this invariant subspace, similar arguments as in Appendix D would imply the existence of barren plateaus (for quantum circuits with enough layers). We leave these questions to future work.

X. CONNECTION TO THE LITERATURE

Given that our work has some overlap with other recent manuscripts, we begin by first discussing how our work connects to the existing literature. First, we recall that Ref. [35] recently provided a characterization of all Lie algebras generated by Pauli operators based on frustration graph techniques [134]. While our Lie algebras for the multi-angle case are contained within the families derived in [35], the classification based on simple properties of a graph as the one presented here is less clear from the optics of frustration graphs, therefore making our results easier to follow from a maxcut perspective.

Then, shortly before our work was finalized, the work of Ref. [37] presented a classification for Lie algebras gen-

erated by spin interactions on undirected graphs using an approach based on interaction graphs. The results in [37] are very close to ours in the sense that the generators are composed from single-qubit operators over vertices of a graph, and of two-qubit operators defined over the vertices of a graph. As such, the results of Theorem 1 are a special case of those in Ref. [37] for special choices of operators (i.e., X on vertices and ZZ on edges). Still, while Ref. [37] characterizes the Lie algebras, our work goes beyond these results as we provide an in-depth description of the symmetries and invariant subspaces, isomorphisms, as well as explicit bases for the Lie algebras.

Here, we also remark that Refs. [35, 37] only consider Pauli generators, and not summations thereof. In this context, we instead recall that Ref. [36] does study Lie algebras for the standard mixer (although they do not consider the multi-angle QAOA ansatz). Therein, the authors present an upper bound on the dimension of the standard Lie algebra by defining a Lie algebra that respects the automorphisms of the considered graph. In this sense, our upper bound of Proposition 2 in terms of the natural Lie algebra (which respects automorphism group and parity) is in general tighter than that of Ref. [36]. But our and their upper bound agree for the complete graph as they consider further symmetries (as we do). The results of [34, 36] for cycle graphs and of [36] for complete graphs go beyond the upper bounds presented in our work. The path graphs are not considered in [34, 36]. For the cycle graphs, we also point the reader to the work of Onsager [44].

XI. DISCUSSION

Computing the Lie algebra of parametrized circuits has become a central and important tool for the study and characterization of variational quantum models. In this context, our work contributes to this body of knowledge by evaluating the Lie algebras for three QAOA ansätze. Our main result constitute a full characterization of the multi-angle Lie algebra for arbitrary circuits. Then, we argue that the presence of hidden symmetries for the orbit and the standard ansätze will likely make a general classification unlikely. Here, we instead define the natural Lie algebra—which respects only the natural symmetries—and use it to upper bound the dimension of the orbit and the standard-ansatz Lie algebras. Importantly, we find evidence that the largest component of the invariant subspaces of the standard-ansatz Lie algebra is of very similar dimension to that of the natural Lie algebra (i.e., their difference may be only polynomially in the number of vertices), and conjecture that this result could hold for the vast majority of graphs.

Our results have several important implications for QAOA, as well as for variational algorithms in general. On the one hand, we show that the multi-angle QAOA ansatz leads to exponentially large Lie algebras, and therefore is extremely prone to exhibiting trainability

barriers such as barren plateaus, even when the circuit contains a single layer. Then, if our conjecture is true, this would mean that the standard QAOA Lie algebra has only exponentially large, or polynomially small components. In this case, the prospects of QAOA become bleak as its action on the polynomial subspace could be classically simulable, while that in the exponentially large subspace could be prone to barren plateaus. As QAOA can likely only significantly outperform state-of-the-art classical methods with a deep enough circuit [135], one would almost be guaranteed to have untrainable models in the regimes where they become truly useful.

A caveat to this argument is the fact that barren plateaus are an average statement that hold for randomly initialized circuits, whereas smart initialization techniques could avoid such average-case issues [9]. Indeed, [46–48, 50, 51] have proposed pre-optimized initial angles for D-regular graphs. This is possible as measured cut values concentrate—in the infinite vertex limit—tightly around maxima both with repeated measurements and varying graph instances [46–49, 136–138]. For this analysis, properties of *D*-regular graphs are connected (in the infinite vertex limit) with the Sherrington-Kirkpatrick model of complete graphs with randomly weighted edges [46-49, 51, 139] (refer to [140] for a review). In particular, the optimal angles for the problem Hamiltonian in Eq. (5a) are rescaled with $1/\sqrt{D}$ as D increases while the angles for the mixer Hamiltonian in Eq. (5b) are not rescaled [46–49]. For proving this, the D-regular graph is assumed to be similar to a tree, where its girth (which is the length of its shortest cycle) is larger than 2L+1 for L layers. The effect of rescaling the optimal angles for the problem Hamiltonian can be clearly seen, e.g., in Figure 9 of [104] where the size of the barren plateau is increasing with D. A similar effect is apparent in Figure 3 of Sec. IV. The rescaling can thus be interpreted as a concentration of the cut values with respect to variations in the angles for large-girth D-regular graphs in the infinite vertex limit.

All of this nicely fits with barren plateaus for the cut value where the variance in the angles vanishes exponentially fast with the number of vertices. Thus our work aims at arbitrary connected graphs (and particularly asymmetric ones) and not only at *D*-regular ones with a large girth. Even though barren plateaus have only been shown for the multi-angle ansatz, our work prepares the ground for a more general symmetry analysis. Connections to the study of smart-initializations are left for future work.

More generally, there has been a string of recent work highlighting limitations of QAOA [137, 141–148], e.g., as a result of clustering of solutions [142, 144], or the fact that QAOA can be outperformed by quantum walks [148], or the detrimental effect of intrinsic shot noise in the measurements for the optimization [146], or by quantum-inspired classical algorithms [145, 147]. On the classical side, there exists highly competitive algorithms [149–154], also including approximation algo-

rithms [62, 63, 155–159]. Moreover, there has been a revolution in solving satisfiability problems (to which maxcut can be reduced to) [160, 161]. This means that QAOA is under pressure due to its seeming limitations and its strong classical competition.

Then, another important implication of our work is the fact that it unveils the crucial importance of the encoding scheme used to embed classical problems in quantum ones. Indeed, while the standard maxcut encoding seems extremely simple and natural, as it uses local operators that respect the parity superselection rule and graph automorphisms, it also leads to hidden symmetries. These spurious symmetries, in turn, lead to unexpected invariant subspaces. Critically, the understanding of these symmetries, and their ensuing effects on the irreducible decompositions, is crucial, as they could avoid using initial states that are not mostly constrained to some subspace which could potentially have a small (or no) overlap with the solution manifold.

Indeed, our work also contributes to developing symmetry tools for a systematic analysis of variational quantum algorithms. Building on tools from [20, 28, 125, 162– 164], our symmetry analysis can be seen as an initial step towards a better understanding of variational quantum algorithms and their strengths and limitations. For QAOA, our work connects methods based on graph automorphisms as in [165, 166] with their impact on the symmetries of the full Hilbert space. We have modeled this using our natural symmetries, also incorporating the parity-superselection operator $X^{\otimes n}$. The presence of hidden symmetries is often related to one-dimensional invariant subspaces and this is curiously connected to quantum many-body scars [112–114], for which one-dimensional invariant subspaces are a necessary condition. Figure 8 highlights an example with hidden symmetries resulting in invariant subspaces of dimension larger than one which cannot be fully explained by quantum many-body scars.

The graph properties also play an important role at the interplay between symmetry and locality and this interplay has been extensively studied in recent years [32, 45, 122, 167, 168]. Thus local unitaries that act only on a fixed number of qubits at a time and that also respect a certain symmetry group cannot in general generate all unitaries that respect that symmetry group, which is in contrast to the universality of one- and two-qubit quantum gates [123, 124]. Such locality restrictions (as studied in [20, 33, 125, 169]) are also exemplified by the parity-superselection symmetry operator $X^{\otimes n}$: it is not contained in the multi-angle Lie algebra, despite obviously respecting its symmetries. This can be understood as a limitation on the control of the relative phase between the even-parity and odd-parity sectors [122]. Or in a more algebraic interpretation, the center of the Lie algebra is highly constraint which has been identified as a potential limitation for the ability to simulate certain quantum dynamics [28]. Section VI highlights the intricacies related to the role that the center of the Lie algebra plays in the hierarchy of QAOA ansätze.

In the grander scheme of things, we believe that our work bring a new and fresh perspective to the Lie-algebra analysis of quantum circuits through the optics of symmetries. As such, we hope that the insights presented here could serve as guiding principle towards the final frontier: Lie algebras that arise from generators expressed as sums of Paulis.

ACKNOWLEDGMENTS

RZ thanks Thomas Schulte-Herbrüggen, Zoltán Zimborás, and Michael Keyl for many discussions and insights on symmetries of controlled quantum systems. RZ also appreciates the illuminating discussions with Armin Römer and Juhi Singh on related projects as well as with Nikkin Devaraju on the original work of [1]. Last but not least, RZ thanks Roberto Gargiulo for many closely related discussions which have also led to the follow-up work [170]. We acknowledge computations with the computer algebra system MAGMA [80].

SK acknowledges initial support by the U.S. DOE through a quantum computing program sponsored by the LANL Information Science & Technology Insti-ML was also supported by the Center for Nonlinear Studies at Los Alamos National Laboratory (LANL). ML and MC acknowledge support by the Laboratory Directed Research and Development (LDRD) program of LANL under project numbers 20230049DR and 20230527ECR. MC was initially supported by LANL's ASC Beyond Moore's Law project. RZ acknowledges funding under Horizon Europe programme HORIZON-CL4-2022-QUANTUM-02-SGA via the project 101113690 (PASQuanS2.1) and from the European High-Performance Computing Joint Undertaking (JU) under grant agreement No 101018180 (HPCQS). The JU receives support from the European Union's Horizon 2020 research and innovation programme and Germany, France, Italy, Ireland, Austria, Spain.

Appendix A: Methods for analyzing symmetries

1. Symmetries and isotypical decomposition

We extend Section IIB by further detailing how to analyze symmetries while pointing to the house graph and the explicit information in Table I (see also Fig. 5). Recall that $\mathfrak{g} = \langle i\mathcal{G} \rangle_{\text{Lie}}$ denotes the (real) Lie algebra generated from a set \mathcal{G} of hermitian generators. Note that \mathfrak{g} is contained in the Lie algebra $\mathfrak{u}(d) \subseteq \mathbb{C}^{d \times d}$ of skew-hermitian matrices for $d = 2^n$. We obtain the Lie group $\exp(\mathfrak{g}) \subseteq \mathbb{U}(d)$ which is contained in the unitary group.

The linear symmetries have been specified by the commutant $\mathcal{C} = \mathfrak{com}(\mathcal{G})$ [see Eq. (8)] which is closed under complex-linear combinations and matrix multiplication. We also introduce the matrix algebra $\mathcal{A} = \langle \mathcal{G} \rangle_{\mathbb{C}} = \langle i\mathcal{G} \rangle_{\mathbb{C}}$

that contains all complex-linear combinations of the identity matrix $\mathbb{1}_d \in \mathbb{C}^{d \times d}$ and arbitrary products of generators in \mathcal{G} . The properties

$$C = com(A) = com(G) = com(g)$$
 and (A1)

$$\mathcal{A} = \mathfrak{com}(\mathcal{C}) = \mathfrak{com}(\mathfrak{com}(\mathcal{A})) \neq \mathfrak{g} \tag{A2}$$

establish a duality between \mathcal{A} and \mathcal{C} . Equation (A2) is the double commutant property of \mathcal{A} . We point to textbooks in algebra [171–174] and representation theory [175–177] as well as original work by Emmy Noether [178–180], which has been publicized by Bartel Leendert van der Waerden [181] and Hermann Weyl [182, 183].

The invariant subspaces induced by the actions of \mathcal{G} , \mathcal{A} , \mathfrak{g} , and $\exp(\mathfrak{g})$ all agree and they decompose into irreducible subspaces as $\exp(\mathfrak{g})$ is contained in the unitary group. Moreover, the centers $\mathcal{Z}(\mathcal{A}) = \mathcal{Z}(\mathcal{C}) = \mathcal{A} \cap \mathcal{C}$ are equal, where [generalizing the definition in Eq. (9)]

$$\mathcal{Z}(\mathcal{M}) = \{ Z \in \mathcal{M} \text{ s.t. } [Z, M] = 0 \text{ for all } M \in \mathcal{M} \}.$$

This implies that the actions of \mathcal{A} and \mathcal{C} induce the same isotypical decomposition $\mathbb{C}^d = \oplus_{\lambda} \mathcal{I}_{(\lambda)}$ as described now: An isotypical decomposition consists of invariant subspaces $\mathcal{I}_{(\lambda)}$ that are the direct sum of all irreducible subspaces isomorphic to one particular irreducible subspace. The isotypical decomposition refines in general into the irreducible decomposition. However, for the free and the standard ansatz corresponding to the house graph (see Table I and Fig. 5), the isotypical and the irreducible decomposition coincide and one respectively obtains $\mathbb{C}^{16} \oplus \mathbb{C}^{16}$ and $\mathbb{C}^{10} \oplus \mathbb{C}^5 \oplus \mathbb{C} \oplus \mathbb{C}^{10} \oplus \mathbb{C}^5 \oplus \mathbb{C}$. Also, the matrix algebra \mathcal{A} is respectively isomorphic to $\mathbb{C}^{16 \times 16} \oplus \mathbb{C}^{16 \times 16}$ and $\mathbb{C}^{10 \times 10} \oplus \mathbb{C}^{5 \times 5} \oplus \mathbb{C}^{1 \times 1} \oplus \mathbb{C}^{10 \times 10} \oplus \mathbb{C}^{5 \times 5} \oplus \mathbb{C}^{1 \times 1}$ and it has the respective dimension 512 and 252.

But the fine structure in the isotypical components $\mathcal{I}_{(\lambda)}$ differs for the action of \mathcal{A} and \mathcal{C} as $\mathcal{I}_{(\lambda)}$ contains irreducible subspaces isomorphic to $\mathcal{I}_{\lambda}^{\mathcal{A}}$ and $\mathcal{I}_{\lambda}^{\mathcal{C}}$ with

$$m_{\lambda} := \operatorname{mult}(\mathcal{I}_{\lambda}^{\mathcal{A}}, \mathbb{C}^{d}) = \operatorname{dim}(\mathcal{I}_{\lambda}^{\mathcal{C}}),$$

$$d_{\lambda} := \operatorname{dim}(\mathcal{I}_{\lambda}^{\mathcal{A}}) = \operatorname{mult}(\mathcal{I}_{\lambda}^{\mathcal{C}}, \mathbb{C}^{d}).$$

Here, the *multiplicity* $\operatorname{mult}(\mathcal{J}, \mathcal{I})$ counts how many times an irreducible \mathcal{J} is equivalent to an irreducible \mathcal{I}_j in the decomposition $\mathcal{I} = \bigoplus_j \mathcal{I}_j$. The dimensions d_{λ} and multiplicities m_{λ} are determined by the commutant \mathcal{C} . Complementing Eq. (10), we have

$$\mathcal{A} \simeq \bigoplus_{\lambda=1}^{\dim[\mathcal{Z}(\mathcal{C})]} \mathbb{1}_{m_{\lambda}} \otimes \mathbb{C}^{d_{\lambda} \times d_{\lambda}}.$$

We now discuss a few prototypical examples in order to highlight the intricacies in identifying Lie algebras and their representations via their linear symmetries. We first consider three two-qubit examples which stress that the Lie algebra $\mathfrak g$ is not uniquely determined even if the gen-

erators act irreducibly, i.e., even if $\dim(\mathcal{C}) = 1$ [20]. Let

$$\mathcal{G}_a := \mathcal{G}_b \cup \{Z_1 Z_2\}, \ \mathcal{G}_b := \{X_1, X_2, Z_1, Z_2\}, \text{ and}$$

$$\mathcal{G}_c := \{ \begin{pmatrix} 0 & \sqrt{3}/2 & 0 & 0 \\ \sqrt{3}/2 & 0 & 1 & 0 \\ 0 & 1 & 0 & \sqrt{3}/2 \\ 0 & 0 & \sqrt{3}/2 & 0 \end{pmatrix}, \begin{pmatrix} 3/2 & 0 & 0 & 0 \\ 0 & 1/2 & 0 & 0 \\ 0 & 0 & -1/2 & 0 \\ 0 & 0 & 0 & -32 \end{pmatrix} \}$$

denote the corresponding generators. We obtain three different Lie algebras of dimension 15, 6, and 3 which are isomorphic to $\mathfrak{su}(4)$, $\mathfrak{su}(2) \oplus \mathfrak{su}(2)$, and $\mathfrak{su}(2)$. We detail how these Lie algebras are irreducibly embedded into $\mathbb{C}^{4\times 4}$. Recall the standard representation κ of a Lie algebra. For the three examples, the representations are κ , $\kappa \otimes \kappa$, and the spin-3/2 representation, respectively. Here,

$$(\gamma \otimes \tilde{\gamma})(g, \tilde{g}) := \gamma(g) \otimes \mathbb{1}_{\dim(\tilde{\gamma})} + \mathbb{1}_{\dim(\gamma)} \otimes \tilde{\gamma}(\tilde{g})$$

is the tensor product of the representations γ and $\tilde{\gamma}$ for the Lie algebras \mathfrak{k} and $\tilde{\mathfrak{k}}$ with $g \in \mathfrak{k}$ and $\tilde{g} \in \tilde{\mathfrak{k}}$. In summary, the examples \mathcal{G}_a , \mathcal{G}_b , and \mathcal{G}_c illustrate three prototypical variants on how generators and the generated Lie algebra can act irreducibly.

Extending the discussion from an irreducible action to a block-diagonal action with two blocks, we examine three three-qubit examples with an irreducible decomposition $\mathbb{C}^4 \oplus \mathbb{C}^4$. The corresponding generators are

$$\begin{split} \mathcal{G}_d &:= \{X_2, X_3, Z_2, Z_3, Z_2 Z_3\} \times (\mathbb{1}_8 \pm Z_1), \\ \mathcal{G}_e &:= \{X_2, X_3, Z_2, Z_2 Z_3, Z_1 X_2 X_3\}, \\ \mathcal{G}_f &:= \{X_2, X_3, Z_2, Z_3, Z_2 Z_3\}. \end{split}$$

For the first two examples, $\dim(\mathcal{C}) = \dim(\mathcal{Z}(\mathcal{C})) = 2$ and the isotypical and the irreducible decompositions agree. We have $\dim(\mathcal{C}) = 4$ and $\dim(\mathcal{Z}(\mathcal{C})) = 1$ for the third example. This results in an isotypical decomposition with a single isotypical component \mathbb{C}^8 which contains the irreducible component \mathbb{C}^4 with multiplicity two. The corresponding Lie algebras have dimensions 30, 15, and 15 and are isomorphic to $\mathfrak{su}(4) \oplus \mathfrak{su}(4)$, $\mathfrak{su}(4)$, and $\mathfrak{su}(4)$. We obtain the respective representations $[\kappa \otimes \epsilon] \oplus [\epsilon \otimes \kappa]$, $\kappa \oplus \overline{\kappa}$, and $\kappa \oplus \kappa$. Here, ϵ denotes the trivial representation and $\overline{\gamma}$ is the dual of a representation γ . One observes characteristic differences and that even the isomorphic Lie algebras of \mathcal{G}_e and \mathcal{G}_f are represented differently.

With all these examples, it is evident that linear symmetries and the commutant will be in general not sufficient to resolve the intricate structure of possibly occurring Lie algebras. Additional techniques are required to analyze general dynamical quantum systems. The intuition leading to the results in Appendices B and C for the free-mixer ansatz is to certain degree based on so-called quadratic symmetries [20, 28, 162–164].

2. Details on natural and hidden symmetries

In this subsection, we further discuss the structure of natural and hidden symmetries following the approach (a) Graph G, automorphisms $\operatorname{Aut}(G)$, symmetries $\mathcal{C}_{\operatorname{std}}$, center $\mathcal{Z}(\mathcal{C}_{\operatorname{std}})$:

$$\begin{array}{ll} \text{Aut}(G) \!=\! \langle (1,2), (3,4) \rangle_{\text{group}} \text{ with } |\text{Aut}(G)| \!=\! 4 \\ \mathcal{C}_{\text{std}} \!=\! \text{span}_{\mathbb{C}} \{P_1, P_{2.1}, P_{2.2}, P_3, P_4, P_5, P_6, P_7, C_2^{1|2}, C_2^{2|1} \} \\ \mathcal{Z}(\mathcal{C}_{\text{std}}) \!=\! \text{span}_{\mathbb{C}} \{P_1, P_{2.1} \!+\! P_{2.2}, P_3, P_4, P_5, P_6, P_7 \} \end{array}$$

(b) Invariant-subspace decomposition of symmetries:

$$\begin{split} |\phi_{2.2}\rangle &= + |0001\rangle - |0010\rangle - |1101\rangle + |1110\rangle \\ |\phi_{3}\rangle &= + |0100\rangle - |0111\rangle - |1000\rangle + |1011\rangle \\ |\phi_{6}\rangle &= + |0001\rangle - |0010\rangle + |0101\rangle - |0110\rangle \\ &+ |1001\rangle - |1010\rangle + |1101\rangle - |1110\rangle \\ |\phi_{7}\rangle &= + |0001\rangle - |0010\rangle - |0101\rangle + |0110\rangle \\ &- |1001\rangle + |1010\rangle + |1101\rangle - |1110\rangle \end{split}$$

(c) Natural and hidden symmetries:

$$\begin{split} \text{Basis } \mathcal{B}_{\text{ext}} = \{ I^{\otimes 4}, \ X^{\otimes 4}, \ \zeta[(1,2)], \ \zeta[(3,4)], \ \zeta[(1,2)(3,4)], \\ X^{\otimes 4}\zeta[(1,2)], \ X^{\otimes 4}\zeta[(3,4)]; \ P_6, \ C_2^{1|2}, \ C_2^{2|1} \} \end{split}$$

Figure 10. Symmetry decomposition of a standard-ansatz QAOA example. Notation as in Fig. 5, but we discuss a case that is not multiplicity-free: the isotypical projector (see App. A1) $P_{2.1}+P_{2.2}$ splits into the projectors $P_{2.1}$ and $P_{2.2}$ and cross terms $C_2^{k|\ell}$ appear in $\mathcal{C}_{\mathrm{std}}$ (see also Fig. 17 in App. H). Relevant parts are marked in blue in (a) and (b). For the natural symmetries in (c), $X^{\otimes 4}\zeta[(1,2)(3,4)]$ does not appear in the basis of natural symmetries $\mathcal{S}_{\mathrm{nat}}$ as it is linear dependent to the other basis elements. Thus $\dim(\mathcal{S}_{\mathrm{nat}}) < 2|\mathrm{Aut}(G)|$.

of Sec. V. To this end, we consider the symmetry decomposition in a more intricate standard-ansatz QAOA example following Fig. 10. Here, we also rely on the isotypical decomposition as detailed in Appendix A 1 and the corresponding isotypical projectors that project onto the respective isotypical component.

Figure 10 highlights a four-vertex graph with an automorphism group consisting of four elements. The symmetries given by the commutant C_{std} are ten dimensional, while the corresponding center $\mathcal{Z}(C_{\text{std}})$ is seven dimensional. We observe that the isotypical projector $P_{2.1}+P_{2.2}$ splits into the one-dimensional projectors $P_{2.1}$ and $P_{2.2}$, which are explicitly specified in Fig. 10(b). This implies that the corresponding representation is not multiplicity-free, i.e., the multiplicity m_{λ} in the decom-

position of Eq. (10) is not equal to one. Moreover, cross terms $C_2^{k|\ell}$ appear in $\mathcal{C}_{\mathrm{std}}$ as specified in Fig. 10(b). As for the example of the house graph in Fig. 5, the basis change in Fig. 10(d) clarifies that the division into natural and hidden symmetries is not unique. The red, nonzero entries in the third-last row of Fig. 10(d) show that both P_6 and P_7 are hidden symmetries, but P_6 and P_7 are—up to natural symmetries—linear-dependent. The projectors $P_{2.1}$, $P_{2.2}$, and P_3 are examples of one-dimensional projectors that are part of the natural symmetries as one can infer from the basis change in Fig. 10(d). Even this simple, low-dimensional example makes the intricate structure of standard-ansatz symmetries and their variability evident.

We finally characterize the one-dimensional projectors and the corresponding cross terms in Fig. 10 while utilizing the corresponding simultaneous eigenvectors $|\psi_j\rangle$ for a given set of Hamiltonians $\mathcal G$ following Eq. (20) in Section V. In particular,

$$H |\psi_i\rangle = \beta(H, |\psi_i\rangle) |\psi_i\rangle$$
 holds for every $H \in \mathcal{G}$.

Clearly, the one-dimensional subspace spanned by the vector $|\psi_j\rangle$ is invariant under the action of every H and the same holds for its orthogonal complement. Thus one verifies H $|\psi_j\rangle\langle\psi_j|-|\psi_j\rangle\langle\psi_j|\,H=0$ and the simultaneous eigenvectors $|\psi_j\rangle$ can be chosen as part of an orthogonal basis. One immediately obtains

$$\begin{split} &(H \mid \psi_{j} \rangle \langle \psi_{k} \mid - \mid \psi_{j} \rangle \langle \psi_{k} \mid H) \mid \psi_{k} \rangle \\ &= H \langle \psi_{k} \mid \psi_{k} \rangle \mid \psi_{j} \rangle - \mid \psi_{j} \rangle \langle \psi_{k} \mid \beta(H) \mid \psi_{k} \rangle \\ &= \left[\beta(H, \mid \psi_{j} \rangle) - \beta(H, \mid \psi_{k} \rangle) \right] \langle \psi_{k} \mid \psi_{k} \rangle \mid \psi_{j} \rangle \end{split}$$

and it follows that $|\psi_j\rangle\langle\psi_k|$ is in the commutant of $\mathcal G$ if and only if the eigenvalues $\beta(H,|\psi_j\rangle)$ and $\beta(H,|\psi_k\rangle)$ are equal for each $H\in\mathcal G$. In other words, the eigenvalues $\beta(H,|\psi_j\rangle)$ of the simultaneous eigenvectors $|\psi_j\rangle$ can used to uniquely identify the corresponding one-dimensional representations up to multiplicity.

Appendix B: Analysis of the free-mixer ansatz

This appendix proves Theorem 1 and thereby determines the free-mixer Lie algebras for connected graphs. We then establish the free-mixer Lie algebras for the particular cases of path graphs (see Thm. 2), cycle graphs (see Thm. 3), connected bipartite graphs different from path and cycle graphs (see Thm. 4), as well as connected non-bipartite graphs different from cycle graphs (see Thm. 5). The results are summarized in Table V, while the general discussion of explicit Pauli string bases is deferred to Appendix C1. We start with some preliminaries in Appendix B1 and summarize two techniques to characterize Lie algebras in Appendix B2 where the first technique is applicable if the Lie algebra acts irreducibly and the second one is based on maximal subalgebras. Path and cycle graphs are then treated in Appendix B3,

while Appendix B 5 contains the most extensive discussion detailing the case of bipartite graphs. The non-bipartite graphs are considered in Appendix B 6. The explicit representations connected to the various cases of free-mixer Lie algebras are determined in Appendices B 4 and B 7. The approach in this appendix is complemented in Appendix C with a focus on bases of Pauli strings and their relation to edges of graphs.

Some of the results and the applied techniques are reminiscent of those in [20, 125]. In particular, the maximal Lie algebra $\mathfrak{su}(2^{n-1}) \oplus \mathfrak{su}(2^{n-1})$ (see Lemma 16 and Thm. 5) is reflected in the parity superselection rule for fermionic systems as discussed in [125, 184, 185]. For path and cycle graphs, we obtain the free-mixer Lie algebras $\mathfrak{so}(2n)$ and $\mathfrak{so}(2n) \oplus \mathfrak{so}(2n)$ with their particular embeddings into $\mathfrak{su}(2^n)$, which manifest as spinor representations of the orthogonal group [186] and which are widely encountered as symmetries in physics [187–194].

1. Preliminaries

In Appendices B and C, G denotes a graph and V its vertex set, which is usually given by $\{1,\ldots,n\}$, while n:=|V| and $E\subset V\times V$ describes the edge set (and similarly for graphs \tilde{G} and \bar{G}). Let $X,Y,Z\in\mathbb{C}^{2\times 2}$ denote the Pauli operators and $I\in\mathbb{C}^{2\times 2}$ the identity operator. The corresponding operators acting on the u-th qubit are $X_u,Y_u,Z_u,I_u\in\mathbb{C}^{2^n\times 2^n}$, e.g. $X_u:=I^{\otimes u-1}\otimes X\otimes I^{\otimes n-u}$. We will usually represent a Lie algebra $\mathfrak{g}\subseteq\mathfrak{u}(2^n)$ explicitly by $2^n\times 2^n$ skew-hermitian matrices [and similarly for $\mathfrak{g}\subseteq\mathfrak{su}(2^n)$]. In this work, a Pauli string is given by a tensor-product operator of the form $P_j=\bigotimes_{u\in V}A_u$ with $A_u\in\{X,Y,Z,I\}$ and the corresponding Lie-algebra element is iP_j . As in Section III, the free-mixer Lie algebra for a connected graph with $n\geqslant 2$ is given by

$$\mathfrak{g}_{\text{free}} := \langle iX_u \text{ for } u \in V; \ iZ_uZ_v \text{ for } \{u,v\} \in E \rangle_{\text{Lie}} \quad (B1)$$

$$= \langle iX_u \text{ for } u \in V; \sum_{\{u,v\} \in E} iZ_uZ_v \rangle_{\text{Lie}} =: \tilde{\mathfrak{g}}_{\text{free}}. \quad (B2)$$

The generators iZ_uZ_v span $\sum_{\{u,v\}\in E}iZ_uZ_v$ and $\mathfrak{g}_{\text{free}}\supseteq \tilde{\mathfrak{g}}_{\text{free}}$. Given an edge $(a,b)\in E$, $[iX_b,[iX_a,[iX_b,[iX_a,\sum_{\{u,v\}\in E}iZ_uZ_v]]]]=16iZ_aZ_b$ and $\mathfrak{g}_{\text{free}}=\tilde{\mathfrak{g}}_{\text{free}}$. Having defined $\mathfrak{g}_{\text{free}}$, we prove its following properties

Lemma 15. (a) The set $\mathfrak{com}(\mathfrak{g}_{\text{free}})$ of complex matrices commuting with $\mathfrak{g}_{\text{free}}$ is spanned by $I^{\otimes n}$ and $X^{\otimes n}$. (b) $iI^{\otimes n}, iX^{\otimes n} \notin \mathfrak{g}_{\text{free}}$. (c) The center $\mathcal{Z}(\mathfrak{g}_{\text{free}}) := \mathfrak{com}(\mathfrak{g}_{\text{free}}) \cap \mathfrak{g}_{\text{free}}$ of $\mathfrak{g}_{\text{free}}$ is trivial and $\mathfrak{g}_{\text{free}}$ is semisimple.

Proof. Clearly, $I^{\otimes n}$ and $X^{\otimes n}$ commute with all generators of $\mathfrak{g}_{\text{free}}$. All elements $S = \sum_j c_j P_j$ of $\mathfrak{com}(\mathfrak{g}_{\text{free}})$ with $0 \neq c_j \in \mathbb{C}$ can be expanded into Pauli strings $P_j = \otimes_{u \in V} A_u$ with $A_u \in \{X, Y, Z, I\}$. For the Pauli strings P_k and $P_{j_1} \neq P_{j_2}$, $[P_k, P_{j_1}]$ and $[P_k, P_{j_2}]$ are either linearly independent or at least one commutator is zero. We obtain $[S, P_k] = 0$ iff $[P_j, P_k] = 0$ for all P_j ,

hence $[S, \mathfrak{g}_{free}] = 0$ iff $[P_j, \mathfrak{g}_{free}] = 0$ for all P_j as all generators of $\mathfrak{g}_{\text{free}}$ in Eq. (B1) are of tensor-product form. Thus we can restrict elements of $\mathfrak{com}(\mathfrak{g}_{free})$ to the form of $S = \bigotimes_{u \in V} A_u$. However, $A_u = Y$ or $A_u = Z$ for any *u* implies $[S, iX_u] \neq 0$. Thus $S = \bigotimes_{u \in V} A_u$ with $A_u \in \{X, I\}$. Now let $A_u = I$ and $A_v = X$ for two $u \neq v$. As the graph is connected, there is a vertex path $u = u_1, u_2, \dots, u_m = v \text{ using edges } \{u_a, u_{a+1}\}$ and there exists an index $1 \leq \ell \leq m-1$ such that $A_{u_{\ell}} = I$ and $A_{u_{\ell+1}} = X$. This implies $[S, iZ_{u_{\ell}}Z_{u_{\ell+1}}] \neq 0$ which proves (a). Recall that $\mathfrak{u}(2^n)$ and all its subalgebras \mathfrak{g} (such as \mathfrak{g}_{free}) are compact Lie algebras and decompose as $\mathfrak{g} = [\mathfrak{g}, \mathfrak{g}] \oplus \mathcal{Z}(g)$ into their semisimple part $[\mathfrak{g}, \mathfrak{g}]$ and their center $\mathcal{Z}(g)$ [77, 78]. Also, $iI^{\otimes n}$ and $iX^{\otimes n}$ (and any reallinear combination thereof) can only be in \mathfrak{g}_{free} if they are in its center $\mathcal{Z}(\mathfrak{g}_{\text{free}}) = \mathfrak{com}(\mathfrak{g}_{\text{free}}) \cap \mathfrak{g}_{\text{free}}$. As all projections of generators in Eq. (B1) onto either $iI^{\otimes n}$ or $iX^{\otimes n}$ are zero, all generators are contained in the semisimple part $\mathfrak{s} := [\mathfrak{g}_{\text{free}}, \mathfrak{g}_{\text{free}}]$. As $[\mathfrak{s}, \mathfrak{s}] \subseteq \mathfrak{s}$ [77], we cannot generate any potential nonzero element of $\mathcal{Z}(\mathfrak{g}_{\text{free}})$. Alternatively, the zero dimensionality of the center $\mathcal{Z}(\mathfrak{g}_{\text{free}})$ can also be verified using Lemma 44 in Appendix G which characterizes the centers of subalgebras of $\mathfrak{g}_{\text{free}}$.

Lemma 15 concludes that $com(g_{free})$ is two dimensional and commutative. Together with representationtheoretic arguments (see, e.g., Theorem 1.5 in [129]), this implies that the representation of $\mathfrak{g}_{\text{free}}$ splits exactly into two irreducible representations (or two irreducible blocks in a suitable basis). Indeed, we can determine these two representations by noting that up to a constant phase factor, Y and Z swap the Hadamard, or X-basis states $|+\rangle$ and $|-\rangle$, while I and X preserve them. Thus $\mathfrak{g}_{\text{free}}$ has invariant subspaces \mathcal{H}_+ and \mathcal{H}_- which are the span of all Hadamard basis states $|b_1\rangle \otimes \cdots \otimes |b_n\rangle$ with $b_i \in \{+, -\}$ with respectively an even or odd number of minus signs. Equivalently, \mathcal{H}_+ and \mathcal{H}_- are respectively the +1 and -1 eigenspaces of $X^{\otimes n}$. Also, \mathcal{H}_+ and \mathcal{H}_{-} have the same dimension. It follows that $\mathfrak{g}_{\mathrm{free}}$ is isomorphic to a subalgebra of $\mathfrak{u}(2^{n-1}) \oplus \mathfrak{u}(2^{n-1}) \cong$ $\mathfrak{su}(2^{n-1}) \oplus \mathfrak{su}(2^{n-1}) \oplus \mathfrak{u}(1) \oplus \mathfrak{u}(1)$. As the center of $\mathfrak{g}_{\text{free}}$ is trivial [see Lemma 15(c)], we obtain

Lemma 16. The free-mixer Lie algebra $\mathfrak{g}_{\text{free}}$ is isomorphic to a subalgebra of $\mathfrak{su}(2^{n-1}) \oplus \mathfrak{su}(2^{n-1})$.

Proof. We project $\mathfrak{g}_{\text{free}}$ onto its two irreducible components $\mathfrak{g}_{\text{free}}^{\pm}:=P_{\pm}\mathfrak{g}_{\text{free}}P_{\pm}$ where $P_{\pm}:=(I^{\otimes n}\pm X^{\otimes n})/2$. We verify $P_{\pm}g_{j}P_{\pm}=P_{\pm}g_{j}$ for $g_{j}\in\mathfrak{g}_{\text{free}}$ as $[X^{\otimes n},\mathfrak{g}_{\text{free}}]=0$ and then establish $[\mathfrak{g}_{\text{free}}^{+},\mathfrak{g}_{\text{free}}^{-}]=[P_{+}g_{1},P_{-}g_{2}]=P_{+}P_{-}[g_{1},g_{2}]=0$. The generators from Eq. (B1) are projected to $i(X_{u}\pm X_{u}X^{\otimes n})$ and $i(Z_{u}Z_{v}\mp\otimes_{w\in V}A_{w})$ where $A_{w}=Y$ if $w\in\{u,v\}$ and $A_{w}=X$ otherwise. And $[P_{\pm}g_{1},P_{\pm}g_{2}]=P_{\pm}^{2}[g_{1},g_{2}]=P_{\pm}[g_{1},g_{2}]$ implies that $\mathfrak{g}_{\text{free}}^{\pm}$ both form a Lie algebra and they are isomorphic as every element $P_{+}gP_{+}\in\mathfrak{g}_{\text{free}}^{+}$ for $g\in\mathfrak{g}_{\text{free}}$ is mapped to $P_{-}gP_{-}\in\mathfrak{g}_{\text{free}}^{-}$. For a center element $0\neq P_{+}cP_{+}\in\mathfrak{g}_{\text{free}}^{+}$ with $c\in\mathfrak{g}_{\text{free}}$, $P_{-}cP_{-}$ is in the center of $\mathfrak{g}_{\text{free}}^{-}$. This implies that c is in $\mathcal{Z}(\mathfrak{g}_{\text{free}})$ which is impossible. Conse-

Table V. Basis, isomorphism type, and dimension of the free-mixer Lie algebra for path, cycle, and connected bipartite graphs, as well as connected non-bipartite graphs different from cycle graphs. Here, #X, #Y, #Z, and #I denote respectively the number of X, Y, Z, and I in a Pauli string. For instance, $\#X|_{V_1}$ indicates the number of X in V_1 for a vertex bipartition $V = V_1 \uplus V_2$ with $|V| = n \geqslant 2$.

Path	n graph	Cycle graph					
Pauli strings	$I \cdot \cdot IXI \cdot \cdot I$ $X \begin{Bmatrix} Y \\ Z \end{Bmatrix} I \cdot \cdot I$	$I \cdot IXI \cdot I, X \cdot XIX \cdot I \cdot I \left\{ {{\frac{Y}{Z}}} \right\} X \cdot X \left\{ {{\frac{Y}{Z}}} \right\} I \cdot I \left\{ {{\frac{Y}{Z}}} \right\} X$	··I	$\#Y + \#Z$ is even and $\#I \neq n$ and $\#X \neq n$ and $\#X + \#Y _{V_1} + \#Z _{V_1}$ is odd		$\#\mathbf{Y} + \#\mathbf{Z}$ is even and $\#\mathbf{I} \neq n$ and $\#\mathbf{X} \neq n$	
				even-even	even-odd	odd-odd	
Lie algebra	$\mathfrak{so}(2n)$	$\mathfrak{so}(2n) \oplus \mathfrak{so}(2n)$	$\mathfrak{so}(2^n)$	$^{-1})\oplus\mathfrak{so}(2^{n-1})$	$\mathfrak{su}(2^{n-1})$	$\mathfrak{sp}(2^{n-1}) \oplus \mathfrak{sp}(2^{n-1})$	$\mathfrak{su}(2^{n-1}) \oplus \mathfrak{su}(2^{n-1})$
Lie dimension	$2n^2-n$	$4n^2-2n$		$2^{2n-2}-2^{n-1}$	$2^{2n-2}-1$	$2^{2n-2}+2^{n-1}$	$2^{2n-1}-2$

quently, both $\mathfrak{g}_{\text{free}}^{\pm}$ have trivial centers (and are semisimple).

To finish this section, we will present a series of maps that will be useful in the proofs of our main result. To begin, consider the map $h(M) := H^{\otimes n}MH^{\otimes n}$ on $2^n \times 2^n$ complex matrices M uses the Hadamard operator

$$H := \frac{1}{\sqrt{2}} \begin{pmatrix} 1 & 1 \\ 1 & -1 \end{pmatrix}$$
,

and maps iX_j , iY_j , iZ_j to iZ_j , $-iY_j$, iX_j . It is a Lie-algebra automorphism of $\mathfrak{su}(2^n)$. The generators from Eq. (B1) are mapped by h to iZ_u for $u \in V$ and iX_uX_v for $\{u,v\} \in E$. We apply the map $\pi_n(g) := \Pi_n g\Pi_n$ where

$$\begin{split} &\Pi_n := I^{\otimes n} \prod_{k=2}^n \mathrm{CNOT}(k,1,n) \\ &= \frac{1}{2} [I^{\otimes n} + Z_2 \cdots Z_n + X_1 - X_1 Z_2 \cdots Z_n] \text{ and } \\ &\mathrm{CNOT}(c,t,n) := \frac{1}{2} [I^{\otimes n} + Z_c + X_t - Z_c X_t]. \end{split}$$

That is, $\mathrm{CNOT}(c,t,n)$ simply denotes a CNOT gate on an n-qubit system where c denotes the control qubit and t the target qubits. The combined transformation $\pi_n \circ h$ maps the symmetry $X^{\otimes n}$ to Z_1 and the projections P_+ and P_- are mapped respectively to $I^{\otimes (n-1)} \oplus \theta^{\otimes (n-1)}$ and $\theta^{\otimes (n-1)} \oplus I^{\otimes (n-1)}$, where θ is the 2×2 zero matrix. The Hamiltonians have been block diagonalized and $\pi_n \circ h$ maps the basis elements $X_u, Z_u Z_v, Z_1 Z_v, X_1$ for $u, v \geqslant 2$ to $Z_u, X_u X_v, X_v, Z^{\otimes n}$. A final basis change $\tilde{h}(g) := H_{n-1}gH_{n-1}$ with $H_{n-1} := I \otimes H^{\otimes n-1}$ leads to $(u, v \geqslant 2)$

(a)
$$X_u$$
, (b) $Z_u Z_v$, (c) Z_v , (d) $Z_1 X_2 \cdot X_n$. (B3)

For later reference, Z_i is transformed by $\tilde{h} \circ \pi_n \circ h$ to

(e)
$$X_1$$
 if $j = 1$ and $X_1 Z_j$ otherwise, (B4)

and the combined basis change leading to Eqs. (B3)-(B4) is given for $n \ge 2$ by the unitary block matrix

$$\mathbf{H}_{n-1} \mathbf{\Pi}_n \mathbf{H}_n = \frac{1}{\sqrt{2}} \begin{pmatrix} I^{\otimes (n-1)} & X^{\otimes (n-1)} \\ I^{\otimes (n-1)} & -X^{\otimes (n-1)} \end{pmatrix}.$$

In the following, we denote the corresponding map by

$$\Lambda(M) := \tilde{h}(\pi_n(h(M))) = (H_{n-1}\Pi_n H_n) M(H_n \Pi_n H_{n-1})
= \frac{1}{2} \begin{pmatrix} I^{\otimes (n-1)} & X^{\otimes (n-1)} \\ I^{\otimes (n-1)} & -X^{\otimes (n-1)} \end{pmatrix} M \begin{pmatrix} I^{\otimes (n-1)} & I^{\otimes (n-1)} \\ X^{\otimes (n-1)} & -X^{\otimes (n-1)} \end{pmatrix}.$$
(B5)

For a Pauli string $P = \bigotimes_{u=1}^n A_u$ with $iP \in \mathfrak{g}_{free}$, Lemma 15(a) implies that the number of A_u with $A_u \in \{Y, Z\}$ is even and $\Lambda(P) = \pm Q$ for a Pauli string Q, i.e.,

$$\Lambda(P) = \begin{cases} \bigotimes_{u=2}^{n} A_u & \text{for } A_1 \in \{I, Z\}, \\ Z_1 \bigotimes_{u=2}^{n} (XA_u) & \text{for } A_1 = X, \\ iZ_1 \bigotimes_{u=2}^{n} (XA_u) & \text{for } A_1 = Y. \end{cases}$$
(B6)

The Hamiltonians under (a) and (b) recover the initial ones from Eq. (B1) without the first vertex. Removing the first vertex will lend itself for an induction step in n.

2. Irreducibility and maximal subalgebras

We recall two tools for characterizing free-mixer Lie algebras. The first one relies on the assumption that a Lie algebra $\mathfrak{g} \subseteq \mathfrak{su}(d)$ acts irreducibly [as on the last n-1 qubits for (a)-(c) in Eq. (B3)]. In this case, \mathfrak{g} can be categorized depending whether or not it is conjugate to a subalgebra of either $\mathfrak{so}(d)$ or $\mathfrak{sp}(d)$. Based on Sec. 3.11 of [195], [196], and Sec. 7 of [20], we summarize this in the following proposition.

Proposition 17. Assume that a subalgebra $\mathfrak{g} \subseteq \mathfrak{su}(d)$ generated by a set of iH_j is irreducibly embedded into $\mathfrak{su}(d)$. It is conjugate to a subalgebra of either (i) $\mathfrak{so}(d)$ and (ii) $\mathfrak{sp}(d)$ iff there exists a nonzero $d \times d$ complex matrix S such that $SH_j + H_j^t S = 0$ for all H_j . Every matrix S is either symmetric or skew-symmetric. If $S \neq 0$ exists, it is unique up to a scalar and one observes either (i) if S is symmetric or (ii) if S is skew-symmetric. Also, $S\bar{S} = \pm \alpha \mathbb{1}_d$ for S symmetric (+) or skew-symmetric (-) where \bar{S} is the complex-conjugated S and $0 < \alpha \in \mathbb{R}$.

Table VI. Example maximal subalgebras \mathfrak{g}^+ of compact \mathfrak{g} .

g	\mathfrak{g}^+
$\mathfrak{su}(2^n)$	$\mathfrak{so}(2^n);\ \mathfrak{sp}(2^n), n {\geqslant} 2;\ \mathfrak{su}(2^{n-1}) \oplus \mathfrak{su}(2^{n-1}) \oplus \mathfrak{u}(1)$
$\mathfrak{so}(2^n)$	$\mathfrak{su}(2^{n-1})\oplus\mathfrak{u}(1), n\geqslant 3;\ \mathfrak{so}(2^{n-1})\oplus\mathfrak{so}(2^{n-1}), n\geqslant 4$
$\mathfrak{sp}(2^n)$	$\mathfrak{su}(2^{n-1})\oplus\mathfrak{u}(1), n\geqslant 2; \ \mathfrak{sp}(2^{n-1})\oplus\mathfrak{sp}(2^{n-1})$
$\mathfrak{su}(2^n) \oplus \mathfrak{su}($	$\mathfrak{su}(2^n)$
$\mathfrak{so}(2m) \oplus \mathfrak{so}$	$\mathfrak{so}(2m) \qquad \mathfrak{so}(2m), m \geqslant 3$
$\mathfrak{so}(m)$	$\mathfrak{so}(m-1), m{\geqslant}5$
$\mathfrak{sp}(2m) \oplus \mathfrak{sp}$	$(2m) \mathfrak{sp}(2m)$

We refer the reader to [20] for a proof of Proposition 17. Our second tool often enables us to simplify and streamline the identification of Lie algebras and it relies on maximality relations between them ([197–200]):

Definition 2. A maximal subalgebra \mathfrak{h} of a Lie algebra \mathfrak{g} is a proper subalgebra $\mathfrak{h} \subsetneq \mathfrak{g}$ such that any subalgebra \mathfrak{k} of \mathfrak{g} containing \mathfrak{h} ($\mathfrak{h} \subseteq \mathfrak{k} \subseteq \mathfrak{g}$) is equal to \mathfrak{h} or \mathfrak{g} . In this case, \mathfrak{h} and any element $g \in \mathfrak{g}$ with $g \notin \mathfrak{h}$ generate \mathfrak{g} .

Fortunately, many relevant cases can also be more easily explained (see [78, Chap. IX, §1, Ex. 7] and [201, 202]) using an *involution* s of a Lie algebra \mathfrak{g} , i.e. an automorphism s of \mathfrak{g} where s^2 is the identity map. Given the eigenspaces \mathfrak{g}^{\pm} of s for the respective eigenvalues ± 1 , \mathfrak{g}^+ is a subalgebra of \mathfrak{g} ($[\mathfrak{g}^+,\mathfrak{g}^+]\subseteq\mathfrak{g}^+$), \mathfrak{g}^+ acts on \mathfrak{g}^- via the commutator with $[\mathfrak{g}^+,\mathfrak{g}^-]\subseteq\mathfrak{g}^-$, and $[\mathfrak{g}^-,\mathfrak{g}^-]\subseteq\mathfrak{g}^+$. The commutator action of \mathfrak{g}^+ on \mathfrak{g}^- is irreducible if and only if \mathfrak{g}^+ is a maximal subalgebra of \mathfrak{g} . If in addition, \mathfrak{g}^+ does not contain any nonzero ideal of \mathfrak{g} , then the pair (\mathfrak{g},s) is called *irreducible*. For compact semisimple Lie algebras, (\mathfrak{g},s) is irreducible iff \mathfrak{g} is either simple or a sum of two simple ideals exchanged by s. Hence, the maximality of \mathfrak{g}^+ is often immediately implied and all possible cases for (\mathfrak{g},s) relate to particular symmetric spaces [201, 202]:

Proposition 18. Table VI lists maximal subalgebras \mathfrak{g}^+ of compact Lie algebras \mathfrak{g} for (a) \mathfrak{g} simple and for (b) $\mathfrak{g} = \mathfrak{h} \oplus \mathfrak{h}$ with \mathfrak{h} simple, $\mathfrak{g}^+ = \{(h,h) \text{ for } h \in \mathfrak{h}\} \cong \mathfrak{h}$, and $\mathfrak{g}^- = \{(h,-h) \text{ for } h \in \mathfrak{h}\}.$

Proof. For (a), we refer to the classification of symmetric spaces [202] and the maximality of \mathfrak{g}^+ follows for compact simple \mathfrak{g} via [78, Chap. IX, §1, Ex. 7] and [201, 202]. We also point to the classification of maximal subalgebras [197–200]. For (b), we apply the preceding analysis or Theorem 15.1 in [198] on maximal subalgebras of semisimple \mathfrak{g} .

At this point it is worth noting that to ease the notation, unless otherwise stated, $\{A,B\}$ will denote the set containing A and B (and not their anticommutator). We shortly discuss cases which will be used later:

Example 1. The Lie algebras

$$\mathfrak{g}_a = \operatorname{span}_{\mathbb{R}} \{ i \, I \otimes \mathcal{C}_{n-1} \} \cong \mathfrak{su}(2^{n-1}) \text{ and}
\mathfrak{g}_b = \operatorname{span}_{\mathbb{R}} \{ i \, \{I, Z\} \otimes \mathcal{C}_{n-1} \} \cong \mathfrak{su}(2^{n-1}) \oplus \mathfrak{su}(2^{n-1})
\text{ with } \mathcal{C}_{n-1} := \{I, X, Y, Z\}^{\otimes n-1} \setminus \{I^{\otimes n-1}\}$$

are block diagonal with equal $(iB_k \oplus B_k)$ and independent $(iB_k \oplus C_\ell)$ blocks where $B_k, C_\ell \in \mathcal{C}_{n-1}$. Also, \mathfrak{g}_a is maximal in \mathfrak{g}_b . Adding iZ_1 to \mathfrak{g}_b generates $\mathfrak{g}_c \cong \mathfrak{su}(2^{n-1}) \oplus \mathfrak{su}(2^{n-1}) \oplus \mathfrak{su}(2^n)$.

Clearly, $iZ_1X_2 \cdot \cdot X_n \notin \mathfrak{g}_a$ but it is contained in \mathfrak{g}_b . Proposition 18 and Example 1 directly imply the first statement in the following lemma:

Lemma 19. (a) The *n*-qubit Lie algebra \mathfrak{g}_a together with the element $iZ_1X_2 \cdots X_n$ generates the Lie algebra \mathfrak{g}_b . (b) We now assume that $n \geq 3$. (b1) Adding X_1Z_j with $j \geq 2$ to \mathfrak{g}_b generates also X_1 . (b2) Adding X_1 to \mathfrak{g}_b generates also Z_1 . (b3) Adding X_1 or X_1Z_j with $j \geq 2$ to \mathfrak{g}_b generates $\mathfrak{su}(2^n)$.

Proof. Statement (a) follows as has been detailed before the lemma. Note the commutator chains

$$-\frac{i}{2}X_{1} = \left[\frac{i}{2}Z_{1}Z_{2}Z_{3}, \left[\frac{i}{2}Z_{1}Z_{2}, \frac{i}{2}X_{1}Z_{3}\right]\right],$$

$$-\frac{i}{2}Z_{1} = \left[\frac{i}{2}X_{1}, \left[\frac{i}{2}Z_{1}X_{2}, \left[\frac{i}{2}Z_{1}X_{2}X_{3}, \left[\frac{i}{2}Z_{1}X_{3}, \frac{i}{2}X_{1}\right]\right]\right]\right].$$
 (B8)

Equation (B7) implies (b1) in general and (b2) follows from Eq. (B8). Statements (b1) and (b2) combined with Example 1 show that \mathfrak{g}_c is generated. As \mathfrak{g}_c is maximal in $\mathfrak{su}(2^n)$, we obtain (b3) via Prop. 18 as the additional element X_1 or X_1Z_i is not contained in \mathfrak{g}_c .

3. Path and cycle graphs

Our analysis of the free-mixer ansatz starts with the path and the cycle graphs with n vertices. An important aspect relates to a Lie-algebra isomorphism from $\mathfrak{so}(2n+2)$ to a subalgebra of $\mathfrak{su}(2^n)$. This isomorphism is detailed by adapting and slightly extending the classical work of [186] (see, e.g., [187–194]) on spinor representations of the orthogonal group. To this end, we provide a matrix N with $(2n+2)\times(2n+2)$ entries which are themselves elements from $\mathfrak{su}(2^n)$ as well as a matrix M with $(2n+2)\times(2n+2)$ entries from $\mathfrak{so}(2n+2)$. The intended Lie isomorphism is then defined by mapping the entries N_{jk} to the entries M_{jk} . Let us introduce the two vectors

$$\alpha := -\frac{i}{2} [Z_1, X_1 Z_2, \dots, X_1 \cdot X_{n-1} Z_n, Y_1, X_1 Y_2, \dots, X_1 \cdot X_{n-1} Y_n],$$

$$\tilde{\alpha} := -\frac{i}{2} [-Y_1 Y_2 \dots Y_n - Y_n \cdot Y_n - Y_n],$$
(B9)

$$\tilde{\alpha} := -\frac{i}{2} [-Y_1 X_2 \cdot X_n, \dots, -Y_{n-1} X_n, -Y_n, Z_1 X_2 \cdot X_n, \dots, Z_{n-1} X_n, Z_n],$$
 (B10)

$$N = -\frac{i}{2} \begin{pmatrix} 0^{\otimes 4} & Z_1 & X_1Z_2 & X_1X_2Z_3 & X_1X_2X_3Z_4 & Y_1 & X_1Y_2 & X_1X_2Y_3 & X_1X_2X_3Y_4 & X^{\otimes 4} \\ -Z_1 & 0^{\otimes 4} & -Y_1Z_2 & -Y_1X_2Z_3 & Y_1X_2X_3Z_4 & X_1 & -Y_1Y_2 & -Y_1X_2Y_3 & -Y_1X_2X_3Y_4 & -Y_1X_2X_3X_4 \\ -X_1Z_2 & Y_1Z_2 & 0^{\otimes 4} & -Y_2Z_3 & -Y_2X_3Z_4 & -Z_1Z_2 & X_2 & -Y_2Y_3 & -Y_2X_3Y_4 & -Y_2X_3X_4 \\ -X_1X_2Z_3 & Y_1X_2Z_3 & Y_2Z_3 & 0^{\otimes 4} & -Y_3Z_4 & -Z_1X_2Z_3 & -Z_2Z_3 & X_3 & -Y_3Y_4 & -Y_3X_4 \\ -X_1X_2X_3Z_4 & Y_1X_2X_3Z_4 & Y_2X_3Z_4 & Y_3Z_4 & 0^{\otimes 4} & -Z_1X_2X_3Z_4 & -Z_2X_3Z_4 & Z_3Z_4 & X_4 & -Y_4 \\ -Y_1 & -X_1 & Z_1Z_2 & Z_1X_2Z_3 & Z_1X_2X_3Z_4 & 0^{\otimes 4} & Z_1Y_2 & Z_2X_2Y_3 & Z_1X_2X_3Y_4 & Z_1X_2X_3X_4 \\ -X_1Y_2 & Y_1Y_2 & -X_2 & Z_2Z_3 & Z_2X_3Z_4 & -Z_1Y_2 & 0^{\otimes 4} & Z_2Y_3 & Z_2X_3Y_4 & Z_2X_3X_4 \\ -X_1X_2Y_3 & Y_1X_2Y_3 & Y_2Y_3 & -X_3 & Z_3Z_4 & -Z_1X_2Y_3 & -Z_2Y_3 & 0^{\otimes 4} & Z_3Y_4 & Z_3X_4 \\ -X_1X_2X_3Y_4 & Y_1X_2X_3Y_4 & Y_2X_3Y_4 & Y_3Y_4 & -X_4 & -Z_1X_2X_3Y_4 & -Z_2X_3Y_4 & -Z_3Y_4 & 0^{\otimes 4} & Z_4 \\ -X_1X_2X_3Y_4 & Y_1X_2X_3Y_4 & Y_2X_3Y_4 & Y_3Y_4 & -X_4 & -Z_1X_2X_3Y_4 & -Z_2X_3Y_4 & -Z_3Y_4 & 0^{\otimes 4} & Z_4 \\ -X_1X_2X_3Y_4 & Y_1X_2X_3Y_4 & Y_2X_3Y_4 & Y_3Y_4 & -X_4 & -Z_1X_2X_3Y_4 & -Z_2X_3Y_4 & -Z_3Y_4 & 0^{\otimes 4} & Z_4 \\ -X_1X_2X_3Y_4 & Y_1X_2X_3Y_4 & Y_2X_3Y_4 & Y_3X_4 & Y_4 & -Z_1X_2X_3Y_4 & -Z_2X_3Y_4 & -Z_3Y_4 & 0^{\otimes 4} & Z_4 \\ -X_1X_2X_3X_4 & Y_1X_2X_3X_4 & Y_2X_3X_4 & Y_3X_4 & Y_4 & -Z_1X_2X_3X_4 & -Z_2X_3X_4 & -Z_4 & 0^{\otimes 4} \end{pmatrix}$$

Figure 11. Example for the matrix N from Eq. (B11). Case of n = 4 which contains 16×16 matrices as its elements.

where the entries α_j and $\tilde{\alpha}_j$ are $2^n \times 2^n$ matrices and $1 \le j \le 2n$. The $(2n+2)\times(2n+2)$ matrix N has entries

$$N_{jk} = -N_{kj} := \begin{cases} 0^{\otimes n} & \text{if } j = k, \\ -\frac{i}{2}X^{\otimes n} & \text{if } j = 0, \ k = 2n+1, \\ [\alpha_k, \alpha_j] & \text{if } 1 \leqslant j, k \leqslant 2n, \\ \alpha_k & \text{if } 0 = j < k \leqslant 2n, \\ \tilde{\alpha}_j & \text{if } 1 \leqslant j < k = 2n+1 \end{cases}$$
(B11)

which are $2^n \times 2^n$ matrices for $j, k \in \{0, \dots, 2n+1\}$. For n = 4, we obtain the 10×10 matrix in Figure 11 which contains 16×16 matrices as its elements.

The matrix M is defined by its $(2n+2)\times(2n+2)$ entries given by the $(2n+2)\times(2n+2)$ matrices $M_{jk}:=e_{jk}-e_{kj}$ where the matrices e_{jk} have entries $(e_{jk})_{ab}:=\delta_{ja}\delta_{kb}$. We map the $(2n+2)\times(2n+2)$ matrices M_{jk} to the $2^n\times 2^n$ matrices N_{jk} for $0\leqslant j< k\leqslant 2n+1$ which induces the desired Lie-algebra isomorphism as one can easily check. This isomorphism is applied to characterize relevant subalgebras of $\mathfrak{su}(2^n)$ by limiting us to suitable submatrices of the matrix N. In particular, we will prove below the following result.

Proposition 20. Let us consider the vector-space bases

$$\begin{split} &\mathcal{B}_a := \{iX^{\otimes n}\}, \quad \mathcal{B}_b := \{iX_j \text{ for } 1 \leqslant j \leqslant n\}, \\ &\mathcal{B}_c := \{i\{Y_j, Z_j\}X_{j+1} \cdots X_{k-1}\{Y_k, Z_k\} \text{ for } 1 \leqslant j < k \leqslant n\}, \\ &\mathcal{B}_d := \{iX_1 \cdots X_{k-1}\{Y_k, Z_k\} \text{ for } 1 \leqslant k \leqslant n\}, \\ &\mathcal{B}_e := \{i\{Y_j, Z_j\}X_{j+1} \cdots X_n \text{ for } 1 \leqslant j \leqslant n\}. \end{split}$$

Using the notation $\mathcal{B}_{i...k} = \mathcal{B}_i \cup \cdots \cup \mathcal{B}_k$, we have

$$\operatorname{span}_{\mathbb{R}}\mathcal{B}_{bc} =: \mathfrak{h}_1 \cong \mathfrak{so}(2n), \ \operatorname{span}_{\mathbb{R}}\mathcal{B}_{bcd} =: \mathfrak{h}_2 \cong \mathfrak{so}(2n+1),$$

 $\operatorname{span}_{\mathbb{R}}\mathcal{B}_{bce} =: \mathfrak{h}_3 \cong \mathfrak{so}(2n+1),$
 $\operatorname{span}_{\mathbb{R}}\mathcal{B}_{abcde} =: \mathfrak{h}_4 \cong \mathfrak{so}(2n+2).$

Note that $\mathfrak{h}_2,\mathfrak{h}_3\supset\mathfrak{h}_1$ and $\mathfrak{h}_4\supset\mathfrak{h}_3,\mathfrak{h}_2,\mathfrak{h}_1$. We present the first result for a free-mixer Lie algebra:

Theorem 2 (Path graphs). The free-mixer Lie algebra for a path graph with $n \ge 2$ and edges $\{v, v+1\}$ for $1 \le v < n$ is $\mathfrak{g}_{\text{free}} = \mathfrak{h}_1 \cong \mathfrak{so}(2n)$ where $\dim(\mathfrak{g}_{\text{free}}) = 2n^2 - n$.

Proof. The generators are iX_u for $1 \leqslant u \leqslant n$ and iZ_vZ_{v+1} for v < n, i.e., $\mathfrak{g}_{\text{free}} \subseteq \mathfrak{h}_1$. Clearly, $iY_vY_{v+1}, iY_vZ_{v+1}, iZ_vY_{v+1} \in \mathfrak{g}_{\text{free}}$ for v < n. We apply $[iZ_1Z_2, iY_2Z_3] = 2iZ_1X_2Z_3$ and similar relations to obtain all of \mathcal{B}_{bc} . \square

Theorem 2 leads together with Propositions 18 and 20 to

Corollary 3. (Fig. 12) For a path graph with $n \ge 2$, the Lie algebras \mathfrak{h}_{\bullet} and $\mathfrak{h}_{\bullet}^{\bullet}$ are generated by $\mathcal{G} := \{iX_u \text{ for } 1 \le u \le n, iZ_vZ_{v+1} \text{ for } 1 \le v < n\}$ and iZ_1 and by \mathcal{G}, iZ_1 , and iZ_n , respectively. (i) They are irreducibly embedded into $\mathfrak{su}(2^n)$. (ii) $\mathfrak{h}_{\bullet} = \mathfrak{h}_2 \cong \mathfrak{so}(2n+1)$; $\mathfrak{so}(5) \cong \mathfrak{sp}(4)$. (iii) $\mathfrak{h}_{\bullet}^{\bullet} = \mathfrak{h}_4 \cong \mathfrak{so}(2n+2)$; $\mathfrak{so}(6) \cong \mathfrak{su}(4)$.

Proof. As $[iZ_1, X^{\otimes n}] \neq 0$, Lemma 15(a) implies that $\mathfrak{com}(\mathfrak{h}_{\bullet})$ and $\mathfrak{com}(\mathfrak{h}_{\bullet}^{\bullet})$ have dimension one which proves (i). The case n=2 is verified directly. Theorem 2 implies that \mathcal{G} generates a Lie algebra that is isomorphic to $\mathfrak{so}(2n)$ and spanned by \mathcal{B}_{bc} . Proposition 20 shows that $\mathfrak{h}_1 \subsetneq \mathfrak{h}_{\bullet} \subseteq \mathfrak{h}_2$. The maximality of \mathfrak{h}_1 in \mathfrak{h}_2 from Prop. 18 implies (ii). The case (iii) is similar.

The Lie algebra $\mathfrak{g}_{\mathrm{free}} \cong \mathfrak{so}(2n)$ in Thm. 2 splits into two irreducible blocks of dimension 2^{n-1} [see Lemma 15(a)]. The basis change leading to Eq. (B3) is applied to the generators of $\mathfrak{g}_{\mathrm{free}}$ and we get (with $2 \leqslant u \leqslant n, \ 2 \leqslant v < n$)

(a')
$$iX_u$$
, (b') iZ_vZ_{v+1} , (c') iZ_2 , (d') $iZ_1X_2 \cdot \cdot X_n$. (B12)

Using Corollary 3(ii), (a')-(c') generate block-diagonal $L_k \oplus L_k$ where the matrices L_k span $\mathfrak{h}_2 \cong \mathfrak{so}(2n-1)$. The generator in (d') is equal to $iX^{\otimes (n-1)} \oplus [-iX^{\otimes (n-1)}]$ and a $\mathfrak{so}(2n)$ is generated in each block using the analysis from Eq. (B11). But the Lie algebra is not spanned by block-diagonal $\tilde{L}_k \oplus \tilde{L}_k$ as the blocks are partially intertwined.

Theorem 3 (Cycle graphs). The free-mixer Lie algebra of a cycle graph with edges $\{1, n\}$, $\{v, v+1\}$ for $1 \le v < n \ge 3$ is $\mathfrak{g}_{\text{free}} \cong \mathfrak{so}(2n) \oplus \mathfrak{so}(2n)$ where $\dim(\mathfrak{g}_{\text{free}}) = 4n^2 - 2n$.

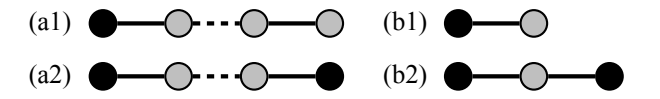


Figure 12. Path graphs with black end vertices. Generators are iX_u for all n vertices u, iZ_vZ_{v+1} for $1 \leqslant v < n$, and iZ_w for black vertices w. (a) General form with Lie algebras (a1) $\mathfrak{so}(2n+1)$ and (a2) $\mathfrak{so}(2n+2)$. (b) Low-dimensional cases with (b1) $\mathfrak{so}(2 \times 2 + 1) \cong \mathfrak{sp}(2^2)$ and (b2) $\mathfrak{so}(2 \times 3 + 2) = \mathfrak{so}(2^3)$.

Proof. The generators from (a')-(c') in Eq. (B12) are extended by iZ_n (which is iZ_1Z_n in the original basis) and get basis matrices $K_j \oplus K_j$ where the K_j span $\mathfrak{so}(2n)$ [see Cor. 3(iii)]. With Prop. 18, the span $\mathfrak{so}(2n)$ of $K_j \oplus K_j$ is maximal in the span $\mathfrak{so}(2n) \oplus \mathfrak{so}(2n)$ of $K_j \oplus K_j$ and $K_j \oplus [-K_j]$. Including (d') completes the proof.

Note that $\mathfrak{g}_{\text{free}} \cong \mathfrak{so}(2n) \oplus \mathfrak{so}(2n)$ in Thm. 3 is spanned by \mathcal{B}_{bc} and $\tilde{\mathcal{B}}_{bc} := \tilde{\mathcal{B}}_b \cup \tilde{\mathcal{B}}_c$ where $\tilde{\mathcal{B}}_r := \{AX^{\otimes n} \text{ for } A \in B_r\}$. This is clear from the form of $\mathfrak{g}_{\text{free}}$ in the basis of Eq. (B12) as detailed in the proof of Thm. 3 (here we recall that $X^{\otimes n}$ corresponds to Z_1 in the basis of Eq. (B12)).

4. Explicit representations: path and cycle graphs

We complement the results in Section B 3 by determining the explicit form of the corresponding representations. Our presentation influenced by the related discussions in [186], [189] (see Chapter VIII and particularly Section §4) and [190] (see Sections 9.5 and 9.6). To enable a more concise presentation, this subsection assumes some familiarity with the highest weight theory for representations of (complex) Lie algebras [72, 78, 192, 203].

Recall from Theorem 2 that the free-mixer Lie algebra $\mathfrak{g}_{\mathrm{free}}$ for the path graph is spanned by

$$iX_{j}$$
 for $2 \leqslant j \leqslant n$, iX_{1} , $i\{Y_{j},Z_{j}\}X_{j+1}\cdots X_{k-1}\{Y_{k},Z_{k}\}$ for $2 \leqslant j < k \leqslant n$, and $iZ_{1}X_{2}\cdots X_{k-1}\{Y_{k},Z_{k}\}$, $iY_{1}X_{2}\cdots X_{k-1}Z_{k}$, $iY_{1}X_{2}\cdots X_{k-1}Y_{k}$ for $2 \leqslant k \leqslant n$.

Applying the basis change from Eqs. (B5)-(B6) leads to

$$\begin{split} &iX_{j} \text{ for } 2 \leqslant j \leqslant n, \, iZ_{1}X_{2} \cdots X_{n}, \\ &i\{Y_{j}, Z_{j}\}X_{j+1} \cdots X_{k-1}\{Y_{k}, Z_{k}\} \text{ for } 2 \leqslant j < k \leqslant n, \text{ and } \\ &iX_{2} \cdots X_{k-1}\{Y_{k}, Z_{k}\}, \, iZ_{1}Y_{k}X_{k+1} \cdots X_{n}, \\ &(-1) \times iZ_{1}Z_{k}X_{k+1} \cdots X_{n} \text{ for } 2 \leqslant k \leqslant n. \end{split} \tag{B13}$$

Clearly, iX_j for $2 \leqslant j \leqslant n$ together with $iZ_1X_2 \cdots X_n$ span a maximal abelian subalgebra $\mathfrak t$ of $\mathfrak g_{\mathrm{free}}$. The complexification [72] of $\mathfrak g_{\mathrm{free}}$ is denoted by $\mathfrak g_{\mathbb C} := \mathfrak g_{\mathrm{free}} \otimes \mathbb C$. We now assume $n \geqslant 4$, while all cases below with n < 4 can be directly verified. We choose a particularly suitable basis

$$\frac{1}{2}(-X_2+Z_1X_2\cdots X_n), \ \frac{1}{2}(X_3-Z_1X_2\cdots X_n),$$
 (B14a)

$$\frac{1}{2}(X_4 - X_3), \dots, \frac{1}{2}(X_{n-1} - X_{n-2}),$$
 (B14b)

$$\frac{1}{2}(-X_n - X_{n-1}), \frac{1}{2}(X_n - X_{n-1}),$$
 (B14c)

in the Cartan subalgebra [72] it of $\mathfrak{g}_{\mathbb{C}}$, where the parts in Eq. (B14b) are missing for n=4. The basis elements are denoted by H_{α} (as in [72, 78]) and they are ordered according to the simple roots $\alpha=\alpha_j$ of $\mathfrak{g}_{\mathbb{C}}\cong\mathfrak{so}(2n,\mathbb{C})$ with $1\leqslant j\leqslant n$ [72]. Restricting to the irreducible $2^{n-1}\times 2^{n-1}$ block in the upper-left corner, the H_{α} are represented as

matrices H_{α}^{+} given by

$$\frac{1}{2}(-X_1+X_1\cdots X_{n-1}), \frac{1}{2}(X_2-X_1\cdots X_{n-1}),$$
 (B15a)

$$\frac{1}{2}(X_3 - X_2), \dots, \frac{1}{2}(X_{n-2} - X_{n-3}),$$
 (B15b)

$$\frac{1}{2}(-X_{n-1}-X_{n-2}), \frac{1}{2}(X_{n-1}-X_{n-2}).$$
 (B15c)

One can identify a particular one-dimensional eigenspace among the common eigenspaces of the H_{α}^{+} which is known as the highest weight space. In our case, it is spanned by the highest weight vector [72] (for $n \ge 4$)

$$v^{+} := \begin{cases} \binom{+1}{-1}^{\otimes (n-1)} & \text{if } n \text{ is even,} \\ \binom{-1}{-1}^{\otimes (n-2)} \otimes \binom{1}{1} & \text{if } n \text{ is odd.} \end{cases}$$
(B16)

The eigenvalues ω_j^+ for $H_{\alpha_j}^+v^+ = \omega_j^+v^+$ are collected in the highest weight $\omega^+ := (\omega_1^+, \dots, \omega_n^+)$ [72] with

$$\omega^{+} = \begin{cases} (0, \dots, 0, 1, 0) & \text{for even } n, \\ (0, \dots, 0, 0, 1) & \text{for odd } n. \end{cases}$$
(B17)

We identify the irreducible representation in the upperleft block as one of the spinor representations of $\mathfrak{so}(2n)$ [or equivalently for $\mathfrak{so}(2n,\mathbb{C})$] which we denote by η_+ . Similarly, the irreducible representation in the lower-right block is the other spinor representation η_- with

$$\omega^{-} = \begin{cases} (0, \dots, 0, 0, 1) & \text{for even } n, \\ (0, \dots, 0, 1, 0) & \text{for odd } n. \end{cases}$$
(B18)

Note that η_{\pm} is conjugate to the dual of η_{\mp} for odd n (i.e. $\eta_{\pm} \simeq \bar{\eta}_{\mp}$); the η_{\pm} are self-dual for even n (i.e., $\eta_{\pm} \simeq \bar{\eta}_{\pm}$).

We continue with the free-mixer Lie algebra $\mathfrak{g}_{\text{free}}$ for the cycle graph. Theorem 3 implies that $\mathfrak{g}_{\text{free}} \cong \mathfrak{g}_+ \oplus \mathfrak{g}_-$ with $\mathfrak{g}_+ \cong \mathfrak{g}_- \cong \mathfrak{so}(2n)$. Using the same frame as in Eq. B13, a basis of \mathfrak{g}_{\pm} is given by

Thus a maximal abelian subalgebra is spanned by $i(X_j \pm Z_1 X_j)/2$ for $2 \leqslant j \leqslant n$ and $i(X_2 \cdots X_n \pm Z_1 X_2 \cdots X_n)/2$. In the Cartan subalgebra of the complexification of \mathfrak{g}_+ , the basis elements corresponding to Eq. (B14) are denoted by \tilde{H}_{α} and are given by

$$\frac{1}{4}(I+Z)\otimes \tilde{b}_i$$
 with $\tilde{b}_i\in [-X_1+X_1\cdots X_{n-1}]$, (B19a)

$$X_2 - X_1 \cdots X_{n-1}, X_3 - X_2, \dots, X_{n-2} - X_{n-3},$$
 (B19b)

$$-X_{n-1}-X_{n-2}, X_{n-1}-X_{n-2}$$
. (B19c)

But the matrices H_{α}^{+} from Eq. (B15) are again recovered when the basis elements \tilde{H}_{α} are restricted to the irreducible $2^{n-1} \times 2^{n-1}$ block in the upper-left corner. Also the highest weight space is spanned by the highest weight vector v^{+} from Eq. (B16). Consequently, the irreducible representation of \mathfrak{g}_{+} in the upper-left block is

given by η_+ . Note that \mathfrak{g}_+ acts on the lower-right block via the trivial representation ϵ . Similarly, the irreducible representation of \mathfrak{g}_- in the lower-right block is also given by η_+ ; \mathfrak{g}_- acts on the upper-left block via ϵ . Putting together the previous, we have thus shown that the following result holds

Proposition 21 (Free-mixer representations for path and cycle graphs). The free-mixer Lie algebras $\mathfrak{g}_{\text{free}}$ for the (i) path and (ii) cycle graph are embedded into $\mathfrak{su}(2^n)$ via the respective representations (i) $\eta_+ \oplus \eta_-$ and (ii) $[\eta_+ \otimes \epsilon] \oplus [\epsilon \otimes \eta_+]$ (up to automorphisms of $\mathfrak{g}_{\text{free}}$).

5. Bipartite graphs

We continue with connected bipartite graphs G different from path and cycle graphs. Their free-mixer Lie algebras $\mathfrak{g}_{\text{free}}$ are determined in Theorem 4 below. To this end, $\mathfrak{g}_{\text{free}}$ is augmented with generators iZ_w for vertices $w \in W$ from a nonempty vertex subset W such that two of its vertices are never connected by an edge (vide infra). The resulting Lie algebra \mathfrak{t}_G^W is, surprisingly, isomorphic to either $\mathfrak{so}(2^n)$ or $\mathfrak{sp}(2^n)$ (see Proposition 28), except for most path graphs from Corollary 3. This enables us to prove Theorem 4.

Working towards this goal, we first establish some basic notation to streamline our discussion. As before, G denotes a graph with n:=|V| vertices V and edges E. If G is connected and bipartite, its vertex bipartition $V=V_1 \uplus V_2$ is unique and every edge $\{u,v\}$ connects $u \in V_1$ and $v \in V_2$ (or vice versa). Here, $V_1 \uplus V_2$ denotes the disjoint union such that $V=V_1 \cup V_2$ and $V_1 \cap V_2=\emptyset$. The parts V_k and $V_{\bar{k}}$ are identified by $k, \bar{k} \in \{1,2\}$ with $k \neq \bar{k}$. Let $\emptyset \neq W \subseteq V_k$ denote a nonempty subset of V_k . Similar notation will be used for further graphs \tilde{G} , \bar{G} . We formally introduce the Lie algebra \mathfrak{t}_G^G :

Definition 3. For a connected bipartite graph G, the Lie algebra \mathfrak{t}_G^W is generated by iX_u for $u \in V$, iZ_uZ_v for $\{u,v\} \in E$, and iZ_w for $w \in W$ with $\emptyset \neq W \subseteq V_k$.

Our objective is to determine \mathfrak{t}_G^W . But as this will require multiple steps, we introduce the target Lie algebra \mathfrak{t}_G^k with the aim of proving that $\mathfrak{t}_G^W = \mathfrak{t}_G^k$ except for most path graphs from Corollary 3:

Definition 4. For a connected bipartite graph G, \mathfrak{t}_G^k is generated by $i \bigotimes_{v \in V} A_v$ with $A_v \in \{I, X, Y, Z\}$ such that the number of $A_v = X$ for $v \in V$ has the opposite parity of the number of $A_w \in \{Y, Z\}$ for $w \in V_k$.

We can now separately establish properties of \mathfrak{k}_G^k and we initially only show that $\mathfrak{k}_G^W \subseteq \mathfrak{k}_G^k$:

Lemma 22 (Properties of \mathfrak{k}_G^k). (i) \mathfrak{k}_G^k is spanned by its generators. (ii) $\mathfrak{k}_G^k \cong \mathfrak{so}(2^n)$ iff $|V_k|$ is even. (iii) $\mathfrak{k}_G^k \cong \mathfrak{sp}(2^n)$ iff $|V_k|$ is odd. (iv) $iZ_v \in \mathfrak{k}_G^k$ iff $v \in V_k$. (v) $iX^{\otimes n} \in \mathfrak{k}_G^k$ iff n is odd. (vi) $\mathfrak{k}_G^W \subseteq \mathfrak{k}_G^k$.

Proof. The statements $iZ_v \in \mathfrak{k}_G^k$ if $v \in V_k$ and $iX^{\otimes n} \in \mathfrak{k}_G^k$ if n is odd follow from Definitions 3-4. As $[iZ_v, X^{\otimes n}] \neq 0$ for $v \in V_k$, Lemma 15(a) shows that $\mathfrak{com}(\mathfrak{k}_G^k)$ is one dimensional. Following Prop. 17, we choose $S = \bigotimes_{v \in V_1} Z_v \bigotimes_{v' \in V_2} Y_{v'}$ such that $SH_j + H_j^t S = 0$ for every generator iH_j of \mathfrak{k}_G^k . $S\bar{S} = \pm \mathbb{1}_2^{\otimes n}$ for $|V_k|$ even (+) or odd (-). Proposition 17 proves the containment $\mathfrak{k}_G^k \subseteq \mathfrak{so}(2^n)$ or $\mathfrak{k}_G^k \subseteq \mathfrak{sp}(2^n)$ depending on the parity of $|V_k|$. Counting the generators proves (i)-(iii) which implies (iv)-(v). The generators of \mathfrak{k}_G^k are contained in \mathfrak{k}_G^k due to Definitions 3-4, hence (vi).

The Lie algebras \mathfrak{h}_{\bullet} or $\mathfrak{h}_{\bullet}^{\bullet}$ from Corollary 3 are particular examples for \mathfrak{k}_{G}^{W} which are contained in either $\mathfrak{so}(2^{n})$ or $\mathfrak{sp}(2^{n})$, except if n is even for which $\mathfrak{h}_{\bullet}^{\bullet} \not\subseteq \mathfrak{so}(2^{n})$ and $\mathfrak{h}_{\bullet}^{\bullet} \not\subseteq \mathfrak{sp}(2^{n})$ hold as $W \subseteq V_{k}$ is not satisfied. In particular, we have $\mathfrak{h}_{\bullet} \subseteq \mathfrak{sp}(2^{n})$ for $n \mod 4 \in \{1, 2\}$ and $\mathfrak{h}_{\bullet} \subseteq \mathfrak{so}(2^{n})$ for $n \mod 4 \in \{3, 0\}$ as well as $\mathfrak{h}_{\bullet}^{\bullet} \subseteq \mathfrak{sp}(2^{n})$ for $n \mod 4 = 1$ and $\mathfrak{h}_{\bullet}^{\bullet} \subseteq \mathfrak{so}(2^{n})$ for $n \mod 4 = 3$. Clearly, these examples will not observe $\mathfrak{t}_{G}^{W} = \mathfrak{t}_{G}^{k}$, except for the two low-dimensional cases in Fig. 12(b).

Assuming that the property $\mathfrak{k}_G^W = \mathfrak{k}_G^k$ holds for some specific connected bipartite graph G, we ask the following question: can we extend this property with the same W to a larger connected bipartite graphs \tilde{G} that contains G as a subgraph? We provide an induction argument for an induction step from n to n+1 assuming that $\tilde{V}-1=V=n\geqslant 4$:

Lemma 23 (bipartite induction). Given a connected bipartite graph G, we add the vertex 0 and the edge $\{0,j\}$ with $j \in V$ and obtain the connected graph \tilde{G} with bipartition $\tilde{V} = \tilde{V}_1 \uplus \tilde{V}_2 = V \cup \{0\}$. This adds iX_0 and iZ_0Z_j and generates $\mathfrak{k}_{\tilde{G}}^W \subseteq \mathfrak{k}_{\tilde{G}}^k$. Let $n \geqslant 4$ and $\mathfrak{k}_{G}^W = \mathfrak{k}_{G}^k$. (i) Either (a) $j \in \tilde{V}_k = V_k$, $\tilde{V}_{\bar{k}} = V_{\bar{k}} \cup \{0\}$, $Z_j \in \mathfrak{k}_{G}^W$, and $Z_0 \notin \mathfrak{k}_{\tilde{G}}^W$ or (b) $\tilde{V}_k = V_k \cup \{0\}$, $j \in \tilde{V}_{\bar{k}} = V_{\bar{k}}$, and $Z_j \notin \mathfrak{k}_{G}^W$ holds. (ii) We obtain that $\mathfrak{k}_{\tilde{G}}^W = \mathfrak{k}_{\tilde{G}}^k$.

Proof. To prove (i), note that the edge (0,j) needs to connect \tilde{V}_1 and \tilde{V}_2 as \tilde{G} is bipartite. Thus 0 and j cannot be both in \tilde{V}_1 or \tilde{V}_2 . We apply Lemma 22(iv) to decide whether $Z_j \in \mathfrak{k}_G^k = \mathfrak{k}_G^W$ or not. In the case (a), $Z_0 \in \mathfrak{k}_{\tilde{G}}^W$ would imply $\mathfrak{k}_G^W \not\subset \mathfrak{k}_G^k$ which is impossible. (ii) \mathfrak{k}_G^k is block-diagonally spanned by $iI \otimes (\bigotimes_{v \in V} A_v)$ with $A_v \in \{I, X, Y, Z\}$ where the number of $A_v = X$ with $v \in V$ has the opposite parity of the number of $A_w \in \{Y, Z\}$ with $w \in V_k$. In case (a), $iZ_j \in \mathfrak{k}_G^W$ and adding iZ_0Z_j results via Prop. 18 in $\mathfrak{k}_G^k \oplus \mathfrak{k}_G^k$ which is maximal in $\mathfrak{so}(2^{n+1})$ if $\mathfrak{k}_G^k \cong \mathfrak{so}(2^n)$ or in $\mathfrak{sp}(2^{n+1})$ if $\mathfrak{k}_G^k \cong \mathfrak{sp}(2^n)$ [see Prop. 18]. Adding iX_0 , we obtain that $\mathfrak{k}_G^W = \mathfrak{k}_G^k$. In case (b), $iZ_j \not\in \mathfrak{k}_G^W$ and adding iZ_0Z_j results in $\mathfrak{su}(2^n)$ via Prop. 18. Its basis is spanned by all $iI \otimes (\bigotimes_{v \in V} A_v)$ and $iZ \otimes B_j$ for Pauli strings $iB_j \not\in \mathfrak{k}_G^k$. Assuming that $iZ_0 \in \mathfrak{k}_G^W$, we generate $\mathfrak{su}(2^n) \oplus \mathfrak{u}(1)$ which is maximal in $\mathfrak{so}(2^n)$ and $\mathfrak{sp}(2^n)$ [see Prop. 18]. Adding iX_0 implies $\mathfrak{k}_G^W = \mathfrak{k}_G^k$ where either $\mathfrak{k}_G^k \cong \mathfrak{so}(2^n)$ and $\mathfrak{k}_G^k \cong \mathfrak{so}(2^n)$ and $\mathfrak{k}_G^k \cong \mathfrak{so}(2^n)$ and $\mathfrak{k}_G^k \cong \mathfrak{so}(2^n)$ and $\mathfrak{k}_G^k \cong \mathfrak{so}(2^n)$. Deciding if $iZ_0 \in \mathfrak{k}_G^W$ for (b), one of

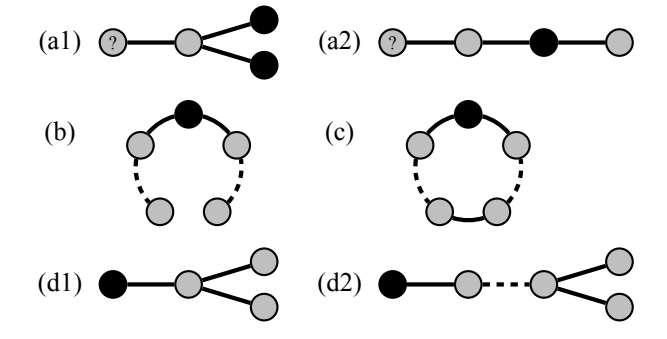


Figure 13. Lemmas 23-26. Notation as in Fig. 12. (a) iZ_q is generated for ?-marked vertices q. (b) Path graph with one black vertex not at the ends. (c) Cycle graph with one black vertex. (d) Y-shaped graphs with one black vertex at the long end with general form (d2).

the two connected, four-vertex subgraphs of \tilde{G} with the vertex q=0 in Fig. 13(a) has to be a possibility and the generation of iZ_0 has been checked.

To apply the induction step, we need to account for all base cases associated to connected bipartite graphs. As $\mathfrak{t}_G^W \subseteq \mathfrak{t}_G^k$ [see Lemma 22(vi)], $\mathfrak{t}_G^W = \mathfrak{t}_G^k$ holds for all $W \subseteq V_k$ if it is valid for |W| = 1. We establish $\mathfrak{t}_G^W = \mathfrak{t}_G^k$ for path graphs with iZ_w where at least one vertex $w \in W$ has degree two, i.e., is not at one end [see Fig. 13(b)]:

Lemma 24 (Figure 13(b)). For a path graph with edges E and bipartition $V = V_1 \uplus V_2$ where $V_1 := \{v \in V \text{ with } v \text{ odd}\}$ and $V_2 := \{v \in V \text{ with } v \text{ even}\}$, \mathfrak{k}_{\bullet} is generated by iX_u for $u \in V$, iZ_uZ_v for $\{u,v\} \in E$, iZ_w for $w \in W \subseteq V_k$. For cases not in Fig. 12(b), W is assumed to contain a degree-two vertex. We obtain $\mathfrak{k}_{\bullet} = \mathfrak{k}_G^k$ and Table VII.

Proof. One can computationally verify the statements for $n \leq 4$. The containment of \mathfrak{k}_{\bullet} in $\mathfrak{so}(2^n)$ or $\mathfrak{sp}(2^n)$ follows from Lemma 22. It is enough to prove the statements for |W| = 1. Lemma 23 completes the proof.

Moving from path graphs in Figure 13(b) to cycle graphs in Figure 13(c), we obtain $\mathfrak{t}_G^W = \mathfrak{t}_G^k$ for cycle graphs:

Lemma 25 (Figure 13(c)). The Lie algebra generated by iX_u for $1 \le u \le n \ge 3$, iZ_vZ_{v+1} for $1 \le v < n$, iZ_1Z_n , and iZ_1 is isomorphic to $\mathfrak{su}(2^n)$ if n is odd, $\mathfrak{so}(2^n)$ if n is divisible by four, and $\mathfrak{sp}(2^n)$ otherwise.

Proof. Removing the edge (2,3) and its generator iZ_2Z_3 so that vertex 1 and iZ_1 are not at the end of the resulting path graph, we obtain either $\mathfrak{so}(2^n)$ or $\mathfrak{sp}(2^n)$ via Lemma 24. For n even, iZ_2Z_3 is already contained in the generated Lie algebra and we stay with $\mathfrak{so}(2^n)$ or $\mathfrak{sp}(2^n)$. For n odd, iZ_2Z_3 is not contained in $\mathfrak{so}(2^n)$ or $\mathfrak{sp}(2^n)$ and Prop. 18 shows that we generate $\mathfrak{su}(2^n)$.

Table VII. Cases in Lemma 24 for n = |V| and $W \subseteq V_k$.

$\frac{1}{n \mod 4}$ $k \mod 2$	$\begin{array}{c} 0\ 0\ 1\ 1\ 2\ 2\ 3\ 3 \\ 1\ 0\ 1\ 0\ 1\ 0\ 1\ 0 \end{array}$	$\begin{smallmatrix} 0 & 0 & 1 & 1 & 2 & 2 & 3 & 3 \\ 1 & 0 & 1 & 0 & 1 & 0 & 1 & 0 \end{smallmatrix}$
$\mathfrak{k}_{ullet} \cong \mathfrak{so}(2^n)$ $\mathfrak{k}_{ullet} \cong \mathfrak{sp}(2^n)$	×× × × × ×	 × × × × × × ×

One challenge arises from the path graphs in Corollary 3 which cannot be used as base cases as either n < 4 or they do not observe $\mathfrak{k}_G^W = \mathfrak{k}_G^k$. To provide a set of base cases consisting of cycle graphs and path graphs extended with one additional vertex, the following Y-shaped graphs play a pivotal role:

Lemma 26 (Figure 13(d)). Given a graph with $n \ge 4$ and edges $E = \{\{1,3\}; \{j,j+1\} \text{ for } 2 \le j < n\}$, the Lie algebra generated by iX_v for $v \in V$, iZ_uZ_v for $\{u,v\} \in E$, and iZ_n is isomorphic to $\mathfrak{sp}(2^n)$ for $n \mod 4 \in \{0,3\}$ and $\mathfrak{so}(2^n)$ for $n \mod 4 \in \{1,2\}$.

Proof. We first prove that we generate iZ_3 for n odd and iZ_4 for n even. Using Corollary 3(ii), iX_2, \ldots, iX_n ; $iZ_2Z_3, \ldots, iZ_{n-1}Z_n$; and iZ_n generate the Lie algebra \mathfrak{f} isomorphic to $\mathfrak{so}(2n-1)$ and the corresponding basis elements have been detailed in Section B 3. We have

$$\begin{split} &[f_1,[f_2,[\frac{i}{2}Z_1Z_3,[f_3,[f_4,[\frac{i}{2}Z_1Z_3,\frac{i}{2}Z_2X_3\cdot\cdot X_{n-2d}]]]]]]\\ &=\frac{i}{2}Z_2X_3\cdot\cdot X_{n-2d-2}, \end{split}$$

where $f_1 := iY_2X_3 \cdot \cdot X_{n-2d-1}Y_{n-2d}/2$, $f_2 := iY_3X_4 \cdot \cdot X_{n-2d-1}Z_{n-2d}/2$, $f_3 := iY_3X_4 \cdot \cdot X_{n-2d-2}Y_{n-2d-1}/2$, $f_4 := iY_2X_3 \cdot \cdot X_{n-2d-2}Z_{n-2d-1}/2$ with $f_j \in \mathfrak{f}$ as well as $0 \leqslant 2d \leqslant n-3$ for n odd and $0 \leqslant 2d \leqslant n-4$ for n even. Thus we can generate iZ_2X_3 for n odd and $iZ_2X_3X_4$ for n even starting from $iZ_2X_3 \cdot \cdot X_n \in \mathfrak{f}$ and using iZ_1Z_3 . As $iZ_2Y_3, iZ_2X_3Y_4 \in \mathfrak{f}$, we obtain $iZ_3/2 = [iZ_2Y_3/2, iZ_2X_3/2]$ and $iZ_4/2 = [iZ_2X_3Y_4/2, iZ_2X_3X_4/2]$ for n odd and even, respectively. Thus iX_2, \ldots, iX_n ; $iZ_2Z_3, \ldots, iZ_{n-1}Z_n$; and iZ_3 for n odd and iZ_4 for n even are used to generate $\mathfrak{so}(2^{n-1})$ and $\mathfrak{sp}(2^{n-1})$ depending on n [see Lemma 24]. With iZ_1Z_3 and iX_1 , Lemma 23 completes the proof.

We formalize the notion of a path graph extended with one additional vertex and the respective free-mixer Lie algebra augmented by one iZ_w with $w \in V_k$ is determined:

Lemma 27. Given a path graph G, an extended path graph \tilde{G} is obtained by adding one vertex 0 and one edge (0,v) with $v \in V$ to G such that \tilde{G} is not a path graph. Then \tilde{G} is bipartite with bipartition $\tilde{V} = \tilde{V}_1 \uplus \tilde{V}_2 = V \cup \{0\}$ and $\tilde{V}_j \supseteq V_j$. For $W = \{w\} \subseteq \tilde{V}_k$, $\mathfrak{k}_{\tilde{G}}^W = \mathfrak{k}_{\tilde{G}}^k$.

Proof. The result is verified for $|V| \leq 3$ and let $|V| \geq 4$. Any extended path graph \tilde{G} with $W = \{w\} \subseteq \tilde{V}_k$ is either obtained from Lemma 26 or by adding vertices and edges to a graph \bar{G} from Lemma 24 or 26 such that the

bipartition of \bar{G} is given by $\bar{V} = \bar{V}_1 \uplus \bar{V}_2$ with $\bar{V}_j \subseteq V_j$ and $W \subseteq \bar{V}_k$. We then apply Lemma 23 multiple times. \square

With the notion of an extended path graph, we can establish this critical statement about $\mathfrak{g}_{\text{free}}$ augmented with generators iZ_w for $w \in W \subseteq V_k$:

Proposition 28. For a connected bipartite graph G with $|V|=n,\ \mathfrak{k}_G^W$ for $\emptyset\neq W\subseteq V_k$ is generated by iX_v for $v\in V,\ iZ_uZ_v$ for edges $\{u,v\},\$ and iZ_w for $w\in W.$ For path graphs not in Fig. 12(b), W is assumed to contain a degree-two vertex. (i) $\mathfrak{k}_G^W=\mathfrak{k}_G^k$. (ii) $\mathfrak{k}_G^W\cong\mathfrak{so}(2^n)$ for even $|V_k|$ and $\mathfrak{k}_G^W\cong\mathfrak{sp}(2^n)$ for odd $|V_k|$.

Proof. Clearly, (ii) follows from (i) and Lemma 22. We have checked all cases with $n \leq 4$, and suitable path and even-cycle graphs are treated in Lemmas 24 and 25 and extended path graphs are considered in Lemma 27. We proceed by induction from a connected bipartite graph G with one vertex q (and its edges) removed from G. From now on, we assume $n \ge 5$ and that G is neither a path graph, a cycle graph, nor an extended path graph. This also implies that G cannot be a path graph. By induction, we assume that Prop. 28 holds for all connected, bipartite graphs with less than n vertices that are neither a path graph, a cycle graph, nor an extended path graph. We pick q as one end vertex of a chosen minimal spanning T tree of G, then \tilde{G} is connected (and clearly bipartite). We divide the proof into three cases: (1) $q \notin W$ and $(V \setminus \{q\}) \cap W \neq \emptyset$, (2) $q \in W$ and $(V \setminus \{q\}) \cap W = \emptyset$, and (3) $q \in W$ and $(V \setminus \{q\}) \cap W \neq \emptyset$. For (1) and (3), Prop. 28 holds for \tilde{G} as it is either a even-cycle graph [see Lemma 25] or an extended path graph [see Lemma 27] or it holds for \tilde{G} by induction. The induction step follows by applying Lemma 23. For (2), we pick a different end vertex of the chosen minimal spanning tree T of G. Then the conditions for (1) apply and we proceed as in (1). \Box

The free-mixer Lie algebra for connected bipartite graphs can now be readily determined:

Theorem 4 (bipartite graphs). Consider a connected bipartite graph G which is neither a path graph nor a cycle graph. Let $V = V_1 \uplus V_2$ be its vertex bipartition and $|V| = n \geqslant 4$. The free-mixer Lie algebra for G is given by (i) $\mathfrak{g}_{\text{free}} \cong \mathfrak{su}(2^{n-1})$ if n is odd (or, equivalently, if $|V_1|$ and $|V_2|$ have opposite parities), (ii) $\mathfrak{g}_{\text{free}} \cong \mathfrak{so}(2^{n-1}) \oplus \mathfrak{so}(2^{n-1})$ if $|V_1|$ and $|V_2|$ are both even, and (iii) $\mathfrak{g}_{\text{free}} \cong \mathfrak{sp}(2^{n-1}) \oplus \mathfrak{sp}(2^{n-1})$ if $|V_1|$ and $|V_2|$ are both odd. Note that $\dim[\mathfrak{su}(2^{n-1})] = 2^{2n-2}-1$, $\dim[\mathfrak{so}(2^{n-1}) \oplus \mathfrak{so}(2^{n-1})] = 2^{2n-2}-2^{n-1}$, and $\dim[\mathfrak{sp}(2^{n-1}) \oplus \mathfrak{sp}(2^{n-1})] = 2^{2n-2}+2^{n-1}$.

Proof. Let G be a connected bipartite graph with one vertex q (and its edges) removed from G. Its vertex bipartition $\tilde{V} = \tilde{V}_1 \uplus \tilde{V}_2 = V \setminus \{q\}$ observes $\tilde{V}_j \subseteq V_j$. We recall from Def. 4 the notation $k, \bar{k} \in \{1, 2\}$ with $k \neq \bar{k}$. We pick q as one end vertex of a chosen minimal spanning tree of G, then \tilde{G} is connected (and clearly bipartite). We permute the numbers of the vertices so that

q becomes the first vertex. We transform the generators iX_v for $v \in V$ and iZ_uZ_v for edges $\{u,v\}$ of Ginto the basis from Eq. (B3) and obtain (for $u, v \in \tilde{V}$) (a) iX_u , (b) iZ_uZ_v , (c) iZ_w for $w \in W \subseteq \tilde{V}_k \subseteq \tilde{V}$ where $W \neq \emptyset$ denotes the set of neighbors of 1, and (d) $iZ_1 \prod_{w \in \tilde{V}} X_w$. As G is neither a path graph nor a cycle graph, W contains at least one vertex of \tilde{G} with degree two if \tilde{G} is a path graph. In the notation of Def. 4, it follows from Prop. 28 that $\mathfrak{k}_{\tilde{G}}^W$ is equal to $\mathfrak{k}_{\tilde{G}}^k$ which is isomorphic to $\mathfrak{so}(2^{n-1})$ if $|\tilde{V}_k|$ is even and to $\mathfrak{sp}(2^{n-1})$ if $|\tilde{V}_k|$ is odd. Here, $\mathfrak{k}_{\tilde{G}}^k$ is block-diagonally spanned by $iI \otimes (\bigotimes_{v \in \tilde{V}} A_v)$ with $A_v \in \{I, X, Y, Z\}$ where the number of $A_v = X$ with $v \in \tilde{V}$ has the opposite parity of the number of $A_u \in \{Y, Z\}$ with $u \in \tilde{V}_k$. We consider the cases (1) $i \prod_{w \in \tilde{V}} X_w \in \mathfrak{k}_{\tilde{G}}^k$ [i.e. n-1 is odd due to Lemma $22(\mathbf{v})$] and (2) $i \prod_{w \in \tilde{V}} X_w \notin \mathfrak{t}_{\tilde{G}}^k$. For (1), we add $iZ_1 \prod_{w \in \tilde{V}} X_w$ and apply Prop. 18 to obtain $\mathfrak{t}_{\tilde{G}}^k \oplus \mathfrak{t}_{\tilde{G}}^k$. For (2), adding the generator $iZ_1 \prod_{w \in \tilde{V}} X_w$ results in $\mathfrak{su}(2^{n-1})$ via Prop. 18. Its basis is spanned by all $iI \otimes (\bigotimes_{v \in \tilde{V}} A_v)$ as defined before and $iZ \otimes B_j$ for Pauli strings $iB_j \notin \mathfrak{t}_{\tilde{C}}^k$.

6. Non-bipartite graphs

Finally, we treat connected non-bipartite graphs also by adding a generator of the form iZ_j and by applying the basis change leading to Eqs. (B3)-(B4):

Proposition 29. Consider a connected, non-bipartite graph with n vertices V and edges E and choose a vertex $j \in V$. Then the generators iX_v for $v \in V$, iZ_uZ_v for $\{u,v\} \in E$, and iZ_j always generate together the Lie algebra $\mathfrak{su}(2^n)$.

Proof. For an odd-cycle graph, the result follows from Lemma 25. We can assume that $n \ge 4$ and that the shortest odd cycle in the non-bipartite graph is shorter than n. We re-order the vertices such that one shortest odd cycle does not contain the first vertex. Now the subgraph without the first vertex is not bipartite. If this subgraph is not connected, pick a connected component not containing the chosen shortest odd cycle. In the subgraph given by this connected component and the first vertex, choose a minimal spanning tree and pick one of its end vertices different from the first vertex as the new first vertex. Then the subgraph not containing the new first vertex is connected. Following the analysis leading to Eqs. (B3)-(B4), the generators from the groups (a), (b), and (c) in Eq. (B3) are of tensor-product form $i(\otimes_i A_i)$ with $A_1 = I$ and they generate by induction the Lie algebra $\mathfrak{g}_a \cong \mathfrak{su}(2^{n-1})$ (Ex. 1). Using the generator $iZ_1X_2 \cdot X_n$ from group (d) in Eq. (B3), Lemma 19(a) shows that we get $\mathfrak{g}_b \cong \mathfrak{su}(2^{n-1}) \oplus \mathfrak{su}(2^{n-1})$ (Ex. 1). Depending on j, we add one of the generators iX_1 or iX_1Z_j from the group (e) in Eq. (B4). Lemma 19(b) shows that we first generate iZ_1 and thus $\mathfrak{g}_c \cong \mathfrak{su}(2^{n-1}) \oplus \mathfrak{su}(2^{n-1}) \oplus \mathfrak{u}(1)$ (Ex. 1), which is maximal in $\mathfrak{su}(2^n)$ [see Prop. 18]. By

the argument in Lemma 19(b3), we obtain the Lie algebra $\mathfrak{su}(2^n)$ by adding one generator from (e) in Eq. (B4). \square

Determining the free-mixer Lie algebra in the nonbipartite case is now immediate:

Theorem 5 (non-bipartite graphs). The free-mixer Lie algebra $\mathfrak{g}_{\text{free}}$ for a connected non-bipartite graph different from a cycle graph with $n \geq 2$ vertices is given by $\mathfrak{g}_{\text{free}} \cong \mathfrak{su}(2^{n-1}) \oplus \mathfrak{su}(2^{n-1})$ with $\dim(\mathfrak{g}_{\text{free}}) = 2^{2n-1} - 2$.

Proof. Similarly as in the proof of Prop. 29, we can assume $n \ge 4$ and we re-order the vertices such that the subgraph without the first vertex is connected and not bipartite. We apply the analysis leading to Eq. (B3). It follows from Proposition 29 that the generators from the groups (a), (b), and (c) in Eq. (B3) generate the Lie algebra $\mathfrak{g}_a \cong \mathfrak{su}(2^{n-1})$ (Ex. 1). Adding $iZ_1X_2 \cdot X_n$ from group (d) in Eq. (B3), Lemma 19(a) shows that we generate $\mathfrak{g}_b \cong \mathfrak{su}(2^{n-1}) \oplus \mathfrak{su}(2^{n-1})$ (Ex. 1).

7. Explicit representations: neither path nor cycle

We complement the results in Sections B 5 and B 6 with the explicit form of the corresponding representations. This determines the embedding of $\mathfrak{g}_{\text{free}}$ into $\mathfrak{su}(2^n)$. The standard representation of a Lie algebra is denoted by κ and $\bar{\kappa}$ identifies its dual; ϵ is the trivial representation.

Proposition 30 (Free-mixer representations for connected graphs different from path and cycle). Consider the free-mixer Lie algebras $\mathfrak{g}_{\text{free}}$ for the bipartite cases (i), (ii), and (iii) from Theorem 4 as well as for the non-bipartite case from Theorem 5. The respective representations are (up to an automorphism of $\mathfrak{g}_{\text{free}}$) given by $\kappa \oplus \bar{\kappa}$ for the first case and by $[\kappa \otimes \epsilon] \oplus [\epsilon \otimes \kappa]$ otherwise.

Proof. Lemma 15 and the discussion in Appendix B1 imply that the commutant $com(\mathfrak{g}_{free})$ is two-dimensional and that the corresponding representation $\xi_1 \oplus \xi_2$ of $\mathfrak{g}_{\text{free}}$ splits into two inequivalent irreducible representations ξ_1 and ξ_2 of degree 2^{n-1} . The reductive decomposition of $\mathfrak{g}_{\text{free}}$ for the considered cases are known from Theorems 4 and 5. We assume $n \ge 5$ as the cases with $n \leq 4$ can be verified by explicit computations. For $n \geqslant 5$, all irreducible representations of degree 2^{n-1} for $\mathfrak{so}(2^{n-1})$, $\mathfrak{sp}(2^{n-1})$, and $\mathfrak{su}(2^{n-1})$ are respectively given (up to equivalence) by the standard representation κ , the standard representation κ , and the standard representation κ and its dual $\bar{\kappa}$. Referring, e.g., to [78], the listed irreducible representations have the required degree and they are the only possibilities up to equivalence, which follows from the well-known enumeration of the respective lowest-dimensional irreducible representations (see, e.g., Chapter VIII, §13, Exercise 2 in [78]). This reduces the possibilities significantly and the results follow as automorphisms of $\mathfrak{su}(2^{n-1})$ switch between κ and $\bar{\kappa}$.

Figure 14. **Commutator graph.** A directed edge with label C connects a vertex A with a vertex B iff $[iC/2, iA/2] = (-1)^s iB/2$ for $s \in \{0, 1\}$.

Appendix C: The free-mixer ansatz via Pauli strings

This appendix complements the proof techniques in Appendix B with an approach focused on Pauli-string bases. For a particular graph, the original generators from Eq. (B1) yield further Lie-algebra elements which in some instances can be interpreted as adding edges to the graph. This enables us to highlight and employ properties of the considered graph. We start with general properties of bases of Pauli strings in Appendix C1. The complete and complete bipartite graphs are considered in Appendix C2. Appendix C3 details the technique of adding edges to a graph. This is then used to treat the bipartite and non-bipartite cases (different from path and cycle graphs). In Appendix C4, more work is needed to identify the Lie algebras for the bipartite graphs that are not path and cycle graphs. We refer to Appendix B3 for the cases of path and cycle graphs.

1. Pauli-string bases

For a given Pauli string

$$P_j = \bigotimes_{u \in V} A_u \text{ with } A_u \in \{X, Y, Z, I\},$$
 (C1)

or its corresponding Lie-algebra element iP_j , let #X, #Y, #Z, and #I denote the respective number of X, Y, Z, and I. We also use the notation $\#X(P_j)$ to identify a particular P_j . And for instance, $\#X|_{V_1}$ indicates the restriction of #X to a subset V_1 of V. We introduce the parity $p(P_j) := \#Y(P_j) + \#Z(P_j)$ (or p for short) of a Pauli string P_j (or similar elements).

Lemma 31. Given a connected graph and its free-mixer Lie algebra $\mathfrak{g}_{\text{free}}$, consider $\sum_j r_j i P_j \in \mathfrak{g}_{\text{free}}$ for Pauli strings P_j as in Eq. (C1) with $0 \neq r_j \in \mathbb{R}$. (i) The parity $p(P_j) := \# Y(P_j) + \# Z(P_j)$ of each P_j is even. (ii) For bipartite graphs with bipartition $V = V_1 \uplus V_2$, $\tilde{p}(P_j) := \# X(P_j) + \# Y|_{V_1}(P_j) + \# Z|_{V_1}(P_j)$ is odd.

Proof. We observe (i) and (ii) for all generators from Eq. (B1). Following Fig. 14, $p(P_j)$ mod 2 and $\tilde{p}(P_j)$ mod 2 are invariant for each P_j under commutators with generators from Eq. (B1). This proves (i) and (ii) for Pauli strings P_j . Linear combinations are similar.

Adding Lemma 15(ii) to the conditions in Lemma 31, we obtain the following set of conditions

$$\#I(P_i) \neq n, \ \#X(P_i) \neq n,$$
 (C2a)

$$p(P_j) = \#Y(P_j) + \#Z(P_j) \text{ is even, and}$$
 (C2b)

$$\tilde{p}(P_j) = \#X(P_j) + \#Y|_{V_1}(P_j) + \#Z|_{V_1}(P_j) \text{ is odd },$$
(C2c)

for Pauli strings P_j where $V = V_1 \uplus V_2$ denotes the bipartition of a bipartite graph. We now count the number of P_j satisfying Eqs. (C2a)-(C2b) or Eqs. (C2a)-(C2c) depending on the number n of vertices as well as the parity of $|V_1|$ and $|V_2|$:

Lemma 32 (Counting Pauli strings). (i) The number of P_j satisfying Eqs. (C2a)-(C2b) is equal to $2^{2n-1}-2$. (ii) The number of P_j observing Eqs. (C2a)-(C2c) for a complete bipartite graph with bipartition $V = V_1 \uplus V_2$ is (a) $2^{2n-2}-1$ for n odd, (b) $2^{2n-2}-2^{n-1}$ for $|V_1| = |V_2|$ even, and (c) $2^{2n-2}+2^{n-1}$ for $|V_1| = |V_2|$ odd.

Proof. The number of P_i that satisfy Eq. (C2b) is with 2^{2n-1} exactly half of all possible ones. Both $I^{\otimes n}$ and $X^{\otimes n}$ observe Eq. (C2b) and (i) follows. For P_j = $\bigotimes_{u \in V} A_u$ with $A_u \in \{X, Y, Z, I\}$ and $p(P_j) \neq n$, let us introduce a map b from P_j to $b(P_j) := \bigotimes_{u \in V} B_u$ with $B_u \in \{I, X\} \setminus \{A_u\}$ for the first vertex $u \in V$ with $A_u \in \{I, X\}$ and $B_u = A_u$ for $u \neq v$. The map b induces a bijection on P_i with $p(P_i) \neq n$ which switches the parity, i.e. $p(P_i) + p(b(P_i))$ is odd. For n odd, $p(P_i) \neq n$ and there is at least one $u \in V$ with $A_u \in \{I, X\}$. Hence b shows that half of P_i satisfying Eq. (C2b) also observe Eq. (C2c). The cases $P_j \in \{I^{\otimes n}, X^{\otimes n}\}$ are ruled out by Lemma 15(ii), but Eq. (C2c) fails for $I^{\otimes n}$, while Eqs. (C2b) and (C2c) hold for $X^{\otimes n}$. This proves (iia). If n is even, there are 2^n operators P_j with $p(P_j) = n$, i.e. $\#X(P_j) = 0$. For Eq. (C2c) to be fulfilled for these 2^n operators, both $\#Y|_{V_1}(P_i) + \#Z|_{V_1}(P_i)$ and $\#Y|_{V_2}(P_i) + \#Z|_{V_2}(P_i)$ need to be odd, i.e., $|V_1| = |V_2|$ is odd. The bijection b is applied to $2^{2n-1}-2^n$ operators, half of which satisfy Eq. (C2c). Both $I^{\otimes n}$ and $X^{\otimes n}$ do not observe Eq. (C2c). We obtain (iib) and (iic).

We know from Lemma 31 that $\mathfrak{g}_{\text{free}}$ is contained in the span of the iP_j with P_j satisfying Eqs. (C2a)-(C2b) for connected graphs. For connected bipartite graphs, the additional condition in Eq. (C2c) has to be observed. The number of P_j agrees with the respective dimensions in Thm. 5 for non-bipartite graphs different from a cycle graph or in Thm. 4 for bipartite graphs which are neither a path graph nor a cycle graph. Thus $\mathfrak{g}_{\text{free}}$ is spanned in these cases by the respective sets of iP_j . Combined with Appendix B, this completes the derivation of Table V.

2. Complete and complete bipartite graphs

Lemma 33. Consider the free-mixer Lie algebra $\mathfrak{g}_{\text{free}}$ for a complete graph. (i) $\mathfrak{g}_{\text{free}}$ is spanned by iP_j for Pauli

strings P_j satisfying Eqs. (C2a)-(C2b). (ii) $\dim(\mathfrak{g}_{\text{free}}) = 2^{2n-1}-2$. (iii) $\mathfrak{g}_{\text{free}} \cong \mathfrak{su}(2^{n-1}) \oplus \mathfrak{su}(2^{n-1})$.

Proof. Lemmas 15 and 31 show that the elements of $\mathfrak{g}_{\text{free}}$ have no support on odd-parity Pauli strings and that $\#I \neq n$ and $\#X \neq n$. The results can readily established for n=2 and we now assume $n \ge 3$. Applying Fig. 14, $iX_u, iX_v, iY_uY_v, iY_uZ_v, \text{ and } iZ_uZ_v \text{ are contained in } \mathfrak{g}_{\text{free}}$ for all vertices $u, v \in V$ with $u \neq v$. We also obtain $iX_uX_v \in \mathfrak{g}_{\text{free}}$ as $[[iY_uY_v, iZ_uZ_w], iZ_vZ_w] = 4iX_uX_v$ for three different vertices $u, v, w \in V$. We prove by induction over k := n - #I that the stated basis elements are contained in $\mathfrak{g}_{\text{free}}$, and we have just verified the base cases of $k \in \{1, 2\}$. We treat the two cases of (a) p > 0 even and (b) p = 0 separately. For (a), we have a iP_i such that $p(P_i) = p \ge 2, \#I(P_i) = n-k, \text{ and } \#X(P_i) = k-p.$ If k>p>0, we can choose $v,w\in V$ such that $A_v=X$ and $A_w \in \{Y, Z\}$. Using Fig. 14, $X_v Z_w$ and $X_v Y_w$ are reached from $Y_v I_w$ with a smaller k. If k = p > 0, we can choose $v_1, v_2, v_3 \in V$ such that $A_{v_j} \in \{Y, Z\}$. Using Fig. 14, for example, $Y_{v_1}Y_{v_2}Y_{v_3}$ is reached from $Y_{v_1}I_{v_2}I_{v_3}$ with a smaller k. For (b), P_j has only X and I in its tensor product with $\#X(P_j) = k \ge 1$ and $\#I(P_j) = n - k \ge 1$. For $k \geq 2$, we choose $v_1, v_2, v_3 \in V$ such that $A_{v_1} = X$, $A_{v_2} = X$, and $A_{v_3} = I$. Using Fig. 14, $X_{v_1} X_{v_2} I_{v_3}$ is reached from $X_{v_1}I_{v_3}I_{v_3}$ with a smaller k. In all three cases, a smaller k is obtained which shows (i) by induction. Lemma 32(i) implies (ii). By Lemma 16, \mathfrak{g}_{free} is isomorphic to a subalgebra of $\mathfrak{su}(2^{n-1}) \oplus \mathfrak{su}(2^{n-1})$. Hence (ii) implies (iii).

Lemma 34. Consider the free-mixer Lie algebra $\mathfrak{g}_{\text{free}}$ for a complete bipartite graph with $n \geq 4$ and its bipartition $V = V_1 \uplus V_2$. (i) $\mathfrak{g}_{\text{free}}$ is spanned by iP_j for Pauli strings P_j satisfying Eqs. (C2a)-(C2c). The number of P_j is (ii) $2^{2n-2}-1$ for n odd, (iii) $2^{2n-2}-2^{n-1}$ for $|V_1|=|V_2|$ even, and (iv) $2^{2n-2}+2^{n-1}$ for $|V_1|=|V_2|$ odd.

Proof. Lemmas 15 and 31 show that no other Pauli strings iP_i can be generated. The proof proceeds by induction on k := n - #I. For k = 1, only iX_u for $u \in V$ are possible and these are contained in Eq. (B1). For k = 2, we obtain iZ_uZ_v , iY_uZ_v , iZ_uY_v , and iY_uY_v for an edge $\{u,v\}$ following Fig. 14 and all other possibilities in Fig. 14 violate Eqs. (C2a)-(C2c). We now assume $3 \leqslant k \leqslant n$ and consider a Pauli string P_i $\bigotimes_{u \in V} A_u$ with $A_u \in \{X, Y, Z, I\}$ as in Eq. (C1). We consider the cases such that either (a) $A_u \in \{Y, Z\}$ and $A_v \in \{X, Y, Z\}$ hold for $u \in V_1$ and $v \in V_2$ (and for V_1 and V_2 exchanged), (b) $A_u \in \{Y, Z\}$ and $A_v = I$ hold for $u \in V_1$ and $v \in V_2$ (and for V_1 and V_2 exchanged), or (c) $p(P_j) = \#Y(P_j) + \#Z(P_j) = 0$. Let $B_{b_1} \dots B_{b_s} | C_{c_1} \dots C_{c_t}$ denote a Pauli string consisting of a subset of P_j , where $b_j \in V_1$, $c_j \in V_2$, $B_{b_j} := A_{b_j}$, $C_{c_i} := A_{c_i} \ s + t \leq n, \ s \leq |V_1|, \ \text{and} \ t \leq |V_2|.$ For (a), we have, e.g., the possibilities Z|X which can be generated from I|Y with a smaller k and Z|Z which can be generated from X|I with a smaller k (see Fig. 14) and all other cases are similar. This resolves (a) by induction.

For (b), we have, e.g., the possibility YY|I which can be generated from XX|I and this case is treated in (c). For (c), $\#X(P_j)$ is odd and thus $\#X(P_j)\geqslant 3$. The case (c) is further divided into the cases (c1) $|V_1|, |V_2|\geqslant 2$ and (c2) $|V_1|=1$ or $|V_2|=1$. For (c1), we have IX|XX which can be generated from IY|IY with a smaller k. For (c2), we have either I|XXX or X|IXX which can be both generated from Y|YII with a smaller k. We resolve (c) by induction, which proves (i). Lemma 32(ii) implies (ii)-(iv).

3. Adding edges to a connected graph

Recall from Eqs. (B1)-(B2) that the problem Hamiltonian $\sum_{\{u,v\}\in E} iZ_uZ_v$ can be split for the free-mixer ansatz into separate iZ_uZ_v for each edge $\{u,v\}\in E$. Thus generating iZ_jZ_k for $\{j,k\}\notin E$ is equivalent to adding $\{j,k\}$ to the edges without changing the free-mixer Lie algebra. More and more edges can be added for graphs different from path and cycle graphs until either a complete or complete bipartite graphs is reached. This explains why only so few classes of free-mixer Lie algebras occur. Two particular configurations that allow us to add edges are Y-configurations and PAW-configurations [see Figs. 15(a)-(b)], which can be directly verified (see Fig. 14):

Lemma 35. Consider a connected graph and either the (a) five- or (b) four-vertex subgraph depicted in Fig. 15(a)-(b) with the generators iX_u for vertices v and iZ_uZ_v for edges $\{u,v\}$. The respective elements (a) iZ_1Z_5 and iZ_2Z_5 or (b) iZ_1Z_4 and iZ_2Z_4 are generated.

For connected graphs that differ from a cycle graph but contain a cycle as depicted in Fig. 15(c), we can generate an additional edge and shorten the cycle by applying Lemma 35(a). Repeating this argument leads to the following two propositions.

Proposition 36. Consider a connected non-bipartite graph different from a cycle graph. Without changing its free-mixer Lie algebra, one can add edges such that the resulting graph (i) has a PAW-configuration (and a triangle) as a subgraph and (ii) is equal to the complete graph. (iii) $\mathfrak{g}_{\text{free}} \cong \mathfrak{su}(2^{n-1}) \oplus \mathfrak{su}(2^{n-1})$.

Proof. A non-bipartite graph contains an odd-cycle. As the graph is also connected and different from a cycle graph, an additional vertex exists that is connected to one of the vertices in the odd-cycle. As the vertices 1 to 5 in Fig. 15(c) form a Y-configuration, we apply Lemma 35(a) to shorten the odd-cycle by adding the edge $\{2,5\}$. This proves (i) by induction. Applying (i), we have a triangle subgraph which is formed by some vertices 1, 2, and 3. Every vertex that is not directly connected to this triangle (say vertex 5) is indirectly connected to one vertex in this triangle (say vertex 3) via some vertex (say vertex 4) as shown in Fig. 15(d). We add further edges without

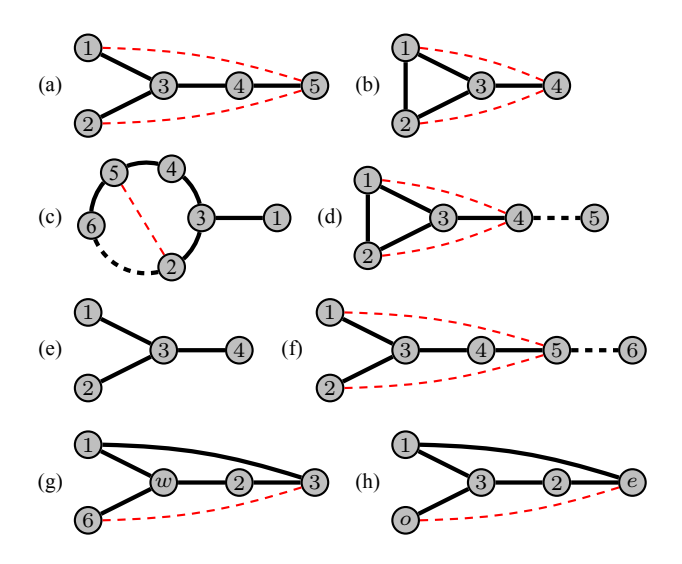


Figure 15. Add red edges, keep Lie algebra. (a) Add the edges $\{1,5\}$ and $\{2,5\}$ to the Y-configuration. (b) Add the edges $\{1,4\}$ and $\{2,4\}$ to the PAW-configuration. (c)-(h) are similar. Generators are iX_u for all vertices u and iZ_uZ_v for edges $\{u,v\}$ (see Fig. 12).

changing $\mathfrak{g}_{\text{free}}$ by repeatedly applying Lemma 35(b) to PAW-configurations, starting with the edges $\{1,4\}$ and $\{2,4\}$ in Fig. 15(d). As 1, 2, and 4 form a new triangle, we can add the edges $\{1,5\}$ and $\{2,5\}$ by induction. This argument shows that any vertex v is directly connected to two vertices in $\{1,2,3\}$, say the vertices 1 and 2. Using the PAW-configuration given by the edge $\{1,3\}$ and the triangle $\{1,2,v\}$, we add the edge $\{3,v\}$. By the previous arguments, any two vertices $v,w\in V\setminus\{1,2,3\}$ with $v\neq w$ are directly connected to 1, 2, and 3. Using the PAW-configuration given by the edge $\{2,w\}$ and the triangle $\{1,2,v\}$, we add the edge $\{v,w\}$. This proves (ii). Lemma 33(iii) implies (iii).

Proposition 37. Consider a connected bipartite graph different from a path or cycle graph. Without changing its free-mixer Lie algebra, one can add edges such that the resulting graph is equal to a complete bipartite graph.

Proof. Clearly, one vertex (say vertex 3) has a degree of at least three and it has three neighbors (say the vertices in $W = \{1, 2, 4\}$) as shown in Fig. 15(e). None of the neighbors of 3 can be directly connected as this would imply a triangle in a bipartite graph which is impossible. If the neighbors of 3 have no additional neighbors except 3 than the graph is a the complete bipartite graph with bipartition $V = V_1 \uplus V_2$ where $|V_1| = 1$ and we have proven the result. So we now assume that $|V_1|, |V_2| > 1$ and one vertex in W (say vertex 4) has a neighbor (say vertex 5) different from 3 as depicted in Fig. 15(a). Let d(v) denote the (minimal) distance of a vertex $v \in V$ from the vertex 3 and the vertex v is called even or odd depending whether d(v) is even or odd (which is well-defined as the graph is bipartite). Our objective is to

add all edges that connect even vertices with odd ones without changing the free-mixer Lie algebra (which is tacitly assumed in the following), which would prove the desired result.

First, we show that (*) one can add edges to connect all even vertices to the vertices in W and all odd vertices to 3. We proceed by induction on d(v). For d(v) = 0, v=3 and it is already directly connected to the vertices in W. For d(v) = 1, v is already a neighbor of 3. For d(v) = 2, there is a path from v (say vertex 5) to 3 via one of its neighbors (say vertex 4) as shown in Fig. 15(a). Lemma 35(a) implies that we can add the edges (1, 5) and (2,5) and the vertex 5 is connected to all vertices in W. For $d(v) \ge 3$, there is a path from v (say vertex 6) to 3 via a neighbor (say vertex 5) of a vertex in W (say vertex 4) as shown in Fig. 15(f). We are free to assume that this path does not contain the other two vertices 1 and 2 in W (as we could shorten the path). If $d(6) \ge 3$ is even, we can apply Lemma 35(a) by induction to add the edges (1,6) and (2,6). Adding the edge (1,6) to the star in Fig. 15(e), Lemma 35(a) implies that edge (4,6) can be added. If $d(6) \ge 3$ is odd, let w be the neighbor of 6 on the path from 3 to 6 where d(w) = d(6) - 1 is even and $w \notin W$. By induction, we can add the edges $\{w, 1\}$, $\{w, 2\}$, and $\{w, 4\}$. We obtain the situation in Fig. 15(g) and can add (3,6). This proves (*) by combining all cases. With the help of Fig. 15(h), it remains to show that any even vertex $e \neq 3$ can be directly connected to any odd vertex $o \notin W$.

4. Identifying the Lie algebras for bipartite graphs

We have already identified the free-mixer Lie algebra for non-bipartite graphs different from cycle graphs as $\mathfrak{g}_{\text{free}} \cong \mathfrak{su}(2^{n-1}) \oplus \mathfrak{su}(2^{n-1})$ and we refer to the direct isomorphisms in Section B 3 for the cases of path and cycle graphs. It remains to tackle all other bipartite graphs (different from path and cycle graphs). Lemma 34 already states the respective dimension for the relevant cases and Proposition 37 reduces the determination of the free-mixer Lie algebra to the case of complete bipartite graphs. We first consider graphs with an even number of vertices while providing a different argument as in Theorem 4:

Proposition 38 (bipartite graphs, n even). Given a connected bipartite graph G that is neither a path graph nor a cycle graph, let $V = V_1 \uplus V_2$ denote its vertex bipartition and assume that $|V| = |V_1| + |V_2| = n \geqslant 4$ is even. The free-mixer Lie algebra for G is given by (i) $\mathfrak{g}_{\text{free}} \cong \mathfrak{so}(2^{n-1}) \oplus \mathfrak{so}(2^{n-1})$ if $|V_1|$ and $|V_2|$ are both even, and (ii) $\mathfrak{g}_{\text{free}} \cong \mathfrak{sp}(2^{n-1}) \oplus \mathfrak{sp}(2^{n-1})$ if $|V_1|$ and $|V_2|$ are both odd.

Proof. Recall from Lemma 15(a) and the discussion in Section B1 that the action of $\mathfrak{g}_{\text{free}}$ splits into two irreducible and invariant subspaces \mathcal{H}_+ and \mathcal{H}_- which

are spanned by Hadamard basis states with respectively an even or odd number of minus signs. Moreover, $\mathfrak{g}_{\mathrm{free}} = \mathfrak{g}_{\mathrm{free}}^+ \oplus \mathfrak{g}_{\mathrm{free}}^-$ decomposes into two isomorphic, semisimple ideals with respect to \mathcal{H}_+ and \mathcal{H}_- . We will apply Proposition 17 to $\mathfrak{g}_{\mathrm{free}}^+$ by identifying a matrix S^+ such that (*) $S^+H_j^+ + (H_j^+)^t S^+ = 0$ for all generators iH_j^+ of $\mathfrak{g}_{\text{free}}^+$ (and similarly for $\mathfrak{g}_{\text{free}}^-$). We can assume that $V_1 = \{1, \dots, |V_1|\}$ with $|V_1| > 1$. Let $S := Z_1 \cdots Z_{|V_1|} Y_{|V_1|+1} \cdots Y_n$ where S is symmetric if $|V_2|$ is even. Switching to the basis of Eq. (B3), S is transformed to $I_1 Z_2 \cdots Z_{|V_1|} Y_{|V_1|+1} \cdots Y_n$. We obtain $S^{\pm} = Z_2 \cdots Z_{|V_1|} Y_{|V_1|+1} \cdots Y_n$ as a matrix on n-1 qubits acting on the respective invariant blocks, where S^{\pm} is symmetric if $|V_2|$ is even. Recalling that n-1 is odd, we can directly verify (*) by referring to the explicit matrices X_u for $u \geqslant 2$, Z_{v_1} Z_{v_2} for $v_1 \in V_1 \setminus \{1\}$ and $v_2 \in V_2$, Z_{v_2} for $v_2 \in V_2$, and $X_2 \cdot X_n$ from Eq. (B3) as acting on n-1 qubits (projected to the respective invariant blocks). Moreover, Proposition 17 implies the desired inclusions into the Lie algebras $\mathfrak{so}(2^{n-1}) \oplus \mathfrak{so}(2^{n-1})$ or $\mathfrak{sp}(2^{n-1}) \oplus \mathfrak{sp}(2^{n-1})$. Finally, we apply Lemma 34(iii)-(iv) to complete the proof.

We also detail a basis-independent argument for the desired inclusions. Note that $P_j^t = (-1)^{\#Y(P_j)}P_j$ for any Pauli string P_j . For the rest of the proof, let P_j denote a Pauli string such that $iP_j \in \mathfrak{g}_{free}$. Recall from Lemma 34(i) that $\#Y(P_j) + \#Z(P_j)$ is even and $\#X(P_j) + \#Y|_{V_1}(P_j) + \#Z|_{V_1}(P_j)$ is odd. We choose $S := \prod_{v \in V_1} Z_v \prod_{w \in V_2} Y_w$ and we obtain $S^t = (-1)^{|V_2|}S$ which implies that S is symmetric or skew-symmetric if $|V_2|$ is even or odd, respectively. As n is even, S commutes with $X^{\otimes n}$ and \mathcal{H}_+ and \mathcal{H}_- are also invariant subspaces of S. Moreover,

$$P_{j}S = SP_{j}(-1)^{\#X+\#Y|_{V_{1}}+\#Z|_{V_{2}}}$$

$$= SP_{j}(-1)^{\#Y|_{V_{1}}+\#Z|_{V_{1}}+1+\#Y|_{V_{1}}+\#Z|_{V_{2}}}$$

$$= SP_{j}(-1)^{\#Z+1} = SP_{j}(-1)^{\#Y+1},$$

which implies that

$$SP_j + P_j^t S = SP_j + (-1)^{\#Y} P_j S$$

= $SP_j + (-1)^{\#Y} (-1)^{\#Y+1} SP_j$
= $SP_j - SP_j = 0$.

Let S^{\pm} and P_j^{\pm} denote the respective projections to \mathcal{H}_+ and \mathcal{H}_- . Note that projection and matrix transposition commutes. Clearly, also $S^{\pm}P_j^{\pm} + (P_j^{\pm})^tS^{\pm} = 0$ holds as terms such as $S^+P_j^-$ and $(P_j^+)^tS^-$ in the expansion of $SP_j + P_j^tS = 0$ are zero. Note that S^{\pm} is symmetric iff S is symmetric. We can apply Prop. 17.

The proof critically relies on the fact that n is even, and a different free-mixer Lie algebra appears if n is odd:

Proposition 39 (bipartite graph, n odd). Given a connected bipartite graph G that is neither a path graph nor a cycle graph, let $V = V_1 \uplus V_2$ denote its vertex bipartition

and assume that $|V| = |V_1| + |V_2| = n \ge 4$ is odd. The free-mixer Lie algebra for G is given by $\mathfrak{g}_{\text{free}} \cong \mathfrak{su}(2^{n-1})$.

Proof. Without loss of generality, we let $|V_1|$ and $|V_2|$ be even and odd, respectively. For Hadamard basis states $|p_1\cdots p_n\rangle$ with $p_j\in\{+,-\}$, let the parity $\pi_j=\pi_j(|p_1\cdots p_n\rangle)\in\{e,o\}$ for $j\in\{1,2\}$ be equal to e iff the number of $v\in V_j$ such that $p_v\in\{-\}$ is even. We define V_{pq} for $p,q\in\{e,o\}$ to be the complex space spanned by Hadamard basis states with $\pi_1=p$ and $\pi_2=q$. We have $\mathcal{H}_+=V_{ee}\oplus V_{oo}$ and $\mathcal{H}_-=V_{eo}\oplus V_{oe}$. Let $\mathcal{B}=(\mathcal{B}_{ee},\mathcal{B}_{oo},\mathcal{B}_{eo},\mathcal{B}_{oe})$ describe bases of the Hadamard basis states from V_{ee},V_{oo} , and V_{eo} and of the negatives of the Hadamard basis states from V_{ee},V_{oo} , and V_{eo} and of the negatives of the Hadamard basis states from V_{oe} . Recall $X\mid \pm \rangle = \pm \mid \pm \rangle$ and $Z\mid \pm \rangle = \mid \mp \rangle$. We define $|\psi^*\rangle := \pm Z^{\otimes n} \mid \psi \rangle$ for Hadamard basis states $|\psi\rangle$ where the plus sign is chosen iff $\pi_j(\mid \psi \rangle) = e$. Our objective now is to show that any generator iH_j of $\mathfrak{g}_{\mathrm{free}}$ has the block-diagonal form

$$iH_j = i \begin{pmatrix} M_j & 0\\ 0 & -M_j^t \end{pmatrix} \tag{C3}$$

in the basis \mathcal{B} for suitable M_j depending on H_j . This would be imply that $\mathfrak{g}_{\text{free}}$ acts on \mathcal{H}_- with the dual of the representation acting on \mathcal{H}_+ . It would follow that $\mathfrak{g}_{\text{free}}$ is isomorphic to a subalgebra of $\mathfrak{su}(2^{n-1})$ and the dimension formula in Lemma 34(ii) then shows $\mathfrak{g}_{\text{free}} \cong \mathfrak{su}(2^{n-1})$.

It remains to verify the form in Eq. (C3) for all generators iX_v for $v \in V$ and iZ_vZ_w for edges (v,w) with $v \in V_1$ and $w \in V_2$. Let $|\psi\rangle$ denote a Hadamard basis state in \mathcal{H}_+ . Note that $X_v |\psi\rangle = f |\psi\rangle$ if and only if $X_v |\psi^*\rangle = -f |\psi^*\rangle$ which implies that $\langle \psi | X_v | \psi \rangle = -\langle \psi^* | X_v | \psi^* \rangle$. For any Hadamard basis $|\phi\rangle$ in \mathcal{H}_+ different from $|\psi\rangle$, we obtain $\langle \phi | X_v | \psi \rangle = 0 = -\langle \psi^* | X_v | \phi^* \rangle$. Hence the matrix X_v in the subspace basis $(\mathcal{B}_{ee}, \mathcal{B}_{oo})$ is the negative transpose of its matrix in the subspace basis $(\mathcal{B}_{eo}, \mathcal{B}_{oe})$.

We continue with $Z_v Z_w$ and we introduce $|\psi_{uv}\rangle := Z_u Z_v |\psi\rangle$ for any Hadamard basis state in \mathcal{H}_+ . It follows that $|\psi_{uv}^*\rangle = -Z_u Z_v |\psi^*\rangle$ and we obtain $\langle \psi_{uv}| Z_u Z_v |\psi\rangle = -\langle \psi^*| X_v |\psi_{uv}^*\rangle$. For any Hadamard basis $|\phi\rangle$ in \mathcal{H}_+ different from $|\psi_{uv}\rangle$, we observe $\langle \phi| Z_u Z_v |\psi\rangle = 0 = -\langle \psi^*| Z_u Z_v |\phi^*\rangle$ which verifies the form in Eq. (C3). \square

Appendix D: Proof of Corollary 2 from Sec. IV

We now prove Corollary 2 which is restated below after some preparations. The QAOA cost function was specified in Eq. (2) as $C(\vec{\theta}) = \langle \psi(\vec{\theta}) | H_p | \psi(\vec{\theta}) \rangle$ for $|\psi(\vec{\theta})\rangle = U(\vec{\theta})|+\rangle^{\otimes n}$, where $|+\rangle^{\otimes n}$ is defined in Eq. (3). This relies on the unitaries $U(\vec{\theta})$ in the circuit from Eq. (7) and $U(\vec{\theta})$ depends on the parameters $\vec{\theta}$ with real entries θ_{ϑ} . For simplicity, the entries θ_{ϑ} of $\vec{\theta}$ are now indexed by the numbers ϑ . Let $\partial_{\vartheta}C(\vec{\theta})$ denote the partial derivative of $C(\vec{\theta})$ with respect to the ϑ -th parameter θ_{ϑ} in $\vec{\theta}$.

More concretely, the parameters $\vec{\theta}$ could be given by the real values $\theta_{\ell u}, \theta_{\ell vw} \in [-\pi, \pi]$ in order to establish

the multi-angle QAOA unitaries [as in Eqs. (4) or (7)]

$$U(\vec{\theta}) = \prod_{\ell=1}^{L} \left[\prod_{u \in V} e^{-i\theta_{\ell u} X_u} \right] \left[\prod_{\{v,w\} \in E} e^{-i\theta_{\ell v w} Z_v Z_w} \right]$$
(D1)

for L layers and a graph with vertices V and edges E. In addition, we could assume that each $\theta_{\ell u}$, $\theta_{\ell vw}$ is sampled independently and uniformly from $(-2\pi, 2\pi)$.

Returning to a more general setting, the parameters $\vec{\theta}$ are sampled according to a given distribution $d\vec{\theta}$ over a chosen parameter domain δ_L . This induces a distribution on the associated unitaries $U(\vec{\theta})$. For a given distribution ν on a compact Lie group $\exp(\mathfrak{g})$ with Lie algebra \mathfrak{g} , we recall the second-order momentum operator

$$M_{\nu} := \int_{U \in e^{\mathfrak{g}}} d\nu(U) \ U^{\otimes 2} \otimes \bar{U}^{\otimes 2}.$$

In particular, we consider the momentum operators

$$M_{e^{\mathfrak{g}}} := \int_{U \in e^{\mathfrak{g}}} d\mu_{e^{\mathfrak{g}}}(U) \ U^{\otimes 2} \otimes \bar{U}^{\otimes 2} \text{ and}$$
$$M_{L} := \int_{\vec{\theta} \in \delta_{L}} d\vec{\theta} \ [U(\vec{\theta})]^{\otimes 2} \otimes [\bar{U}(\vec{\theta})]^{\otimes 2}$$

for the Haar measure $d\mu_{e^{\mathfrak{g}}}$ on the (compact) Lie group $e^{\mathfrak{g}}$ and a general distribution $d\vec{\theta}$ on the parameters $\vec{\theta}$ over a parameter domain δ_L . This leads to the following

Definition 5 (Approximate unitary 2-design). A distribution ν on a compact Lie group $\exp(\mathfrak{g})$ with Lie algebra \mathfrak{g} is an ε -approximate unitary 2-design if

$$||M_{\nu} - M_{e^{\mathfrak{g}}}||_{\infty} \leqslant \varepsilon.$$

Here, $\|\cdot\|_{\infty}$ denotes the Schatten ∞ -norm (or operator norm) which is given by the largest singular value of its argument. We are particularly interested under which assumptions the condition $\|M_L - M_{e^g}\|_{\infty} \le \varepsilon$ holds. The distribution of unitaries in a multi-angle QAOA circuit has to be an approximate unitary 2-design in the following result (which we restate from Sec. IV):

Corollary 2. For the free ansatz, consider any archetypal graph from Def. 1 with n>3 vertices and |E| edges. Recall the QAOA cost function $C(\vec{\theta})$ from Eq. (2) and its partial derivative $\partial_{\vartheta}C(\vec{\theta})$ with respect to the ϑ -th parameter θ_{ϑ} in $\vec{\theta}$. Assume that the multi-angle QAOA circuit has enough layers such that the distribution of unitaries is an ε -approximate unitary 2-design. Then, the expectation value of the partial derivatives is $E_{\vec{\theta}}[\partial_{\vartheta}C(\vec{\theta})]=0$ and their variance is given by (with $d=2^n$)

$$\operatorname{Var}_{\vec{\theta}}[\partial_{\vartheta}C(\vec{\theta})] = 4d^{2}|E|/[(d^{2}-4)(d+2)] \leqslant 4n^{2}/2^{n}.$$

We start the proof by first collecting relevant notation and results, while partially relying on Appendix B 1. Recall that $X^{\otimes n}$ commutes with the free-mixer Lie algebra

 $\mathfrak{g}_{\text{free}}$ and all its generators in $\mathcal{G}_{\text{free}}$ [see Lemma 15(a)] and that the vector space $\mathcal{H}=(\mathbb{C}^2)^{\otimes n}$ of dimension $d=2^n$ splits into the invariant subspaces $\mathcal{H}=\mathcal{H}_+\oplus\mathcal{H}_-$ where the +1 and -1 eigenspaces $\mathcal{H}_\pm=\{|\psi\rangle\in\mathcal{H}\,|\,X^{\otimes n}\,|\psi\rangle=\pm|\psi\rangle\}$ of $X^{\otimes n}$ are spanned by all Hadamard basis states $|b_1\rangle\cdots|b_n\rangle$ with $b_j\in\{+,-\}$ and respectively an even or odd number of minus signs (i.e. $b_j=-$). Clearly, \mathcal{H}_+ and \mathcal{H}_- have the same dimension $d_+=d_-=2^{n-1}$ and the fiduciary state $|+\rangle^{\otimes n}$ [see Eq. (3)] is contained in \mathcal{H}_+ .

The corresponding $d \times d$ projection matrices $P_{\pm} = (I^{\otimes n} \pm X^{\otimes n})/2$ can be represented as $P_{\pm} = Q_{\pm}^{\dagger} Q_{\pm}$ using the rectangular reduction matrices $Q_{\pm} \in \mathbb{C}^{d \pm \times d}$ where the columns of $Q_{\pm}^{\dagger} \in \mathbb{C}^{d \times d \pm}$ are given by the associated (orthonormalized) Hadamard basis states. Note that $Q_{\pm}Q_{\pm}^{\dagger} = I^{\otimes (n-1)}$. For a Pauli string (or any suitable matrix) A, we define the reduced operators

$$A^{(\pm)} := Q_{\pm} A Q_{\pm}^{\dagger} \in \mathbb{C}^{d_{\pm} \times d_{\pm}}. \tag{D2}$$

Lemma 40. For a Pauli string A on n qubits that is different from the identity and $X^{\otimes n}$ and that commutes with $X^{\otimes n}$, the reduced operators $A^{(\pm)}$ are unitarily equivalent to a Pauli string on n-1 qubits. In particular, $\text{Tr}[A^{(\pm)}] = 0$ and $\text{Tr}[A^{(\pm)}A^{(\pm)}] = 2^{n-1}$.

Proof. Clearly, A and $A^{(\pm)}$ are hermitian. The proof proceeds in two steps verifying that (i) the eigenvalues of $A^{(\pm)}$ are ± 1 and that (ii) their multiplicity is equal to 2^{n-2} (or, equivalently, $\text{Tr}[A^{(\pm)}] = 0$). We compute

$$\begin{split} A^{(\pm)}A^{(\pm)} &= Q_{\pm}AQ_{\pm}^{\dagger}Q_{\pm}AQ_{\pm}^{\dagger} = Q_{\pm}AP_{\pm}AQ_{\pm}^{\dagger} \\ &= (Q_{\pm}AAQ_{\pm}^{\dagger} \pm Q_{\pm}AAX^{\otimes n}Q_{\pm}^{\dagger})/2 \\ &= (Q_{\pm}Q_{\pm}^{\dagger} \pm Q_{\pm}X^{\otimes n}Q_{\pm}^{\dagger})/2 \\ &= (I^{\otimes (n-1)} + I^{\otimes (n-1)})/2 = I^{\otimes (n-1)}, \end{split}$$

where we have used that A commutes with $X^{\otimes n}$, that the square A^2 of the Pauli string A is equal to $I^{\otimes n}$, that $Q_{\pm}Q_{\pm}^{\dagger}=I^{\otimes(n-1)}$, and that $Q_{\pm}X^{\otimes n}Q_{\pm}^{\dagger}=\pm I^{\otimes(n-1)}$ as the columns of Q_{\pm}^{\dagger} contain the eigenvectors of $X^{\otimes n}$ to the eigenvalues ± 1 . Thus $A^{(\pm)}$ has only ± 1 as eigenvalues. In particular, $\text{Tr}[A^{(\pm)}A^{(\pm)}]=2^{n-1}$. We complete the proof by computing the trace (for $A \notin \{I^{\otimes n}, X^{\otimes n}\}$)

$$\operatorname{Tr}[A^{(\pm)}] = \operatorname{Tr}[Q_{\pm}AQ_{\pm}^{\dagger}] = \operatorname{Tr}[AP_{\pm}]$$
$$= (\operatorname{Tr}[A] + \operatorname{Tr}[AX^{\otimes n}])/2 = 0. \qquad \Box$$

The proof of Corollary 2 is based on a general result from [21, 90] which describes the variance of the cost function of a randomly initialized parametrized quantum circuit that is deep enough and observes certain controllability conditions. We recall a special case of this result:

Fact 1 (special case of Thm. 2 in [21]). Let the action of a Lie algebra $\mathfrak{g} = \langle H_1, \dots, H_m \rangle_{\text{Lie}}$ induce a Hilbert space splitting $\mathcal{H} = \mathcal{H}_1 \oplus \mathcal{H}_2$ into invariant subspaces such that \mathcal{H}_1 is irreducible and has dimension $d_1 = \dim(\mathcal{H}_1)$ and

 $P_1\mathfrak{g}P_1 = \mathfrak{su}(d_1)$ holds for the respective projector P_1 . We consider a variational quantum circuit [see Eq. (7)]

$$U(\vec{\theta}) = \prod_{\ell=1}^{L} \prod_{k=1}^{m} e^{-i\theta_{\ell k} H_k} = \prod_{\vartheta} e^{-i\theta_{\vartheta} H_{\vartheta}}$$

with L layers and the notation $\vartheta = \vartheta(\ell,k) = (\ell-1)m + k$ and $H_{\vartheta(\ell,k)} = H_k$. The corresponding cost function $\tilde{C}(\vec{\theta}) = \text{Tr}[U(\vec{\theta})\rho U(\vec{\theta})^{\dagger}O]$ depends on a hermitian measurement operator O and a fiduciary mixed state ρ with $\rho = P_1 \rho P_1$. Suppose that the number of layers L in $U(\vec{\theta})$ is large enough so that the distribution of $U(\vec{\theta})$ is an ε -approximate 2-design. Then, the variance of the partial derivative with respect to the parameter θ_{μ} of $\tilde{C}(\vec{\theta})$ is

$$\operatorname{Var}_{\vec{\theta}}[\partial_{\vartheta} \tilde{C}(\vec{\theta})] = \frac{2d_1}{(d_1^2 - 1)^2} \, \Delta[H_{\vartheta}^{(1)}] \, \Delta[O^{(1)}] \, \Delta[\rho^{(1)}] \quad (D3)$$

where the reduced operator $B^{(1)}$ of a matrix B acting on \mathcal{H} is defined using the orthonormalized eigenvectors of P_1 to the eigenvalue one as in and before Eq. (D2) and

$$\Delta(B) = \text{Tr}[B^2] - \text{Tr}[B]^2 / \dim(\mathcal{H}) = \dim(\mathcal{H}) \text{Var}[\text{Eig}(B)],$$
 where Eig(B) denotes the set of eigenvalues of B.

We set $O=H_p,\ \rho=|\psi\rangle\langle\psi|$ for $|\psi\rangle=|+\rangle^{\otimes n}$, and $d_1=d_+=d/2$ in Fact 1 and recover the setting of Corollary 2 with $\tilde{C}(\vec{\theta})=\langle\psi(\vec{\theta})|H_p|\psi(\vec{\theta})\rangle=C(\vec{\theta})$. We can now directly prove Corollary 2 by applying Eq. (D3) and the following Lemma 41 as all the generators H_{ϑ} in the multi-angle ansatz are Pauli strings that are different from $I^{\otimes n}$ and $X^{\otimes n}$ and that commute with $X^{\otimes n}$.

Lemma 41. In the setting of Corollary 2, we have |E| edges and $d_+ = d/2 = 2^{n-1}$ for n qubits. Let A denote any Pauli string that is different from the identity and $X^{\otimes n}$ and that commutes with $X^{\otimes n}$. Moreover, H_p is the parent Hamiltonian from Eq. (1) and $\rho = |\psi\rangle\langle\psi|$ is the projector for $|\psi\rangle = |+\rangle^{\otimes n}$ from Eq. (3). We obtain

$$\Delta[A^{(+)}] = d_{+} = d/2,$$

$$\Delta[H_{p}^{(+)}] = |E| d_{+} = |E| d/2,$$

$$\Delta[\rho^{(+)}] = (d_{+}-1)/d_{+} = (d-2)/d.$$

Proof. Applying Lemma 40, we compute

$$\Delta(A^{(+)}) = \text{Tr}[A^{(+)}A^{(+)}] - \text{Tr}[A^{(+)}]^2/d_+ = d_+ = d/2.$$

Recall the notation Q_{+} from Eq. (D2) and we obtain

$$Tr[H_p^{(+)}] = Tr[Q_+ H_p Q_+^{\dagger}] = Tr(H_p P_+)$$

$$= \frac{1}{2} \sum_{\{k,\ell\} \in E} \left[Tr(Z_k Z_{\ell} I^{\otimes n}) + Tr(Z_k Z_{\ell} X^{\otimes n}) \right] = 0 \quad (D4)$$

as the trace of a Pauli string (different from the identity) is always zero. Since $\text{Tr}[H_p^{(+)}] = 0$, we similarly get

$$\Delta[H_p^{(+)}] = \text{Tr}[H_p^{(+)}H_p^{(+)}] = \text{Tr}(H_pH_pP_+)$$
$$= \sum_{\{u,v\}\in E} \sum_{\{u',v'\}\in E} \text{Tr}(Z_uZ_vZ_{u'}Z_{v'}P_+)$$

where all terms not observing u = u' and c = v' do not contribute as in Eq. (D4), and it follows that

$$\Delta[H_p^{(+)}] = \sum_{\{u,v\} \in E} P_+ = |E| \, d_+ = |E| \, d/2.$$

Note $\rho^2 = \rho$ and $P_+ \rho P_+ = \rho$. We compute $\text{Tr}[\rho^{(+)}] =$ $\text{Tr}(\rho P_{+}) = \text{Tr}(\rho P_{+} P_{+}) = \text{Tr}(P_{+} \rho P_{+}) = \text{Tr}(\rho) = 1.$ Also, $\text{Tr}[\rho^{(+)}\rho^{(+)}] = \text{Tr}(\rho P_+ \rho P_+) = \text{Tr}(\rho^2) = \text{Tr}(\rho) = 1,$ which implies the stated formula for $\Delta[\rho^{(+)}]$.

Appendix E: Proofs for Section VII

This appendix collects proofs for Section VII. In particular, Appendix E1 provides the proof of Lemma 6, Proposition 7 is verified in Appendix E2, and Appendix E3 proves Proposition 9.

Proof of Lemma 6

In the following, we assume n > 5 as one can directly verify that $\mathfrak{g}_{nat} \cong \mathfrak{u}(n)$ for all $n \in \{2, 3, 4, 5\}$. By analyzing suitable commutators, one concludes that the semisimple part $\mathfrak{s}_{nat} = [\mathfrak{g}_{nat}, \mathfrak{g}_{nat}]$ of \mathfrak{g}_{nat} has dimension n^2-1 , while the center $\mathcal{Z}(\mathfrak{g}_{nat})$ is one dimensional and it is spanned by the single element

$$z_{\text{nat}} = \begin{cases} \sum_{o=1}^{\bar{n}} i P_{oo}^{YY} + i P_{oo}^{ZZ} & \text{for } n \text{ even,} \\ -i X_{\bar{n}+1} + \sum_{o=1}^{\bar{n}} i P_{oo}^{YY} + i P_{oo}^{ZZ} & \text{for } n \text{ odd.} \end{cases}$$

In particular, using the indices $o \in \{1, ..., \bar{n}\}, \tilde{o} \in$ $\{1, \dots, \bar{n}-1\}$, and $p, q \in \{1, \dots, n\}$ with p < n+1-qand $p \neq q$, a basis for \mathfrak{s}_{nat} is given by

$$iX_{\bar{n}+1} - iP_{\bar{n}\bar{n}}^{YY}$$
 if n is odd, (E1a)

$$iP_{oo}^{YY} - iP_{oo}^{ZZ}, \ iP_{\tilde{o}+1}^{ZZ} - iP_{\tilde{o}\tilde{o}}^{YY}, \tag{E1b}$$

$$iX_{o} + iX_{n+1-o}, iP_{oo}^{YZ} + iP_{oo}^{ZY},$$
 (E1c)

$$iX_{o}+iX_{n+1-o}, iP_{oo}^{YZ}+iP_{oo}^{ZY},$$
 (E1c)
 $iP_{pq}^{YY}+iP_{qp}^{YY}, iP_{pq}^{ZZ}+iP_{qp}^{ZZ}, iP_{pq}^{YZ}+iP_{qp}^{ZY}.$ (E1d)

In order to prove $\mathfrak{g}_{nat} \cong \mathfrak{u}(n)$, the induction hypothesis is that the elements in Eq. (31) with o > 1, p > 1, and q>1 generate the Lie algebra $\mathfrak{k}\cong\mathfrak{u}(n-2)$. Its center $\mathcal{Z}(\mathfrak{k})$ is spanned by the element

$$\tilde{z}_{\text{nat}} = \begin{cases} \sum_{o=2}^{\bar{n}} i P_{oo}^{YY} + i P_{oo}^{ZZ} & \text{for } n \text{ even,} \\ -i X_{\bar{n}+1} + \sum_{o=2}^{\bar{n}} i P_{oo}^{YY} + i P_{oo}^{ZZ} & \text{for } n \text{ odd,} \end{cases}$$

and we denote the semisimple part of \mathfrak{k} by $\mathfrak{k} \cong \mathfrak{su}(d-2)$. Note that a basis of \mathfrak{k} is given by all the elements in Eq. (E1) with o > 1, $\tilde{o} > 1$, p > 1, and q > 1, and possibly the one from Eq. (E1a).

First, we prove that \mathfrak{s}_{nat} is simple. Recall that \mathfrak{s}_{nat} is semisimple and that all its ideals are semisimple. We compute the ideal i in \mathfrak{s}_{nat} that contains the simple Lie algebra \mathfrak{k} in order to show that \mathfrak{i} is simple and $\mathfrak{i} = \mathfrak{s}_{nat}$.

To the contrary, we will assume that there exists a complementary ideal j with $i \oplus j \subseteq \mathfrak{s}_{nat}$. But then [i,j] = 0holds. Thus $[g, \mathfrak{i}] = 0$ holds for all elements $g \in \mathfrak{s}_{nat}$ outside of i. We systematically verify that all elements in Eq. (E1) with o = 1, $\tilde{o} = 1$, p = 1, or q = 1 are also contained in i. Each element in Eq. (E1d) with p = 1 or q = 1 does not commute with the element

$$iX_r + iX_{n+1-r}$$
 if n is even or $r \neq \bar{n}+1$ and $iP_{\bar{n}+1}^{ZZ} + iP_{\bar{n}\bar{n}+1}^{ZZ}$ if n is odd and $r = \bar{n}+1$

from \mathfrak{k} where $1 \neq r \in \{p,q\}$. The conditions in the previous equation are sufficient for the element to not commute (but not necessary). Thus all elements in Eq. (E1d) need to be contained in i. Moreover, the elements from Eqs. (E1b)-(E1c) with o = 1 and $\tilde{o} = 1$ do not commute with $iP_{12}^{ZZ}+iP_{21}^{ZZ}$, which implies that all elements from Eqs. (E1b)-(E1c) are contained in i. We have shown that $\mathfrak{i} = \mathfrak{s}_{nat}$. In each step, our proof technique also verifies that newly added elements do not commute with all elements already contained in i. While starting from the simple \mathbf{t}, this implies that \mathbf{i} never splits into two (or more) simple ideals. Thus $i = \mathfrak{s}_{nat}$ is simple.

An abelian subalgebra of $\mathfrak{s}_{\mathrm{nat}}$ is spanned by the n-1 elements from Eqs. (E1a)-(E1b) and it is maximal abelian. Otherwise, the rank of $\mathfrak{s}_{\mathrm{nat}}$ would be at least n while its dimension is equal to n^2-1 . But this conflicts with $\mathfrak{s}_{\rm nat}$ being simple. Indeed, all compact simple Lie algebras are $\mathfrak{su}(m+1)$, $\mathfrak{so}(2m+1)$, $\mathfrak{sp}(m)$, $\mathfrak{so}(2m)$, \mathfrak{g}_2 , \mathfrak{f}_4 , \mathfrak{e}_6 , \mathfrak{e}_7 , \mathfrak{e}_8 with respective ranks m, m, m, m, 2, 4, 6, 7, 8 and dimensions m^2+2m , $2m^2+m$, $2m^2+m$, $2m^2-m$, 14, 52, 78, 133, 248. Clearly, a rank of $m \ge n > 5$ is not possible for \mathfrak{s}_{nat} . For n > 5, the rank of m = n-1 implies that $\mathfrak{s}_{\mathrm{nat}} \cong \mathfrak{su}(n)$ and $\mathfrak{g}_{\mathrm{nat}} \cong \mathfrak{u}(n)$. This completes the proof by induction.

Proof of Proposition 7

We again can directly verify that the statement holds for $n \in \{2, 3, 4, 5\}$ and we assume now that n > 5. We shortly recall the standard generators

$$g_p := i \sum_{w=1}^{n-1} Z_w Z_{w+1}$$
 and $g_m := i \sum_{v=1}^n X_v$

for the path graph and introduce the elements

$$\tilde{g}_p := iZ_1Z_2 + iZ_{n-1}Z_n$$
 and $\tilde{g}_m := iX_1 + iX_n$.

It is straightforward to verify that

$$\tilde{g}_m = (-[g_p, [g_p, [g_p, [g_p, g_m]]]] - 16[g_p, [g_p, g_m]])/48,$$

$$\tilde{g}_p = -[\tilde{g}_m, [\tilde{g}_m, g_p]]/4.$$

Consequently, $g_p - \tilde{g}_p$ and $g_m - \tilde{g}_m$ are contained in $\mathfrak{g}_{\mathrm{std}}$ and we can assume as induction hypothesis that these two elements generate $\mathfrak{k} \cong \mathfrak{u}(n-2)$. Following Eq. (31), clearly $iP_{22}^{YY} \in \mathfrak{k}$ and one obtains that

$$\begin{split} g_1 &:= i P_{11}^{ZZ} &= [g_p, [g_p, i P_{22}^{YY}]]/8 + i P_{22}^{YY}, \\ g_2 &:= i P_{11}^{YZ} + i P_{11}^{ZY} = [\tilde{g}_m, i P_{11}^{ZZ}]/2, \\ g_3 &:= i P_{11}^{YY} &= [\tilde{g}_m, i P_{11}^{YZ} + i P_{11}^{ZY}]/4 + i P_{11}^{ZZ}. \end{split}$$

Consequently, \tilde{g}_m , g_1 , g_2 , and g_3 generate the Lie algebra $\mathfrak{g}_2 \cong \mathfrak{u}(2)$ such that all elements of \mathfrak{g}_2 commute with all elements of \mathfrak{k} . We summarize

$$\mathfrak{u}(2) \oplus \mathfrak{u}(n-2) \cong \mathfrak{g}_2 \oplus \mathfrak{k} \subsetneq \mathfrak{g}_{\mathrm{std}} \subseteq \mathfrak{g}_{\mathrm{nat}} \cong \mathfrak{u}(n),$$

but $\mathfrak{u}(2)\oplus\mathfrak{u}(n-2)$ is a maximal subalgebra of $\mathfrak{u}(n)$ [204, 205]. Thus the induction step is complete.

3. Proof of Proposition 9

For this proof, let $n_I = n_I(S)$, $n_X = n_X(S)$, $n_Y =$ $n_Y(S)$, and $n_Z = n_Z(S)$ denote respectively the number of I, X, Y, and Z in a Pauli string S. Recall from Table III that $n_Y + n_Z$ is even, $n_X \neq n$, and $n_I \neq n$ for the Pauli-string basis of $\mathfrak{g}_{\text{free}}$ for a complete graph. In order to determine \mathfrak{g}_{nat} , we are counting the Pauli strings that are also invariant under the action of the automorphism group $Aut(K_n) = S_n$. We assume that the two Pauli strings S_1 and S_2 contain the same number of X, Y, Z, and I, i.e., $n_I(S_1) = n_I(S_2)$, $n_X(S_1) = n_X(S_2)$, $n_Y(S_1) = n_Y(S_2)$, and $n_Z(S_1) = n_Z(S_2)$. Then there clearly exits an automorphism $\sigma \in \mathcal{S}_n$ of the complete graph that maps S_1 to S_2 , in the sense that $\zeta[\sigma]S_1 =$ $S_2\zeta[\sigma]$, where ζ maps permutations to n-qubit matrices and has been defined in Sec. V. A weak 4-composition of n is an ordered quadruple of nonnegative integers (n_I, n_X, n_Y, n_Z) with $n_I + n_X + n_Y + n_Z = n$. Thus a basis of \mathfrak{g}_{nat} is given by all possible sums of Pauli strings (with identity coefficients) such that the Pauli strings in each sum correspond to a fixed weak 4-composition (n_I, n_X, n_Y, n_Z) of n while observing the additional conditions that $n_Y + n_Z$ is even and neither n_I nor n_X is equal to n. Now all that remains is to count these allowed weak 4-compositions. Ignoring all restrictions, we have $\binom{n+3}{3}$ weak 4-compositions (as is easily verified by the stars-and-bars method [206, pp. 17–18]).

If n is odd, then $n_I + n_X$ and $n_Y + n_Z$ have opposite parity, so the map $(n_I, n_X, n_Y, n_Z) \mapsto (n_Z, n_Y, n_X, n_I)$ establishes a bijection between weak 4-compositions that satisfy the \mathbb{Z}_2 symmetry and that do not. So, there are exactly $\frac{1}{2}\binom{n+3}{3}$ weak 4-compositions that satisfy the parity condition. Removing the weak 4-compositions (n, 0, 0, 0) and (0, n, 0, 0), we obtain the final answer of $\dim(\mathfrak{g}_{\mathrm{nat}}) = \frac{1}{2}\binom{n+3}{3} - 2$ if n is odd.

If n is even, then the map $(n_I, n_X, n_Y, n_Z) \mapsto (n_I + 1, n_X, n_Y, n_Z - 1)$ establishes a bijection from the set of weak 4-compositions with $n_Y + n_Z$ even and $n_Z \ge 1$ to the set of weak 4-compositions with $n_Y + n_Z$ odd and $n_I \ge 1$. The only weak 4-compositions that have not

been accounted for are the ones with $n_Y + n_Z$ even and $n_Z = 0$ and the ones with $n_Y + n_Z$ odd and $n_I = 0$.

The former cases can be thought of as weak 3-compositions of n of the form (n_I, n_X, n_Y) with n_Y even; all of these are allowed, as long as neither n_I nor n_X equals n. Letting n_Y range over all even values from 0 to n, we see that there are $(n+1)+(n-1)+\cdots+3+1=(n/2+1)^2$ possibilities. The latter weak 4-compositions can be thought of as weak 3-compositions of n of the form (n_X, n_Y, n_Z) with n_X odd (since n is even); all of these are not allowed. Letting n_X range over all odd values from 1 to n-1, we see that there are $n+(n-2)+\cdots+4+2=n(n/2+1)/2$ possibilities.

The total of the two quantities from the last paragraph is $\binom{n+2}{2}$, which is exactly the number of weak 4-compositions missing from the bijection established for even n. Putting this all together, we conclude that the number of allowed weak 4-compositions is

$$\dim(\mathfrak{g}_{\text{nat}}) = \left[\left(\frac{n}{2} + 1 \right)^2 - 2 \right] + \frac{1}{2} \left[\left(\frac{n+3}{3} \right) - \left(\frac{n+2}{2} \right) \right]$$
$$= \frac{1}{2} \binom{n+3}{3} + \frac{n}{4} - \frac{3}{2}$$

if n is even, which completes the proof.

Appendix F: Proofs for Section VIII

This appendix details the proofs for Section VIII. In particular, Appendix F 1 provides the proof of Lemma 10, Proposition 11 is shown in Appendix F 2, Appendix F 3 verifies Lemma 12, and finally the proof of Proposition 14 is given in Appendix F 4.

1. Proof of Lemma 10

Notice that X_v anticommutes with $Z^{\otimes n}$ for each qubit v, which means hat any mixer Hamiltonian created from terms with X_v also anticommutes with $Z^{\otimes n}$. However, $Z_w Z_{\tilde{w}}$ commutes with $Z^{\otimes n}$ for any two qubits w and \tilde{w} and any Hamiltonian created by adding terms with $Z_w Z_{\tilde{w}}$ also commutes with $Z^{\otimes n}$. Consequently, any nested commutator of such Hamiltonians commutes with $Z^{\otimes n}$ if it has an even number of mixer Hamiltonian terms or anticommutes with $Z^{\otimes n}$ if it has an odd number of mixer Hamiltonian terms. All of these nested commutators span g. By definition, $g|\psi\rangle \in W$ for $|\psi\rangle \in W$ and a nested commutator $g \in \mathfrak{g}$. Moreover, $Z^{\otimes n} | \psi \rangle$ is an arbitrary element in $(Z^{\otimes n})W$. Since either commutes or anticommutes with $Z^{\otimes n}$, it follows that $g(Z^{\otimes n}|\psi\rangle) =$ $\pm Z^{\otimes n}(g|\psi\rangle) \in (Z^{\otimes n})W$. Hence $(Z^{\otimes n})W$ is also an invariant subspace of \mathfrak{g} .

2. Proof of Proposition 11

As $Z \mid + \rangle = \mid - \rangle$ and $Z \mid - \rangle = \mid + \rangle$ and n is odd, $Z^{\otimes n}$ maps states in \mathcal{H}_{+} to states in \mathcal{H}_{-} and vice versa via the preceding discussion. Alternatively, we notice that $Z^{\otimes n}$ anticommutes with $X^{\otimes n}$ if n is odd, so it must map a ± 1 eigenstate of $X^{\otimes n}$ to a ∓ 1 eigenstate.

The symmetries of \mathfrak{g} induce a subspace decomposition of \mathcal{H}_+ and \mathcal{H}_- . In particular, any invariant subspace V_i within \mathcal{H}_+ will lead to a corresponding invariant subspace $(Z^{\otimes n}) V_j$ within \mathcal{H}_- due to Lemma 10 and the preceding paragraph showing that $Z^{\otimes n}$ swaps \mathcal{H}_+ and \mathcal{H}_- (as n is odd). Conversely, any invariant subspace within \mathcal{H}_{-} will lead to a corresponding invariant subspace within \mathcal{H}_{+} for the same reason. It follows that \mathcal{H}_{+} and \mathcal{H}_{-} must have matching decompositions into irreducible, invariant subspaces, with the correspondence is induced by multiplication with $Z^{\otimes n}$, exactly as desired.

3. Proof of Lemma 12

An automorphism $\sigma_2 \in \operatorname{Aut}(G) \subseteq \mathcal{S}_n$ acts on a basis state $|x\rangle = |x_1\rangle \otimes \cdots \otimes |x_n\rangle$ via (see Section V)

$$\sigma_2\cdot|x\rangle=\,|x_{\sigma_2^{-1}(1)},\!\dots,x_{\sigma_2^{-1}(n)}\rangle=\,|x_{\sigma_2^{-1}(1)}\rangle\otimes\dots\otimes|x_{\sigma_2^{-1}(n)}\rangle\,.$$

This is described using the map $\Upsilon(\sigma_1, \sigma_2) = \vartheta[\sigma_1] \zeta[\sigma_2]$ from the permutation group $G_{nat} = S_2 \times Aut(G)$ to the group of natural symmetries $\mathbb{G}_{\mathrm{nat}} = \mathbb{Z}_2 \times \zeta[\mathrm{Aut}(G)]$ where the form of $\zeta[\sigma_2]$ is detailed in Section V and $\vartheta[\sigma_1]$ is given in Eq. (35). For the proof, we compute the character $\chi_{\text{nat}}(\sigma_1, \sigma_2)$ from Eq. (36). Based on the statement of this lemma, we need to consider three cases: (i) For $\sigma_1 = 1, \chi_{\text{nat}}(\sigma_1, \sigma_2) = 2^{c(\sigma_2)}$. (ii) If $\sigma_1 = (1, 2)$ and every cycle in the decomposition in Eq. (38) for $\sigma = \sigma_2$ has even length, then $\chi_{\rm nat}(\sigma_1, \sigma_2) = 2^{c(\sigma_2)}$. (iii) If $\sigma_1 = (1, 2)$ and there exists a cycle of odd length in the decomposition of Eq. (38), then $\chi_{\text{nat}}(\sigma_1, \sigma_2) = 0$.

Recall that $I^{\otimes n}$ and $X^{\otimes n}$ from Eq. (35) as well as $\zeta[\sigma_2]$ act as permutation matrices on $\mathbb{C}^{d\times d}$. Thus the same applies to $\Upsilon(\sigma_1, \sigma_2)$ and the number of fix points in the set of basis states determines the value of the trace as non-invariant basis states do not contribute. Given a computational basis state $|x\rangle$, we observe that

$$\Upsilon(\mathbf{1},\sigma_2)\left|x\right> = \left|x_{\sigma_2^{-1}(1)},..,x_{\sigma_2^{-1}(n)}\right>, \tag{F1a}$$

$$\Upsilon((1,2),\sigma_2)|x\rangle = |\neg x_{\sigma_2^{-1}(1)},...,\neg x_{\sigma_2^{-1}(n)}\rangle,$$
 (F1b)

where $\neg x_i$ again denotes the negation of x_i by swapping the basis states $|0\rangle$ and $|1\rangle$.

The case (i) corresponds to Eq. (F1a) and $|x\rangle$ is fixed if and only if $x_j = x_{\sigma_2^{-1}(j)}$ for each $1 \leqslant j \leqslant n$. In order words, x needs to be constant on each cycle in the decomposition of Eq. (38). Consequently, the result $\chi_{\rm nat}(\sigma_1,\sigma_2)=2^{c(\sigma_2)}$ follows for (i) as one has two possible values 0 and 1 for each cycle of σ_2 .

If $\sigma_1 = (1, 2)$, Eq. (F1b) applies and it is necessary and sufficient for a fixed point to observe $x_j = \neg x_{\sigma_2^{-1}(j)}$ for each $1 \leq j \leq n$. Hence the fixed points are exactly the basis states that alternate between zero and one on each cycle in the cycle decomposition of σ_2 . But this is impossible for any cycle of odd length and we obtain $\chi_{\rm nat}(\sigma_1,\sigma_2)=0$ in the case (iii). For the case (ii), we again have $\chi_{\rm nat}(\sigma_1,\sigma_2)=2^{c(\sigma_2)}$ as there are also two choices for each cycle.

4. Proof of Proposition 14

Lemma 13 implies case (b) as we only need to sum over the identity element $1 \in Aut(G)$. As all terms in the sum in Lemma 13 are positive, case (c) is obtained by restricting the sum to the identity element $1 \in Aut(G)$. For (a), we state two formulas

$$\sum_{\sigma \in \mathcal{S}_n} 2^{c(\sigma)} = (n+1)! \text{ and } (F2a)$$

$$\sum_{\sigma \in \mathcal{S}_n} 2^{c(\sigma)} = (n+1)! \text{ and } (F2a)$$

$$\sum_{\sigma \in \mathcal{S}_{2m}} 2^{c(\sigma)} \wp(\sigma) = (2m)!$$
(F2b)

where Eq. (F2a) is a special case of Proposition 1.3.7 on p. 27 in [206]. We will prove Eq. (F2b) below. The proof of (a) now continues separately for odd and even n. If n=2m+1 is odd, then $\wp(\sigma)=0$ for all $\sigma\in \operatorname{Aut}(G)$. Thus Lemma 13 and Eq. (F2a) imply for n = 2m+1 that

$$\mathbf{m}_{(\mathrm{t,t})} = (2m+2)!/[2(2m+1)!] = m+1 = \left\lfloor \frac{n}{2} \right\rfloor + 1.$$

For n = 2m even, combining Eqs. (F2a) and (F2b) proves

$$\mathbf{m}_{(t,t)} = \frac{(2m+1)!}{[2(2m)!]} + \frac{(2m)!}{[2(2m)!]}$$

= $\frac{(m+\frac{1}{2})}{1} + \frac{1}{2} = m+1 = \frac{n}{2} + 1.$

Thus we are left with verifying Eq. (F2b). Let $\mathcal{P}(n,k)$ denote the set of all partitions p of n with k parts [206], i.e., $p = [p_1, \dots, p_k]$ where each part is given by an integer $p_j > 0$ such that $\sum_{j=1}^k p_j = n$ and $p_j \geqslant p_{j+1}$. Similarly, let $\mathcal{P}_e(n,k) \subseteq \mathcal{P}(n,k)$ denote the set of partitions that have only even parts p_i . Also, we describe a partition pas in Eq. (37) using its cycle type $(1^{b_1}, \ldots, n^{b_n})$ where the multiplicity $b_a \ge 0$ of a in p is given by $b_a = \sum_{j=1}^k \delta_{ap_j}$ with $1 \le a \le n$. The number of permutations $\sigma \in S_n$ with cycle type $(1^{b_1}, \ldots, n^{b_n})$ as determined by a partition p of n is equal to (see Prop. 1.3.2 on p. 23 in [206])

$$n!/\mathbf{z}_{(n,p)}$$
 where $\mathbf{z}_{(n,p)} := \prod_{a=1}^{n} a^{b_a} b_a!$.

Let 2p denote the partition obtained by multiplying each part of p by 2. We now compute

$$\sum_{\sigma \in \mathcal{S}_{2m}} 2^{c(\sigma)} \wp(\sigma) = \sum_{k=1}^{m} \sum_{p \in \mathcal{P}_{c}(2m,k)} 2^{k} (2m)! / \mathbf{z}_{(2m,p)} \quad (F3a)$$

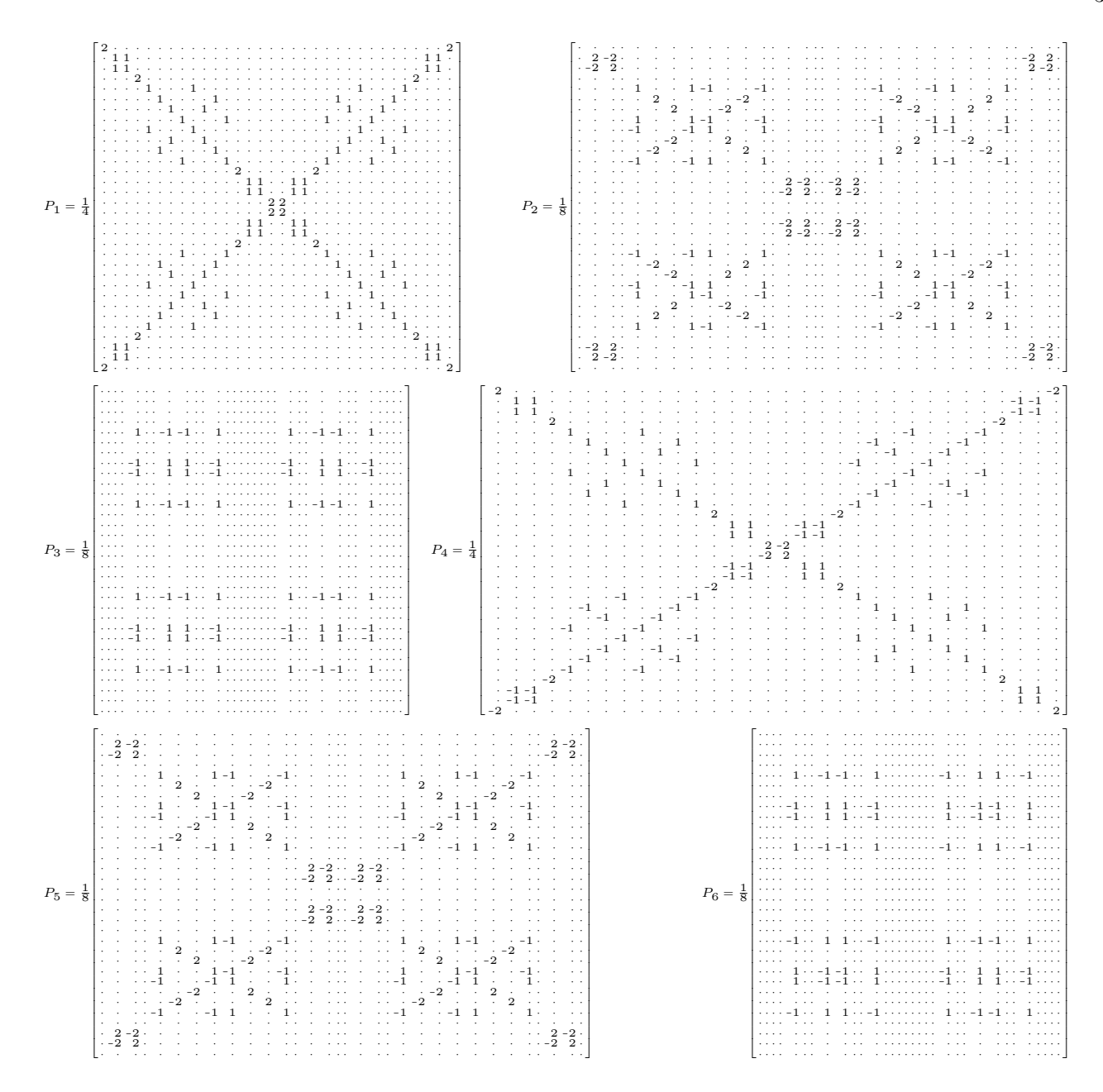


Figure 16. Explicit matrices for the projectors P_j from Fig. 5. Zeros are replaced by dots.

$$= (2m)! \sum_{k=1}^{m} \sum_{p \in \mathcal{P}(m,k)} 2^{k} / \mathbf{z}_{(2m,2p)}$$

$$= (2m)! \sum_{k=1}^{m} \sum_{p \in \mathcal{P}(m,k)} \frac{2^{k}}{\mathbf{z}_{(m,p)} \prod_{a=1}^{m} 2^{b_{a}}}$$

$$= (2m)! \sum_{k=1}^{m} \sum_{p \in \mathcal{P}(m,k)} \frac{2^{k}}{\mathbf{z}_{(m,p)} 2^{\sum_{a=1}^{m} b_{a}}}$$

$$= (2m)! \sum_{k=1}^{m} \sum_{p \in \mathcal{P}(m,k)} 1/\mathbf{z}_{(m,p)} = (2m)!,$$
(F3c)

where we can limit the summation over k in Eq. (F3a)

to values of up to m as all partitions have even parts $p_j \geq 2$. Equation (F3b) follows as all even partitions in $\mathcal{P}_e(2m,k)$ are obtained from all partitions in $\mathcal{P}(m,k)$ by multiplying each part by two and all occurring parts are less than equal to m. Finally, we conclude by comparing Eq. (F3c) with $\sum_{k=1}^m \sum_{p \in \mathcal{P}(m,k)} m!/\mathbf{z}_{(m,p)} = |\mathcal{S}_m| = m!$.

Appendix G: Properties of centers for general compact Lie algebras and subalgebras of $\mathfrak{g}_{\mathrm{free}}$

In this appendix, we shortly state some useful properties related to the centers of certain Lie algebras \mathfrak{g} such that \mathfrak{g} is a general compact Lie algebra (i.e. $\mathfrak{g} \subseteq \mathfrak{u}(m)$

for a suitable m), \mathfrak{g} is contained in $\mathfrak{g}_{\text{free}}$, or \mathfrak{g} is equal to $\mathfrak{g}_{\text{std}}$. Recall that any element g contained in a compact Lie algebra $\mathfrak{g} \subseteq \mathfrak{u}(m)$ can be uniquely decomposed into g = s + c where $s \in [\mathfrak{g}, \mathfrak{g}]$ is contained in the semisimple part $[\mathfrak{g}, \mathfrak{g}]$ of \mathfrak{g} and $c \in \mathcal{Z}(\mathfrak{g})$ is contained in the center $\mathcal{Z}(\mathfrak{g})$ of \mathfrak{g} . This is a consequence of \mathfrak{g} being contained in a unitary Lie algebra and thus being reductive [77, 78]. The number of elements in a generating set for a compact Lie algebra constraints the dimension of its center:

Lemma 42. Consider a Lie algebra $\langle g_1, \ldots, g_k \rangle_{\text{Lie}} = \mathfrak{g} \subseteq \mathfrak{u}(m)$ that is contained in a unitary Lie algebra $\mathfrak{u}(m)$ and that is generated by k elements g_1, \ldots, g_k . Then the dimension $|\mathcal{Z}(\mathfrak{g})|$ of the center $\mathcal{Z}(\mathfrak{g})$ of \mathfrak{g} is less than equal to the number k of generators, i.e., $|\mathcal{Z}(\mathfrak{g})| \leq k$.

Proof. The generators $g_j = s_j + c_j$ can be uniquely decomposed into $s_j \in [\mathfrak{g},\mathfrak{g}]$ and $c_j \in \mathcal{Z}(\mathfrak{g})$. Clearly, $[g_j,g_k] \subseteq [\mathfrak{g},\mathfrak{g}]$ and all s_j are obtained from the generators via linear combinations of higher-order commutators. Thus, we obtain $c_j = g_j - s_j$ and $\mathcal{Z}(\mathfrak{g})$ is spanned by the elements c_j , which completes the proof.

Interestingly, we can interpret the center of a compact Lie algebra as a subset of the center of its commutant:

Lemma 43. Given a compact Lie algebra $\mathfrak{g} \subseteq \mathfrak{u}(m)$ and its commutant $\mathcal{C} = \mathfrak{com}(\mathfrak{g})$, we have (i) $\mathcal{Z}(\mathfrak{g}) = \mathcal{C} \cap \mathfrak{g} \subseteq \mathcal{C}$ and (ii) $\mathcal{Z}(\mathfrak{g}) \subseteq \mathcal{Z}(\mathcal{C})$.

Proof. The case (i) is obvious from the definitions. Assume that there exists $g \in \mathcal{Z}(\mathfrak{g})$ and $M \in \mathcal{C}$ such that $[g,M] \neq 0$. But this conflicts with the definition of the commutant \mathcal{C}_{std} and the statement follows.

This allows us to bound the dimension of the centers for Lie algebras that include the standard-ansatz and the free Lie algebras $\mathfrak{g}_{\mathrm{std}}$ and $\mathfrak{g}_{\mathrm{free}}$:

Lemma 44. Given a Lie algebra $\mathfrak{g} \subseteq \mathfrak{g}_{free}$, the dimension $\dim[\mathcal{Z}(\mathfrak{g})]$ of its center $\mathcal{Z}(\mathfrak{g})$ is bounded as $\dim[\mathcal{Z}(\mathfrak{g})] \leq \dim[\mathcal{Z}(\mathcal{C})] - 2$ where $\mathcal{C} = \mathcal{C}(\mathfrak{g})$ is the commutant of \mathfrak{g} .

Proof. Clearly. $\mathfrak{g} \subseteq \mathfrak{g}_{\text{free}}$ and $\mathcal{C} \supseteq \mathcal{C}_{\text{free}}$. Lemma 15(a) and (b) now imply $iX^{\otimes n}, iI^{\otimes n} \notin \mathfrak{g}$ and $iX^{\otimes n}, iI^{\otimes n} \in \mathcal{C}$. Clearly, $iX^{\otimes n}, iI^{\otimes n} \notin \mathcal{Z}(\mathfrak{g})$ follows. This then verifies $\dim[\mathcal{Z}(\mathfrak{g})] \leq \dim(\mathcal{C})-2$.

Lemma 43 implies $\mathcal{Z}(\mathfrak{g}) \subseteq \mathcal{Z}(\mathcal{C})$. The statement of the current lemma is immediate after we have shown $iI^{\otimes n}, iX^{\otimes n} \in \mathcal{Z}(\mathcal{C})$. We have $iI^{\otimes n} \in \mathcal{Z}(\mathcal{C})$. Moreover, $iX^{\otimes n} \in \mathcal{Z}(\mathcal{C})$ follows, e.g., as the projectors $P_{\pm} = (X^{\otimes n} \pm I^{(n)})/2$ are linear combinations of the isotypical projectors contained in $\mathcal{Z}(\mathcal{C})$ associated to the isotypical decomposition of \mathcal{C} (see Appendix A).

We now bound the dimension of the center $\mathcal{Z}(\mathfrak{g}_{std})$ for the standard-ansatz Lie algebra \mathfrak{g}_{std} :

Lemma 45. Given the Lie algebra \mathfrak{g}_{std} of the standard ansatz, the dimension $\dim[\mathcal{Z}(\mathfrak{g}_{std})]$ of its center $\mathcal{Z}(\mathfrak{g}_{std})$ is bounded as $\dim[\mathcal{Z}(\mathfrak{g}_{std})] \leq \min\{2,\dim[\mathcal{Z}(\mathcal{C}_{std})]-2\}$ where $\mathcal{C}_{std} = \mathcal{C}(\mathfrak{g}_{std})$ is the commutant of \mathfrak{g}_{std} . *Proof.* Lemma 42 directly verifies $\dim[\mathcal{Z}(\mathfrak{g}_{std})] \leq 2$. Lemma 44 completes the proof.

Appendix H: Explicit projection matrices from Figures 5 and 10

The explicit form of the projection matrices from Figures 5 and 10 are shown in Figures 16 and 17, respectively.

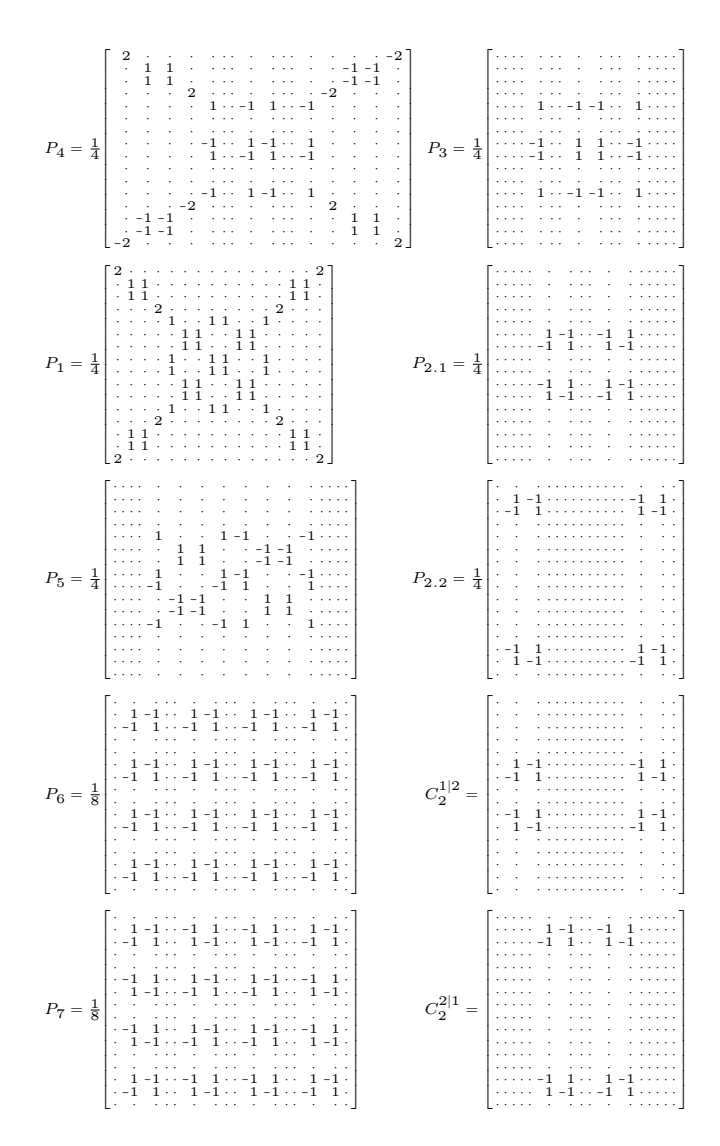


Figure 17. Explicit matrices for the projectors P_j and cross terms $C_2^{k|\ell}$ from Fig. 10. Dots denote zeros.

- E. Farhi, J. Goldstone, and S. Gutmann, A quantum approximate optimization algorithm (2014), arXiv:1411.4028.
- [2] E. Farhi and A. W. Harrow, Quantum supremacy through the quantum approximate optimization algorithm (2016), arXiv:1602.07674.
- [3] M. Cerezo, A. Arrasmith, R. Babbush, S. C. Benjamin, S. Endo, K. Fujii, J. R. McClean, K. Mitarai, X. Yuan, L. Cincio, and P. J. Coles, Nat. Rev. Phys. 3, 625–644 (2021).
- [4] K. Bharti, A. Cervera-Lierta, T. H. Kyaw, T. Haug, S. Alperin-Lea, A. Anand, M. Degroote, H. Heimonen, J. S. Kottmann, T. Menke, et al., Rev. Mod. Phys. 94, 015004 (2022).
- [5] S. Endo, Z. Cai, S. C. Benjamin, and X. Yuan, J. Phys. Soc. Jpn. 90, 032001 (2021).
- [6] M. Schuld, I. Sinayskiy, and F. Petruccione, Contemp. Phys. 56, 172 (2015).
- [7] J. Biamonte, P. Wittek, N. Pancotti, P. Rebentrost, N. Wiebe, and S. Lloyd, Nature 549, 195 (2017).
- [8] M. Cerezo, G. Verdon, H.-Y. Huang, L. Cincio, and P. J. Coles, Nat. Comput. Sci. 2, 567–576 (2022).
- [9] M. Larocca, S. Thanasilp, S. Wang, K. Sharma, J. Bia-monte, P. J. Coles, L. Cincio, J. R. McClean, Z. Holmes, and M. Cerezo, Nat. Rev. Phys. 7, 174 (2025).
- [10] J. R. McClean, S. Boixo, V. N. Smelyanskiy, R. Babbush, and H. Neven, Nat. Commun. 9, 1 (2018).
- [11] M. Cerezo, A. Sone, T. Volkoff, L. Cincio, and P. J. Coles, Nat. Commun. 12, 1 (2021).
- [12] E. R. Anschuetz and B. T. Kiani, Nat. Commun. 13, 7760 (2022).
- [13] E. R. Anschuetz, in *International Conference on Learning Representations* (2022).
- [14] L. Bittel and M. Kliesch, Phys. Rev. Lett. 127, 120502 (2021).
- [15] X. You and X. Wu, in Proceedings of the 38th International Conference on Machine Learning, edited by M. Meila and T. Zhang (PMLR, 2021) pp. 12144–12155.
- [16] E. Fontana, M. Cerezo, A. Arrasmith, I. Rungger, and P. J. Coles, Quantum 6, 804 (2022).
- [17] G. Koßmann, L. Binkowski, L. van Luijk, T. Ziegler, and R. Schwonnek, Deep-Circuit QAOA (2023), arXiv:2210.12406v2.
- [18] J. Rajakumar, J. Golden, A. Bärtschi, and S. Eidenbenz, in *Proceedings of the 21st ACM International Conference on Computing Frontiers* (ACM, New York, NY, 2024) p. 199–206.
- [19] P. Bermejo, B. Aizpurua, and R. Orús, Phys. Rev. Res. 6, 023069 (2024).
- [20] R. Zeier and T. Schulte-Herbrüggen, J. Math. Phys. 52, 113510 (2011).
- [21] M. Larocca, P. Czarnik, K. Sharma, G. Muraleedharan, P. J. Coles, and M. Cerezo, Quantum 6, 824 (2022).
- [22] M. Ragone, B. N. Bakalov, F. Sauvage, A. F. Kemper, C. Ortiz Marrero, M. Larocca, and M. Cerezo, Nat. Commun. 15, 7172 (2024).
- [23] E. Fontana, D. Herman, S. Chakrabarti, N. Kumar, R. Yalovetzky, J. Heredge, S. H. Sureshbabu, and M. Pistoia, Nat. Commun. 15, 7171 (2024).
- [24] N. L. Diaz, D. García-Martín, S. Kazi, M. Larocca, and M. Cerezo, Showcasing a Barren Plateau The-

- ory Beyond the Dynamical Lie Algebra (2023), arXiv:2310.11505.
- [25] M. Larocca, N. Ju, D. García-Martín, P. J. Coles, and M. Cerezo, Nat. Comput. Sci. 3, 542 (2023).
- [26] L. Schatzki, M. Larocca, Q. T. Nguyen, F. Sauvage, and M. Cerezo, npj Quantum Inf. 10, 12 (2024).
- [27] M. L. Goh, M. Larocca, L. Cincio, M. Cerezo, and F. Sauvage, Lie-algebraic classical simulations for variational quantum computing (2023), arXiv:2308.01432.
- [28] Z. Zimborás, R. Zeier, T. Schulte-Herbrüggen, and D. Burgarth, Phys. Rev. A 92, 042309 (2015).
- [29] F. Albertini and D. D'Alessandro, J. Math. Phys. 59, 052102 (2018).
- [30] S. Lloyd, Quantum approximate optimization is computationally universal (2018), arXiv:1812.11075.
- [31] M. E. Morales, J. Biamonte, and Z. Zimborás, Quantum Inf. Process. 19, 1 (2020).
- [32] S. Kazi, M. Larocca, and M. Cerezo, New Journal of Physics 26, 053030 (2024).
- [33] R. Wiersema, E. Kökcü, A. F. Kemper, and B. N. Bakalov, npj Quantum Inf. 10, 110 (2024).
- [34] D. D'Alessandro and Y. Isik, J. Phys. A 58, 115202 (2025).
- [35] G. Aguilar, S. Cichy, J. Eisert, and L. Bittel, Full classification of Pauli Lie algebras (2024), arXiv:2408.00081.
- [36] J. Allcock, M. Santha, P. Yuan, and S. Zhang, On the dynamical Lie algebras of quantum approximate optimization algorithms (2024), arXiv:2407.12587.
- [37] E. Kökcü, R. Wiersema, A. F. Kemper, and B. N. Bakalov, Classification of dynamical Lie algebras generated by spin interactions on undirected graphs (2024), arXiv:2409.19797.
- [38] M. B. Mansky, S. L. Castillo, V. R. Puigvert, and C. Linnhoff-Popien, Permutation-invariant quantum circuits (2023), arXiv:2312.14909.
- [39] M. B. Mansky, M. A. Martinez, A. B. de la Serna, S. L. Castillo, D. Nikoladou, G. Sathish, Z. Wang, S. Wölckert, and C. Linnhoff-Popien, Scaling of symmetry-restricted quantum circuits (2024), arXiv:2406.09962.
- [40] E. Kökcü, T. Steckmann, Y. Wang, J. Freericks, E. F. Dumitrescu, and A. F. Kemper, Phys. Rev. Lett. 129, 070501 (2022).
- [41] F. Sauvage, M. Larocca, P. J. Coles, and M. Cerezo, Quantum Sci. Technol. 9, 015029 (2024).
- [42] R. Herrman, P. C. Lotshaw, J. Ostrowski, T. S. Humble, and G. Siopsis, Sci. Rep. 12, 6781 (2022).
- [43] K. Shi, R. Herrman, R. Shaydulin, S. Chakrabarti, M. Pistoia, and J. Larson, in 2022 IEEE/ACM 7th Symposium on Edge Computing (SEC) (Seattle, WA, 2022) pp. 414–419.
- [44] L. Onsager, Phys. Rev. 65, 117 (1944).
- [45] I. Marvian, Phys. Rev. Res. 6, 043292 (2024).
- [46] S. Boulebnane and A. Montanaro, Predicting parameters for the Quantum Approximate Optimization Algorithm for MAX-CUT from the infinite-size limit (2021), arXiv:2110.10685.
- [47] J. Basso, E. Farhi, K. Marwaha, B. Villalonga, and L. Zhou, in 17th Conference on the Theory of Quantum Computation, Communication and Cryptography (TQC 2022), Leibniz International Proceedings in Informatics (LIPIcs), Vol. 232, edited by F. Le Gall and

- T. Morimae (Schloss Dagstuhl Leibniz-Zentrum für Informatik, Dagstuhl, Germany, 2022) pp. 7:1–7:21.
- [48] J. Basso, E. Farhi, K. Marwaha, B. Villalonga, and L. Zhou, The Quantum Approximate Optimization Algorithm at High Depth for MaxCut on Large-Girth Regular Graphs and the Sherrington-Kirkpatrick Model (2022), arXiv:2110.14206v3.
- [49] S. Boulebnane, On the power of the Quantum Approximate Optimization Algorithm, Ph.D. thesis, University College London (2024).
- [50] L. Zhou, S.-T. Wang, S. Choi, H. Pichler, and M. D. Lukin, Phys. Rev. X 10, 021067 (2020).
- [51] E. Farhi, J. Goldstone, S. Gutmann, and L. Zhou, Quantum 6, 759 (2022).
- [52] C. Moore and S. Mertens, *The Nature of Computation* (Oxford University Press, New York, 2011).
- [53] C. W. Commander, Maximum Cut Problem, MAX-CUT, in *Encyclopedia of Optimization*, edited by C. A. Floudas and P. M. Pardalos (Springer, Boston, 2008) pp. 1991–1999.
- [54] A. Newman, Max Cut, in *Encyclopedia of Algorithms*, edited by M.-Y. Kao (Springer, Boston, 2008) pp. 489– 492.
- [55] M. R. Garey and D. S. Johnson, Computers and Intractibility (W. H. Freeman and Company, San Francisco, 1979).
- [56] R. Diestel, *Graph Theory*, 5th ed. (Springer, Berlin, 2017).
- [57] R. M. Karp, in Complexity of Computer Computations, edited by R. E. Miller and J. W. Thatcher (Plenum Press, New York, 1972) pp. 85–103.
- [58] M. R. Garey, D. S. Johnson, and L. Stockmeyer, Theor. Comput. Sci. 1, 237 (1976).
- [59] M. M. Deza and M. Laurent, Geometry of Cuts and Metrics (Springer, Berlin, 1997).
- [60] E. W. Mayr, H. J. Prömel, and A. Steger, eds., Lectures on Proof Verification and Approximation Algorithms (Springer, Berlin, 1998).
- [61] V. V. Vazirani, Approximation Algorithms (Springer, Berlin, 2001).
- [62] D. P. Williamson and D. B. Shmoys, *The Design of Approximation Algorithms* (Cambridge University Press, Cambridge, 2011).
- [63] M. X. Goemans and D. P. Williamson, J. ACM 42, 1115 (1995).
- [64] H. Karloff, SIAM J. Comput. 29, 336 (1999).
- [65] U. Feige and G. Schechtman, Random Struct. Alg. 20, 403 (2002).
- [66] J. Håstad, J. ACM 48, 798 (2001).
- [67] S. Hadfield, Z. Wang, B. O'Gorman, E. G. Rieffel, D. Venturelli, and R. Biswas, Algorithms 12, 34 (2019).
- [68] M. P. Harrigan, K. J. Sung, M. Neeley, K. J. Satzinger, F. Arute, K. Arya, J. Atalaya, J. C. Bardin, R. Barends, S. Boixo, et al., Nat. Phys. 17, 1 (2021).
- [69] I. Gaidai and R. Herrman, Sci. Rep. 14, 18911 (2024).
- [70] A. Wilkie, J. Ostrowski, and R. Herrman, An angle rounding parameter initialization technique for ma-QAOA (2024), arXiv:2404.10743.
- [71] Z. Holmes, K. Sharma, M. Cerezo, and P. J. Coles, PRX Quantum 3, 010313 (2022).
- [72] B. C. Hall, *Lie Groups, Lie Algebras, and Representa*tions, 2nd ed. (Springer, New York, 2015).
- [73] N. Jacobson, *Lie Algebras* (Dover Publications, New York, 1979).

- [74] W. A. de Graaf, Lie Algebras: Theory and Algorithms (Elsevier, Amsterdam, 2000).
- [75] D. D'Alessandro, Introduction to Quantum Control and Dynamics, 2nd ed. (CRC Press, Boca Raton, 2022).
- [76] D. Elliott, Bilinear Control Systems (Springer, London, 2009).
- [77] N. Bourbaki, Elements of Mathematics, Lie Groups and Lie Algebras, Chapters 1–3 (Springer, Berlin, 1989).
- [78] N. Bourbaki, Elements of Mathematics, Lie Groups and Lie Algebras, Chapters 7–9 (Springer, Berlin, 2008).
- [79] D. A. Roozemond, Algorithms for Lie algebras of algebraic groups, Ph.D. thesis, Technische Universiteit Eindhoven, Netherlands (2010).
- [80] W. Bosma, J. Cannon, and C. Playoust, J. Symbolic Comput. 24, 235 (1997).
- [81] M. Grötschel and W. R. Pulleyblank, Oper. Res. Lett. 1, 23 (1981).
- [82] R. Herrman, P. C. Lotshaw, J. Ostrowski, T. S. Humble, and G. Siopsis, Sci. Rep. 12, 1 (2022).
- [83] F. Lowenthal, Rocky Mt. J. Math. 1, 575 (1971).
- [84] F. Silva Leite, Rocky Mt. J. Math. 21, 879 (1991).
- [85] D. D'Alessandro, Syst. Control Lett. 47, 87 (2002).
- [86] B. T. Kiani, S. Lloyd, and R. Maity, Learning unitaries by gradient descent (2020), arXiv:2001.11897.
- [87] V. Akshay, H. Philathong, M. E. Morales, and J. D. Biamonte, Phys. Rev. Lett. 124, 090504 (2020).
- [88] A. W. Harrow and R. A. Low, Commun. Math. Phys. 291, 257 (2009).
- [89] R. A. Low, Pseudo-randomness and Learning in Quantum Computation, Ph.D. thesis, University of Bristol, UK (2010).
- [90] W. G. Brown and L. Viola, Phys. Rev. Lett. 104, 250501 (2010).
- [91] F. G. S. L. Brandão, A. W. Harrow, and M. Horodecki, Commun. Math. Phys. 346, 397 (2016).
- [92] F. G. S. L. Brandão, W. Chemissany, N. Hunter-Jones, R. Kueng, and J. Preskill, PRX Quantum 2, 030316 (2021).
- [93] J. Haferkamp and N. Hunter-Jones, Phys. Rev. A 104, 022417 (2021).
- [94] M. Oszmaniec, A. Sawicki, and M. Horodecki, IEEE Trans. Inf. Theory 68, 989 (2022).
- [95] J. Haferkamp, Quantum 6, 795 (2022).
- [96] A. W. Harrow and S. Mehraban, Commun. Math. Phys. 401, 1531 (2023).
- [97] T. Schuster, J. Haferkamp, and H.-Y. Huang, Science 389, 92 (2025).
- [98] N. Laracuente and F. Leditzky, in 16th Innovations in Theoretical Computer Science Conference (ITCS 2025), Leibniz International Proceedings in Informatics (LIPIcs), Vol. 325, edited by R. Meka (Schloss Dagstuhl – Leibniz-Zentrum für Informatik, Dagstuhl, Germany, 2025) pp. 69:1–69:2.
- [99] A. E. Deneris, P. Bermejo, P. Braccia, L. Cincio, and M. Cerezo, Exact spectral gaps of random onedimensional quantum circuits (2024), arXiv:2408.11201.
- [100] R. O'Donnell, R. A. Servedio, and P. Paredes, in 2023 IEEE 64th Annual Symposium on Foundations of Computer Science (FOCS) (2023).
- [101] J. Haah, Y. Liu, and X. Tan, in 2024 IEEE 65th Annual Symposium on Foundations of Computer Science (FOCS) (2024) pp. 463–475.
- [102] D. Belkin, J. Allen, S. Ghosh, C. Kang, S. Lin, J. Sud, F. T. Chong, B. Fefferman, and B. K. Clark, PRX Quan-

- tum 5, 040344 (2024).
- [103] A. Pesah, M. Cerezo, S. Wang, T. Volkoff, A. T. Sorn-borger, and P. J. Coles, Phys. Rev. X 11, 041011 (2021).
- [104] V. Vijendran, A. Das, D. E. Koh, S. M. Assad, and P. K. Lam, Quantum Sci. Technol. 9, 025010 (2024).
- [105] A. Kandala, A. Mezzacapo, K. Temme, M. Takita, M. Brink, J. M. Chow, and J. M. Gambetta, Nature 549, 242 (2017).
- [106] M. Larocca, F. Sauvage, F. M. Sbahi, G. Verdon, P. J. Coles, and M. Cerezo, PRX Quantum 3, 030341 (2022).
- [107] B. E. Sagan, *The Symmetric Group*, 2nd ed. (Springer, New York, 2001).
- [108] D. Shemesh, Lin. Alg. Appl. 62, 11 (1984).
- [109] A. Jamiołkowski and G. Pastuszak, Lin. Multilin. Alg. 63, 314 (2015).
- [110] E. Malvetti, Computing common eigenvectors and simultaneous triangulation (2023), arXiv:2309.14344.
- [111] P.-G. Rozon and K. Agarwal, Phys. Rev. Research 6, 023041 (2024).
- [112] S. Moudgalya, N. Regnault, and B. A. Bernevig, Phys. Rev. B 102, 085140 (2020).
- [113] S. Moudgalya and O. I. Motrunich, Phys. Rev. X 12, 011050 (2022).
- [114] S. Moudgalya and O. I. Motrunich, Phys. Rev. X 14, 041069 (2024).
- [115] C. J. Turner, A. A. Michailidis, D. A. Abanin, M. Serbyn, and Z. Papié, Nat. Phys. 14, 745 (2018).
- [116] M. Serbyn, D. A. Abanin, and Z. Papié, Nat. Phys. 17, 675 (2021).
- [117] K. Pakrouski, P. N. Pallegar, F. K. Popov, and I. R. Klebanov, Phys. Rev. Lett. 125, 230602 (2020).
- [118] K. Pakrouski, P. N. Pallegar, F. K. Popov, and I. R. Klebanov, Phys. Rev. Res. 3, 043156 (2021).
- [119] P. Sala, T. Rakovszky, R. Verresen, M. Knap, and F. Pollmann, Phys. Rev. X 10, 011047 (2020).
- [120] K. Bull, J.-Y. Desaules, and Z. Papić, Phys. Rev. B 101, 165139 (2020).
- [121] S. Moudgalya, N. Regnault, and B. A. Bernevig, Phys. Rev. B 107, 224312 (2023).
- [122] I. Marvian, Nat. Phys. 18, 283 (2022).
- [123] D. P. DiVincenzo, Phys. Rev. A 51, 1015 (1995).
- [124] S. Lloyd, Phys. Rev. Lett. **75**, 346 (1995).
- [125] Z. Zimborás, R. Zeier, M. Keyl, and T. Schulte-Herbrüggen, EPJ Quantum Technol. 1, 11 (2014).
- [126] D. S. Dummit and R. M. Foote, Abstract Algebra, 3rd ed. (John Wiley & Sons, Hoboken, 2004).
- [127] W. A. Adkins and S. H. Weintraub, Algebra: An Approach via Module Theory (Springer, New York, 1992).
- [128] J.-P. Serre, Linear Representations of Finite Groups (Springer, New York, 1977).
- [129] W. Ledermann, Introduction to group characters, 2nd ed. (Cambridge University Press, Cambridge, 1987).
- [130] A. N. Sengupta, Representing Finite Groups: A Semisimple Introduction (Springer, New York, 2012).
- [131] P. Erdős and A. Rényi, Acta Math. Acad. Sci. Hung. 14, 295 (1963).
- [132] C. Godsil and G. Royle, *Algebraic Graph Theory* (Springer, New York, 2001).
- [133] M. Cerezo, M. Larocca, D. García-Martín, N. L. Diaz, P. Braccia, E. Fontana, M. S. Rudolph, P. Bermejo, A. Ijaz, S. Thanasilp, E. R. Anschuetz, and Z. Holmes, Does provable absence of barren plateaus imply classical simulability? or, why we need to rethink variational quantum computing (2023), arXiv:2312.09121.

- [134] A. Chapman and S. T. Flammia, Quantum 4, 278 (2020).
- [135] G. E. Crooks, Performance of the quantum approximate optimization algorithm on the maximum cut problem (2018), arXiv:1811.08419.
- [136] F. G. Brandão, M. Broughton, E. Farhi, S. Gutmann, and H. Neven, For fixed control parameters the quantum approximate optimization algorithm's objective function value concentrates for typical instances (2018), arXiv:1812.04170.
- [137] J. Basso, D. Gamarnik, S. Mei, and L. Zhou, in 2022 IEEE 63rd Annual Symposium on Foundations of Computer Science (FOCS) (2022).
- [138] J. Basso, D. Gamarnik, S. Mei, and L. Zhou, Performance and limitations of the QAOA at constant levels on large sparse hypergraphs and spin glass models (2024), arXiv:2204.10306.
- [139] A. Dembo, A. Montanari, and S. Sen, Ann. Probab. 45, 1190 (2017).
- [140] K. Blekos, D. Brand, A. Ceschini, C.-H. Chou, R.-H. Li, K. Pandey, and A. Summer, Phys. Rep. 1068, 1 (2024).
- [141] S. Bravyi, A. Kliesch, R. Koenig, and E. Tang, Phys. Rev. Lett. 125, 260505 (2020).
- [142] E. Farhi, D. Gamarnik, and S. Gutmann, The Quantum Approximate Optimization Algorithm Needs to See the Whole Graph: A Typical Case (2020), arXiv:2004.09002.
- [143] E. Farhi, D. Gamarnik, and S. Gutmann, The Quantum Approximate Optimization Algorithm Needs to See the Whole Graph: Worst Case Examples (2020), arXiv:2005.08747.
- [144] C.-N. Chou, P. J. Love, J. S. Sandhu, and J. Shi, Limitations of Local Quantum Algorithms on Random MAX-k-XOR and Beyond, in 49th International Colloquium on Automata, Languages, and Programming (ICALP 2022), Leibniz International Proceedings in Informatics (LIPIcs), Vol. 229, edited by M. Bojańczyk, E. Merelli, and D. P. Woodruff (Schloss Dagstuhl – Leibniz-Zentrum für Informatik, Dagstuhl, Germany, 2022) pp. 41:1–41:20.
- [145] A. Misra-Spieldenner, T. Bode, P. K. Schuhmacher, T. Stollenwerk, D. Bagrets, and F. K. Wilhelm, PRX Quantum 4, 030335 (2023).
- [146] G. Scriva, N. Astrakhantsev, S. Pilati, and G. Mazzola, Phys. Rev. A 109, 032408 (2024).
- [147] M. H. Muñoz-Arias, S. Kourtis, and A. Blais, Phys. Rev. Res. 6, 023294 (2024).
- [148] L. Gerblich, T. Dasanjh, H. Wong, D. Ross, L. Novo, N. Chancellor, and V. Kendon, Advantages of multistage quantum walks over QAOA (2024), arXiv:2407.06663.
- [149] F. Rendl, G. Rinaldi, and A. Wiegele, Math. Program., Ser. A 121, 307 (2010).
- [150] I. Dunning, S. Gupta, and J. Silberholz, INFORMS J. Comput. 30, 608 (2018).
- [151] M. Jünger, E. Lobe, P. Mutzel, G. Reinelt, F. Rendl, G. Rinaldi, and T. Stollenwerk, ACM J. Exp. Algorithmics 26, 1.9 (2021).
- [152] V. H. Nguyen and M. Minoux, Optim. Lett. 15, 1041 (2021).
- [153] D. Rehfeldt, T. Koch, and Y. Shinano, Math. Program. Comput. 15, 445 (2023).
- [154] J. Charfreitag, M. Jünger, S. Mallach, and P. Mutzel, in *Proceedings of the Symposium on Algorithm Engi-*

- neering and Experiments, ALENEX, edited by C. A. Phillips and B. Speckmann (SIAM, 2022) pp. 54–66.
- [155] C. H. Papadimitriou and M. Yannakakis, J. Comput. Syst. Sci. 43, 425 (1991).
- [156] S. Arora, D. Karger, and M. Karpinski, J. Comput. Syst. Sci. 58, 193 (1999).
- [157] K. Jansen, M. Karpinski, and A. L. E. Seidel, SIAM J. Comput. 35, 110 (2005).
- [158] S. Gharibian and O. Parekh, Almost Optimal Classical Approximation Algorithms for a Quantum Generalization of Max-Cut, in Approximation, Randomization, and Combinatorial Optimization. Algorithms and Techniques (APPROX/RANDOM 2019), Leibniz International Proceedings in Informatics (LIPIcs), Vol. 145, edited by D. Achlioptas and L. A. Végh (Schloss Dagstuhl Leibniz-Zentrum für Informatik, Dagstuhl, Germany, 2019) pp. 31:1–31:17.
- [159] E. Gaar and F. Rendl, Math. Program., Ser. B 183, 283 (2020).
- [160] J. K. Fichte, D. L. Berre, M. Hecher, and S. Szeider, SIAM J. Comput. 66, 64 (2023).
- [161] D. E. Knuth, The Art of Computer Programming, Volume 4B: Combinatorial Algorithms, Part 2 (Addison-Wesley, Upper Saddle River, New Jersey, 2023).
- [162] R. Zeier and Z. Zimborás, J. Math. Phys. 56, 081702 (2015).
- [163] T. Schulte-Herbrüggen, G. Dirr, and R. Zeier, Open Sys. Information Dyn. 24, 1740019 (2017).
- [164] T. Schulte-Herbrüggen, R. Zeier, M. Keyl, and G. Dirr, in *Quantum Information: From Foundations to Quan*tum Technology Applications, Vol. 2, edited by D. Bruss and G. Leuchs (Wiley, Weinheim, 2019) 2nd ed., pp. 607–641.
- [165] R. Shaydulin and S. M. Wild, IEEE Trans. Quantum Eng. 2, 3101409 (2021).
- [166] R. Shaydulin, S. Hadfield, T. Hogg, and I. Safro, Quantum Inf. Process. 20, 359 (2021).
- [167] I. Marvian, H. Liu, and A. Hulse, Phys. Rev. Lett. 132, 130201 (2024).
- [168] I. Marvian, H. Liu, and A. Hulse, Qudit circuits with SU(d) symmetry: Locality imposes additional conservation laws (2021), arXiv:2105.12877.
- [169] C. V. Kraus, M. M. Wolf, and J. I. Cirac, Phys. Rev. A. 75, 022303 (2007).
- [170] R. Gargiulo, M. Rizzi, and R. Zeier, in ReAQCT '24: Proceedings of Recent Advances in Quantum Computing and Technology, June 19–20, 2024, Budapest, Hungary (ACM, 2024) pp. 20–50.
- [171] M. Brešar, Introduction to Noncommutative Algebra (Springer, Cham, 2014).
- [172] F. Lorenz, Algebra, Volume II (Springer, New York, 2008).
- [173] N. Jacobson, Basic Algebra I, 2nd ed. (Freeman, San Francisco, 1985).
- [174] N. Jacobson, Basic Algebra II, 2nd ed. (Freeman, San Francisco, 1989).
- [175] K. Lux and H. Pahlings, Representations of Groups: A Computational Approach (Cambridge University Press, Cambridge, 2010).
- [176] C. W. Curtis and I. Reiner, Representation Theory of Finite Groups and Associative Algebras (Wiley, New

- York, 1962).
- [177] C. W. Curtis and I. Reiner, Methods of Representation Theory, Volume I (Wiley, New York, 1981).
- [178] E. Noether, Math. Z. 30, 641 (1929).
- [179] E. Noether, Math. Z. 37, 514 (1933).
- [180] E. Noether, Gesammelte Abhandlungen Collected Papers (Springer, Berlin, 1983).
- [181] B. L. van der Waerden, Algebra, Volume II, 3rd ed. (Springer, New York, 1991).
- [182] H. Weyl, Ann. Math. 37, 709 (1936).
- [183] H. Weyl, The Classical Groups (Princeton University Press, Princeton, 1953).
- [184] M.-C. Bañuls, J. I. Cirac, and M. M. Wolf, Phys. Rev. A 76, 022311 (2007).
- [185] G. C. Wick, A. S. Wightman, and E. P. Wigner, Phys. Rev. 88, 101 (1952).
- [186] R. Brauer and H. Weyl, Am. J. Math. 57, 425 (1935).
- [187] F. D. Murnaghan, The Theory of Group Representations (Dover Publications, New York, 1963).
- [188] B. Kaufman, Phys. Rev. 76, 1232 (1949).
- [189] H. Boerner, Representation of Groups, 2nd ed. (North-Holland, Amsterdam, 1969).
- [190] W. Miller, Jr., Symmetry Groups and Their Applications (Academic Press, New York, 1972).
- [191] D. H. Sattinger and O. L. Weaver, Lie Groups and Algebras with Applications to Physics, Geometry, and Mechanics (Springer, New York, 1986).
- [192] W. Fulton and J. Harris, Representation Theory: A First Course (Springer, New York, 1991).
- [193] H. Georgi, Lie Algebras in Particle Physics, 2nd ed. (CRC Press, Boca Ration, 1999).
- [194] A. Zee, Group Theory in a Nutshell for Physicists (Princeton University Press, Princeton, 2016).
- [195] H. Samelson, Notes on Lie Algebras, 2nd ed. (Springer, New York, 1999).
- [196] M. Obata, Trans. Am. Math. Soc. 87, 347 (1958).
- [197] E. B. Dynkin, Amer. Math. Soc. Transl. Ser. 2 6, 245 (1957).
- [198] E. B. Dynkin, Amer. Math. Soc. Transl. Ser. 2 6, 111 (1957).
- [199] V. V. Gorbatsevich, A. L. Onishchik, and E. B. Vinberg, Structure of Lie Groups and Lie Algebras, in *Lie Groups and Lie Algebras III* (Springer, Berlin, 1994) pp. 1–244.
- [200] F. Antoneli, M. Forger, and P. Gaviria, J. Lie Theory 22, 949 (2012).
- [201] A. Borel, Semisimple Groups and Riemannian Symmetric Spaces (Hindustan Book Agency, New Delhi, 1998).
- [202] S. Helgason, Differential Geometry, Lie Groups, and Symmetric Spaces (Academic Press, New York, 1978).
- [203] N. Bourbaki, Elements of Mathematics, Lie Groups and Lie Algebras, Chapters 4–6 (Springer, Berlin, 2008).
- [204] A. Borel and J. de Siebenthal, Comment. Math. Helv. 23, 200–221 (1949).
- [205] M. Goto and F. D. Grosshans, Semisimple Lie Algebras (Marcel Dekker, New York, 1978).
- [206] R. P. Stanley, *Enumerative Combinatorics, Vol. I*, 2nd ed. (Cambridge University Press, Cambridge, 2012).